# Unraveling brain oscillatory correlates of memory encoding

Dissertation zur Erlangung des
akademischen Grades
eines Doktors der Naturwissenschaften

vorgelegt von
Fellner, Marie-Christin

an der

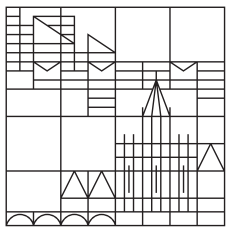

Universität Konstanz

Mathematisch-naturwissenschaftliche Sektion
Fachbereich Psychologie

Tag der mündlichen Prüfung: 7. Dezember 2015

1.Referent: Dr. Simon Hanslmayr

2. Referent: Dr. Sarang Dalal

# ACKNOWLEDGEMENTS

First and foremost, thank you Simon Hanslmayr for being a great supervisor, thanks for all the discussions, ideas, support and independence. Without your help and ideas this work would never have been possible. More importantly, without you I probably would have never considered that being a scientist is something I could be.

Thank you, Simon, for science.

A big thank you to all the volunteers who have participated in the experiments, especially the patients, thank you all for your time and patience.

Thank you, Sarang Dalal for all the help and discussions.

Thank you, Maria Wimber, for all the help in fMRI analysis .

Thank you, to all the people involved in the EEG-fMRI project, thank you Gregor Volberg, Markus Goldhacker, Mark Greenlee, Daniel Kaiser, Steffi Birkner.

Thank you, Karen Mullinger, for the great help in discovering the effects of motion on simultaneous EEG-fMRI and for all the great input on the project.

Thank you also to all the people involved in the intracranial measurements, Stefanie Gollwitzer, Stefan Rampp, Gernot Kreiselmeyer and Hajo Hamer.

Thank you to Ursula Lommen and Barbara Awiszus for all the help in the MEG recordings.

Thanks to all the Hiwis that helped with data acquisitions. Thank you, Marina, Janin, Anne, Julia, Irina, Martin.

Thanks to all of my colleagues Tobi, Tzvetan, Britta, Maite, Hanna, Johanna, Ursel, Cati for all the discussions, and lunch and coffee breaks.

Thanks to my flatmates for all the distraction.

Thanks to my parents for all your support.

Thank you Gerd, for being Gerd.

# SUMMARY

It is a common phenomenon that some occurrences in our life are well remembered, whereas others seem to be forgotten just after a glimpse. This observation leads to the assumption that some special process during experiencing an event determines later remembrance. In the present work the neural correlates of successful memory formation are investigated. To this end, brain oscillations as a correlate of neural activity and neural communication were recorded and contrasted for remembered and forgotten events. This contrast is commonly denoted subsequent memory effect (SME). SMEs are capturing two different processes: the forming of cortical representations needed to process information and the binding of these distributed representations into a memory trace.

Commonly, it is assumed that processing of information is carried out by distributed networks in the neocortex. The binding of these distributed representations into a unified memory trace then additionally relies on the medial temporal lobe as a major hub for tying together activity distributed across the cortex. Such distributed networks are thought to be characterized by specific spectral fingerprints. The goal of the presented studies is to identify the specific spectral fingerprints of memory encoding processes.

In study 1 SMEs were contrasted during a typical deep semantic judgment task and during a more elaborative survival encoding task. In the survival task participants were asked to judge presented words according to their relevance in a survival situation In the survival condition increases in alpha and beta long-range phase synchrony indexed successful encoding, whereas alpha/beta power decreases indexed semantic encoding. Additionally, pre-item subsequent memory effects in theta power were found, which did not vary with encoding condition. These results show that measures of local synchrony (power) and global long range-synchrony (phase synchronization) in the alpha/beta frequency range dissociate between memory encoding processes depending on the level of elaboration during encoding, potentially reflecting the involvement of a more distributed cortical network than during the more item related semantic judgment task.

Study 2 was specifically designed to investigate the alleged relation of theta oscillations and MTL activity. fMRI studies consistently demonstrate MTL activity in episodic memory formation. Spatial navigation and electrophysiological recordings have also emphasized the role of theta oscillations in these tasks. However, how and especially whether increases or decreases in theta power are linked to memory formation through MTL activity remains debated. To this

end, EEG and fMRI were recorded separately while participants used two mnemonic encoding strategies: the spatial Method of Loci and the non-spatial Pegword Method. Both encoding strategies are highly associative, but only the method of loci employs processing of spatial cues. The more effective spatial mnemonic technique induced a pronounced theta power decrease in the left MTL compared to the non-spatial associative mnemonic strategy. In addition, successful encoding during both strategies was related to a decrease in theta power. In the fMRI data these theta decreases were mirrored by BOLD increases in the MTL. This pattern of concurrent MTL BOLD increases and theta power decreases implies that indeed decreases in theta activity index MTL involvement during memory encoding and additionally demonstrate that associative memory formation irrespective of the encoding task is related to theta decreases.

Study 3 emerged from study 2, initially designed to investigate trial-by-trial correlations of oscillatory power and BOLD signals during encoding. We observed that low frequency EEG (<20 Hz) was strongly correlated with in-scanner movement. Thereby, minor head motion (<0.2 mm) induced spurious effects in a twofold manner: Small differences in task correlated motion elicit spurious low frequency effects, and, as motion concurrently influences fMRI data, EEG-BOLD correlations closely matched motion-fMRI correlations. These findings highlight an important caveat that needs to be addressed by future EEG-fMRI studies. For instance in the present study, results misleadingly showed an increase in theta power during memory formations, where out-of-scanner control data revealed that indeed an decrease in theta power is related to memory formation.

In study 4 memory encoding effects in MEG and iEEG were contrasted during encoding of two different stimuli: words and faces. Processing of words and faces elicits activity in well defined dissociable areas: left lateralized fronto-temporo-parietal regions for word processing and right ventral occipito-temporal areas for processing of unfamiliar faces. Decreases in alpha/beta power were found to index activity in these word and face areas during item processing and successful encoding of the respective material. These alpha/beta decreases were more strongly related to successful encoding of words, whereas successful encoding of faces was indexed by visual gamma increases. Additional post- and prestimulus decreases in theta power were found during memory formation, independently of material.

In all studies a common pattern was apparent: whereas alpha/beta oscillatory effects varied with encoding tasks and material, theta effects indexed memory formation independent of material and task. This finding demonstrates that oscillatory memory encoding effects reflect at least two cognitive processes involved in memory formation: alpha/beta activity seems to

index cortical information processing, potentially indexing activity in distributed semantic networks. In addition to the more distributed alpha/beta effects, gamma oscillations might index processing of sensory features. In contrast to the material and task dependent alpha/beta and gamma effects, theta power decreases were connected to memory encoding independent of cortical processing. Furthermore, theta decreases were found concurrent to MTL BOLD activity. Consequently, theta oscillatory networks during memory encoding can be interpreted as a MTL related memory binding process.

# ZUSAMMENFASSUNG

Während man sich an manche Ereignisse außergewöhnlich gut erinnert, scheinen andere Ereignisse schon nach kurzer Zeit nie passiert zu sein. Diese Beobachtung führt zur Überlegung, dass bestimmte neuronale Aktivität während dieser Ereignisse über das spätere Erinnern bestimmt. In der hier vorgelegten Arbeit sollen eben diese neuralen Korrelate untersucht werden späteres Erinnern bestimmen. Dazu wurde in mehreren Experimenten die Gehirn-oszillatorische Aktivität während der Formierung von später abrufbaren Gedächtnispuren untersucht. Oszillatorische Aktivität während des Enkodierens wurde hierfür in Abhängigkeit von der späteren Gedächtnisleistung zwischen erinnerten und nichterinnerten Episoden verglichen. Diese Differenz zwischen Aktivität von erinnerten und vergessenen Stimuli wird meist als Subsequent Memory Effect (SME) bezeichnet.

Dieser Kontrast zwischen neuronaler Aktivität während erinnerter und vergessener Stimuli umfasst zwei Prozesse: zum einem die Verarbeitung und kortikale Repräsentation des Stimulus, zum anderen das „Binding“ dieser kortikalen Repräsentationen zu einer Gedächtnisspur. Die neuronale Repräsentation und Verarbeitung wird dem Cortex zugesprochen, während der mediale Temporallappen eine tragende Rolle in der Zusammenführung dieser Repräsentationen zu einer Gedächtnisspur hat. Beide dieser Prozesse umfassen Aktivierung in komplexen neuronalen Netzwerken. Ein Mechanismus, der die neuronale Kommunikation und die Zusammenarbeit solcher spezifischer verteilten Netzwerke ermöglichen könnte, sind Gehirnoszillationen. Aktivierung in spezifischen kortikalen Netzwerken könnte daher zu spezifische “spektralen Fingerprints” in diesen Netzwerken führen. Das Ziel dieser Arbeit ist es diese spektralen Fingerprints von Gedächtnisenkodierprozessen zu messen und zu charakterisieren.

Mit diesem Zielen wurde in drei Studien Gedächtnisenkodierprozesse und die Abhängigkeit dieser Prozesse von Enkodieraufgaben und zu enkodierende Material untersucht. In einem multimodal Messansatz wurde in EEG, MEG, fMRI und intrakranielles EEG aufgezeichnet. Studie 1 untersuchte den Einfluss von verschiedener Enkodierstrategien, semantischer Verarbeitung und von sogenannten „survival processing“, auf SMEs. In Studie 2 wurde der Zusammenhang von fMRI BOLD Aktivierung und EEG Theta Oszillationen untersucht. In Studie 3, werden artifizielle Gedächtniseffekte in simultanen EEG-fMRI Daten berichtet. In Studie 4 wurden SMEs während verschiedener Materialen (Gesichtern und Wörtern) verglichen.

In allen Studien war ein übereinstimmendes Muster zu erkennen: Alpha/beta Oszillationen variierten mit den Enkodieraufgaben und dem zu enkodierenden Material. Im Gegensatz dazu waren Effekte im Theta Frequenzband, unabhängig von Material und Aufgabe, korreliert mit erfolgreicher Gedächtnisenkodierung. Dieses Ergebnismuster zeigt, dass kortikale Verarbeitungsprozesse, die zur Gedächtnisendkodierung beitragen mit oszillatorischer Aktivität im Alpha/Beta Bereich korreliert sind. Theta Oszillationen hingegen scheinen MTL "binding" Prozesse zu reflektieren.

# CONDUCTED STUDIES AND OWN RESEARCH CONTRIBUTIONS

All reported studies were co-authored and supported by a number of colleagues. See below for own research contributions in each reported study.

## STUDY 1: BRAIN OSCILLATORY SUBSEQUENT MEMORY EFFECTS DIFFER IN POWER AND LONG-RANGE SYNCHRONIZATION BETWEEN SEMANTIC AND SURVIVAL PROCESSING.

Authors: Marie-Christin Fellner, Karl-Heinz T. Bäuml, Simon Hanslmayr

I supported the design of the experiment and was involved in data collection. I conducted all analysis on behavioral and electrophysiological data, and drafted the manuscript.

Status: published in NeuroImage (2013), 79, 361-370.

## STUDY 2: SPATIAL MNEMONIC ENCODING IS RELATED TO THETA POWER DECREASES AND MEDIAL TEMPORAL LOBE BOLD INCREASES

Authors: Marie-Christin Fellner, Gregor Volberg, Maria Wimber , Markus Goldhacker, Mark W. Greenlee, Simon Hanslmayr

I designed the experiment and collected EEG-fMRI data in Regensburg and collected additional EEG data in Konstanz. I analyzed EEG and fMRI data and drafted the manuscript.

Status: submitted to Cerebral Cortex (Status on 20th September 15)

## STUDY 3: SPURIOUS CORRELATIONS IN SIMULTANEOUS EEG-FMRI DRIVEN BY IN-SCANNER MOVEMENT

Authors: Marie-Christin Fellner, Gregor Volberg, Karen Mullinger, Maria Wimber, Markus Goldhacker, Mark W. Greenlee, Simon Hanslmayr

I designed the experiment and collected EEG-fMRI and an additional EEG dataset (same data as used in Study 2). I analyzed the data and drafted the manuscript.

Status: submitted to NeuroImage (Status on 20th September 15)

## STUDY 4: SPECTRAL FINGERPRINTS OF MEMORY ENCODING: MATERIAL SPECIFC AND MATERIAL UNSPECIFIC SUBSEQUENT MEMORY EFFECTS

Authors: Marie-Christin Fellner, Stefanie Gollwitzer, Stefan Rampp, Hajo Hamer, Simon Hanslmayr

I designed the experiment and recorded iEEG data from patients in Erlangen and MEG data from a student sample in Konstanz. I analyzed iEEG and MEG data and drafted the manuscript.

Status: in preparation

# ABBREVIATIONS

BA, Brodmann areal

BCG, ballisto-cardiogram

BOLD, blood-oxygenation-level-dependent

ECG, electrocardiogram

EEG, electroencephalography

ERP, event related potential

fMRI, functional magnetic resonance imaging

FWE, family-wise error

FWHM, full-width at half maximum

GLM, general linear model

HRF, hemodynamic response function

ICA, independent component analysis

IC, independent component

iEEG, intracranial recorded electroencephalogram

IFG, Inferior frontal lobe

LCMV, linear constraint minimum variance

MEG, magnetoencephalography

MNI, Montreal Neurological Institute

MTL, medial temporal lobe

MRI, magnet resonance imaging

OBS, optimal basis set

PLV, phase locking value

QRS complex, complex of characteristical ECG deflections

ROI, region of interest

SEM, standard error of the mean

SME, subsequent memory effect

SPM, statistical parametric mapping

TR, time resolution

# CONTENT

# THEORETICAL BACKGROUND

## EPISODIC MEMORY ENCODING

### *COGNITIVE PERSPECTIVE*

From our daily life we know that some events we can remember very well and other events we seem to never have experienced. Common experience already leads to the conception that there must be something special about the things we can later remember, which was lacking for the events we later cannot remember. What one would commonly denote "memory" is usually labeled declarative memory in psychological theory. It encompasses memory for certain life events (i.e. "I had pizza for dinner yesterday") and facts ("Pizza is a round piece of dough with tomatoes and cheese"). Declarative memory is separated form other, non-declarative, implicit memory systems (e.g. skills or conditioning; Squire (2004)). Several cognitive theories define what determines successful encoding into declarative memory in terms of information processing.

One of the most influential theories on memory encoding, the levels of processing framework, by Craik and Lockheart (1972) states that successful encoding is merely a function of processing information. Depending on how "deep" an item is processed, the more likely it will be later remembered. Deepness is conceptualized from ranging from perceptual feature processing to abstract semantic processing. For example, judging words concerning a specific visual feature (e.g. what font a word is written) signifies shallow processing and leads to lower later recall rates than judging words for pleasantness, a form of deep processing. Other experiments have shown that not only deepness determines encoding, but also distinctiveness of the encoding task and elaboration during encoding (Craik, 2002; Hunt & Einstein, 1981; Klein & Saltz, 1976). Deducing from this line of theories, memory formation seems to be a mere byproduct of processing; a complex neural representation and processing of stimuli is all that is needed to form memories.

This pure processing view of memory encoding, however, cannot explain memory impairments in amnestic patients. Famously, patient H. M. after a bilateral medial temporal lobe (MTL) resection, did perform normally on a wide range of tasks, but was not able to form any new memories (Corkin, 2002; Scoville & Milner, 1957). For example, he still enjoyed solving crossword puzzles, but he could not remember what he had for dinner last night. Consequently, pure processing is not sufficient for memory formation leading to the notion that an additional process, crucially involving MTL is needed, to successfully encode a memory. In addition to

forming an internal representation during processing, these representations must be bound to an enduring trace (Paller & Wagner, 2002). Furthermore, not all of these declarative memories are created the same way. Other studies focusing on memory patients with brain lesions showed that declarative memory is not monolithic, but separable in semantic memory and episodic memory (Patterson, Nestor, & Rogers, 2007; Tulving, 1984, 2002; Vargha-Khadem et al., 1997). Episodic memory, memories for events that encompass autonoetic consciousness (i.e. first person remembering, e.g. "*me* eating pizza last night") (Tulving, 1984) crucially rely on medial temporal lobe function and specifically the hippocampus. Semantic memory, memory for facts (e.g. pizza is food), or more precise every knowledge in a propositional form (Tulving, 1993), is supported by different neural processes.

Despite the distinction between these memory systems, interactions of semantic and episodic memory are considered crucial for memory encoding. Encoding in episodic memory is thought to always involve semantic knowledge (Tulving, 2002; see also for a more recent account van Kesteren, Ruiter, Fernandez, and Henson (2012)). The previously highlighted levels of processing framework also can be interpreted as a framework for how semantic memory operations support episodic memory encoding (Craik, 2002). The formation of an episodic memory trace, as a unified multimodal representation, therefore always involves two processes: the processing and representation of the content of the presented stimuli and the binding of these representations to a durable memory trace.

### *NEURAL CORRELATES OF MEMORY ENCODING*

The neural correlates of memory encoding have been studied using the subsequent memory paradigm in numerous experiments (Paller & Wagner, 2002). In these studies, the correlates of memory encoding are conceptualized as the difference in activity between later remembered stimuli and later forgotten stimuli. This contrast between subsequent remembered and forgotten items is referred to as the subsequent memory effect (SME). First SMEs were reported more than 35 years ago investigating event related potentials (ERP) in EEG (Paller, McCarthy, & Wood, 1988; Sanquist, Rohrbaugh, Syndulko, & Lindsley, 1980). These studies already reported a reliable marker of subsequent memory: an enhanced positivity starting ~400ms after item onset correlated with successful memory formation.

With the advent of imaging techniques (PET and fMRI) it was possible to determine which brain structures show differences in activity during memory formation. First studies using block designs reported increased activity in MTL and frontal regions during encoding phases (Gabrieli et al., 1996; Kapur et al., 1994; Kelley et al., 1998; Stern et al., 1996). With the

emergence of event-related fMRI studies it was also possible to calculate more temporally resolved SMEs by modeling hemodynamic brain responses on a shorter time-scale (Brewer, Zhao, Desmond, Glover, & Gabrieli, 1998; Wagner et al., 1998). To this date, numerous fMRI studies have been carried out investigating memory encoding related activity in various paradigms.

Most of the studies investigating memory formation have focused on MTL activity, because of the crucially involvement of this region in memory formation known since the infamous amnestic patient H.M. (Scoville & Milner, 1957). The MTL and specifically the hippocampus as hypothesized general connector of cortical activity is thought to form complex spatio-temporal representations (Buzsaki, 1996, 2010; Eichenbaum, 2000). MTL activity is not exclusively related to memory encoding, but also to spatial processing and navigation. Spatial navigation similar as episodic memory operation is based on the integration of, mainly sensorimotor, information to an abstract representation (Burgess, 2008; Buzsaki, 2005; Ekstrom et al., 2005). Similar mechanisms are proposed to underlie spatial navigation and episodic memory formation (Buffalo, 2015; Buzsaki & Moser, 2013; Ekstrom, 2014; Zucker & Ranganath, 2015). The role of the hippocampus and MTL regions in memory encoding is therefore hypothesized to connect distributed cortical representation into a self-referenced spatio-temporal memory trace (Buzsaki & Moser, 2013).

A meta-analysis including 74 fMRI studies showed successful encoding reliably involves several areas (Kim, 2011): BOLD activity in MTL is increased during memory formation, and generally more so during associative memory encoding (Davachi, 2006; Diana, Yonelinas, & Ranganath, 2007; Ranganath, 2010; Staresina & Davachi, 2009) confirming the important role of MTL regions. The left IFG, a brain region also involved in semantic memory operations (Binder, Desai, Graves, & Conant, 2009; Noppeney, Phillips, & Price, 2004; Patterson et al., 2007; Pulvermuller, 2013), also shows increased activity during memory formation. Accordingly, especially in studies investigating word encoding and/or employing encodings task involving semantic judgment have reported SMEs in the left IFG (Kim, 2011; Kirchhoff, Wagner, Maril, & Stern, 2000; Otten & Rugg, 2001b). In contrast to left IFG effects during encoding of semantic information, encoding of pictorial stimuli and perceptual details leads to increased activity in fusiform gyrus and along the ventral occipito-temporal stream (Dickerson et al., 2007; Garoff, Slotnick, & Schacter, 2005; Kim, 2011). These fusiform BOLD increases during memory formation, similar to left IFG semantic effects, are attributable to processing the to-be-encoded material, as the fusiform gyrus is generally involved in processing visual features

(Kanwisher & Yovel, 2006; Logothetis, Pauls, & Poggio, 1995; McCandliss, Cohen, & Dehaene, 2003).

Consequently, SMEs in cortical areas like the left IFG and fusiform gyrus are related to processes involved in the cortical representation and processing of stimuli, whereas MTL activity is hypothesized to bind these representations to a unified memory trace. On a more functional level, cell assemblies in specific cortical areas are thought to represent specific features (Pulvermuller, 2013) and complex processing of the represented features involves the interplay and connectivity of these distributed areas to enable e.g. judging an item for its semantic content (Buzsaki, 2010; Patterson et al., 2007). Whereas semantic processing is thought to rely on connectivity between cortical areas, interplay between MTL and cortical areas is thought to be crucial for encoding a self referenced spatio-temporal episode into memory. MTL related activity is considered to interact with cortical representations to form a memory trace (Buzsaki, 1996). For example, increased connectivity between MTL and left IFG has been shown during semantic memory encoding (Schott et al., 2013).

Summed up, fMRI experiments so far have identified areas correlating with memory encoding, indexing cortical information processing and memory binding processes. Areas like left IFG and fusiform gyrus, which show variation in activation depending on encoding task and to-be-encoded material, are involved in the cortical representation and processing of information. Especially during associative encoding tasks, when these distributed cortical representations have to be bound into a unified representation, involvement of MTL structures has been reported. This interpretation of results implies that memory encoding involves a complex neural network that flexibly interacts during formation of memories.

### *BRAIN OSCILLATIONS AND MEMORY ENCODING*

Measuring fMRI data with high spatial resolution reveals a lot about which brain areas are involved in memory formation. However, memory cannot be strictly localized but involves representations distributed across cortex (Fuster, 1997). Therefore, mapping areas reliably involved in encoding alone cannot reveal the functional correlates of memory formation, as memory formation depends on the dynamic interaction between different areas. The general mechanism of forming lasting neural representations relies on changes of the synaptic weights between neurons by concurrent neuronal spiking, condensed in Hebb's famous "fire together, wire together" principle (Hebb, 1949). Such temporally correlated firing of neurons is reflected in brain oscillations: increases in amplitude and coherence of brain oscillations are thought to be a crucial prerequisite of information transfer and neural information coding (Salinas &

Sejnowski, 2001; Singer & Gray, 1995). Such brain oscillations are thought to enable the formation of distributed neural networks (Varela, Lachaux, Rodriguez, & Martinerie, 2001) and to facilitate communication within these networks (Fries, 2005). Consequently, brain oscillations as a mechanism of neural communication and integration might play a major role in integrating distributed cortical representations into a unified memory trace.

Specific cognitive processes relying on distributed networks are proposed to be characterized by distinct spectral fingerprints (M. Siegel, Donner, & Engel, 2012). By enabling communication between distributed areas, specific oscillations are thought to index specific neural networks, for example networks involved in memory formation (Watrous & Ekstrom, 2014; Watrous, Fell, Ekstrom, & Axmacher, 2015). Information transfer in such a network might be achieved by the control of local spiking through an oscillation, as neural spiking has been shown to correlate with power (Haegens, Nacher, Luna, Romo, & Jensen, 2011) and phase (Jacobs, Kahana, Ekstrom, & Fried, 2007; Rutishauser, Ross, Mamelak, & Schuman, 2010) of ongoing low frequency oscillations. Through these mechanisms, neural spiking is controlled by oscillatory activity. Also, slower oscillations have been shown to reflect operations in larger networks (Buzsaki & Draguhn, 2004; von Stein, Chiang, & Konig, 2000) and there seems to be a hierarchy of slower oscillations controlling faster oscillations (Lakatos et al., 2005). In a similar vein, lower frequency oscillations have been related to top-down processes controlling higher frequencies, which are considered to index more bottom-up sensory activity (Buffalo, Fries, Landman, Buschman, & Desimone, 2011; Donner & Siegel, 2011; Jensen, Bonnefond, Marshall, & Tiesinga, 2015; von Stein et al., 2000).

Several review papers have emphasized the crucial role of brain oscillation in memory processes (Duzel, Penny, & Burgess, 2010; Fell & Axmacher, 2011; Hanslmayr & Staudigl, 2014; Hanslmayr, Staudigl, & Fellner, 2012; Kahana, 2006; Nyhus & Curran, 2010; Watrous & Ekstrom, 2014; Watrous et al., 2015). The majority of studies investigating oscillatory correlates of memory encoding focused on theta oscillations (~2-8 Hz). This "theta-centric" encoding view stems from the connection of theta oscillations and the hippocampus in rodents (Buzsaki, 2005; Buzsaki & Moser, 2013), but also in humans (Watrous, Lee, et al., 2013). Furthermore, theta oscillations are a core element in several models of memory functions (Burgess, Barry, & O'Keefe, 2007; Hasselmo & Stern, 2014; Lisman & Jensen, 2013). One of the first studies reporting oscillatory encoding effects found increases in theta power during successful memory formation (Klimesch, 1996). Klimesch, Doppelmayr, Russegger, and Pachinger (1996) theorized that this positive theta SME (i.e. increases in power signifying successful memory formation)

indexes hippocampo-cortical feedback loops involved in memory encoding. Several following studies also reported theta increases during successful memory formation (Friese et al., 2013; Hanslmayr, Spitzer, & Bauml, 2009; Hanslmayr et al., 2011; Klimesch, Doppelmayr, et al., 1996; Klimesch, Doppelmayr, Schimke, & Ripper, 1997; Osipova et al., 2006; Staudigl & Hanslmayr, 2013). However, more recently, theta decreases related to memory encoding (i.e. negative theta SMEs) were reported (Burke et al., 2013; Fell et al., 2011; Greenberg, Burke, Haque, Kahana, & Zaghloul, 2015; Guderian, Schott, Richardson-Klavehn, & Duzel, 2009; Long, Burke, & Kahana, 2014; Sederberg et al., 2007). Note, that the majority of studies reporting theta decreases recorded in intracranial implanted patients, in part directly in the MTL. This finding of intracranial theta decreases did shatter the very straightforward assumption of theta power increases being a correlate of postulated memory binding processes. It therefore still remains a debated question how theta oscillatory power, MTL activity and memory encoding are related.

Not only theta power changes have been observed during memory formation, several studies also reported alpha (~8-12 Hz) and beta (~13-30 Hz) oscillations indexing successful encoding. Here, mainly decreases in power have been found to relate to memory encoding (Klimesch, Schimke, et al., 1996; Sederberg, Kahana, Howard, Donner, & Madsen, 2003; Sederberg et al., 2007; Weiss & Rappelsberger, 2000). A few studies also reported memory encoding-related alpha increases (Khader, Jost, Ranganath, & Rosler, 2010; Meeuwissen, Takashima, Fernandez, & Jensen, 2011). However, these alpha increases were not found in classical memory encoding paradigms, but during working memory maintenance and therefore possible reflect active inhibition to prevent task interfering input (Jensen, Gelfand, Kounios, & Lisman, 2002; Jensen & Mazaheri, 2010; Klimesch, Sauseng, & Hanslmayr, 2007). Whereas increases in alpha power are seen as a deactivation of cortical areas, decreases in alpha and also beta power have been found to correlate positively with neural activity (Haegens et al., 2011; Hanslmayr et al., 2011; Scheeringa et al., 2011). Desynchronized alpha/beta power has been hypothesized to be a general marker of cortical information processing during memory encoding (Hanslmayr, Staudigl, et al., 2012). SMEs in the alpha and beta frequency range have also been reported to correlate (Sederberg et al., 2003), suggesting alpha and beta decreases are at least partially related to similar processes.

A first study investigating the effect of varying encoding tasks on brain oscillatory SMEs, contrasted a typical shallow alphabetical encoding task with a semantic animacy judgment task and found memory related alpha/beta power decreases specifically during semantic processing (Hanslmayr et al., 2009). In a follow up simultaneous EEG-fMRI study, beta power decreases

were found to be correlated with BOLD activity in the left IFG on a trial by trial basis (Hanslmayr et al., 2011). This demonstrates that task-related decreases of oscillatory beta power directly index the BOLD activity in the left IFG. To test if these beta decreases in the left IFG are functionally relevant for memory formation or a mere epiphenomenon, an additional study was carried out using repetitive transcranial magnetic stimulation (rTMS) (Hanslmayr, Matuschek, & Fellner, 2014). rTMS can entrain a focal cortical area in a specific oscillation (Thut & Miniussi, 2009) to probe for causal involvement of brain oscillations in cognitive tasks. In the experiment, participants encoded word lists while their left IFG was stimulated using different frequencies. Only during stimulation in the beta frequency, and thereby preventing beta power decreases, memory performance was significantly attenuated when compared to stimulation with other frequencies and sham. This pattern of results underlines the importance of power decreases during memory encoding processes and the localization of these decreases left IFG, a area considered an important hub in complex semantic processing (Sharon, 2003), suggests that these beta decreases are specifically indexing information processing during memory formation.

In addition to memory encoding effects in the lower frequency range effects in the gamma frequency range (~35 -120 Hz) have been reported. Memory-related gamma increases have been mostly found in posterior brain areas (Osipova et al., 2006), but also distributed across the cortex and in the MTL (Burke et al., 2014; Fell et al., 2001; Sederberg et al., 2007). It has been pointed out that increases in gamma power during memory closely match typical memory related fMRI activations (Burke et al., 2014). These gamma power increases are hypothesized to be an unspecific marker of local neural activity (Burke, Ramayya, & Kahana, 2015). Generally, gamma oscillation haven been specifically related to local information processing (Jensen, Kaiser, & Lachaux, 2007), like the processing of visual features (Fries, 2009; Fries, Nikolic, & Singer, 2007).

# GOALS OF THE PRESENTED STUDIES

Despite the wealth of findings by the studies reported above, there are several open questions regarding how and which oscillations are involved in the formation of memories. Whereas numerous ERP and fMRI studies have investigated how encoding-related activity varies depending on differing material and various encoding tasks, only very few studies have investigated the impact of different information processing on the oscillatory correlates of memory encoding. In the present work, encoding strategies (Study 1 & 2) and the to-be-encoded material (study 3) was manipulated in order to disentangle spectral fingerprints of dissociable memory encoding processes.

Cognitive theories, as summarized in the "Cognitive Perspective" section above, propose that memory encoding is dependent on processing and building cortical representations of to-be-encoded material. However, the pure processing of material is not sufficient for memory formation, an additional process is needed to unify the cortical representation into a durable memory trace. Brain oscillations, as assumed correlates of neural communication, are a possible mechanism to enable the distributed processing of information and the binding of these representations to an episodic memory. We hypothesized therefore that these memory encoding sub-processes are reflected by differing oscillations, signifying spectral fingerprints of distinct processing networks. Alpha and beta oscillatory power decreases have been implicated in cortical information processing and semantic processing (Hanslmayr et al., 2014; Hanslmayr et al., 2009; Hanslmayr, Staudigl, et al., 2012) and also material-specific alpha/beta retrieval effects have been reported (Khader & Rosler, 2011; Staudigl, Vollmar, Noachtar, & Hanslmayr, 2015; Waldhauser, Johansson, & Hanslmayr, 2012). Therefore, alpha/beta oscillations are a likely candidate for indexing material- and task-dependent SMEs. Theta oscillations, in contrast, are classically related to the MTL (Buzsaki, 2005), the brain region crucially involved in memory binding processes (Paller & Wagner, 2002; Ranganath, 2010; Staresina & Davachi, 2009) and therefore should be independent of cortical processing task and material specific processing. By varying encoding tasks and to-be-encoded material the present work tried to identify distinct spectral fingerprints of these processes in these frequency bands.

In study 1, SMEs in EEG elicited by two efficient encoding strategies were contrasted. One of the encoding tasks was a classical semantic encoding task, in which participants were asked to judge presented material regarding its animacy (Hanslmayr et al., 2009; Otten & Rugg, 2001b). This semantic encoding task was contrasted to a survival processing encoding task, a

more unusual, but previously shown to be very efficient encoding strategy (Nairne, Thompson, & Pandeirada, 2007), stimulating elaborative encoding (Burns, Burns, & Hwang, 2011; Kroneisen & Erdfelder, 2011). The open question this study was designed to answer was, if SMEs do vary for two encoding task with different levels of elaboration.

The goal of study 2 was to identify the relation of theta oscillatory power and MTL activity. To this end, EEG and fMRI was measured separately while participants used two different mnemonic strategies: The Method of Loci and the Pegword method. Both encoding methods are based on associative encoding, but only the Method of Loci additionally involves spatial processing. Besides memory functions, spatial processing is one of the major functions associated with the MTL (Burgess, 2008; Buzsaki & Moser, 2013). Therefore, theta oscillatory activity during the Method of Loci should be especially boosted. As the relationship of theta power, memory encoding and MTL activity remains highly debated, the goal of the study was to investigate whether increases or decreases in theta power are related to BOLD MTL activity. Of additional interest was, whether theta oscillations and MTL activity are specifically involved in spatial memory encoding or more generally in associative memory encoding.

The data presented in study 3 were originally collected to be included in study 2. Simultaneous EEG-fMRI was actually recorded to investigate trial-by-trial theta power and BOLD correlations. However, extended data analysis showed that SMEs in simultaneously recorded EEG are largely driven by artifacts caused by in-scanner movement. Possibly this difference in movement is attributable to physiological movements like respiration. Thereby, SMEs in simultaneous EEG were in stark contrast to data recorded outside. Furthermore, motion by concurrently driving artifacts in EEG and fMRI recordings also caused spurious EEG-fMRI correlations. The finding that in-scanner movement correlated positively with later memory performance shows how artifacts in EEG-fMRI, which have not been considered problematic before, can induce spurious effects that are seemingly neurophysiological plausible and that may dramatically bias interpretation of the results.

In study 4 the effects of to-be-encoded material on SMEs was investigated. MEG was measured in a healthy subject sample and a patient sample with intracranial implanted electrodes. Here, the research question was how oscillatory activity varies with to-be-encoded material and which effects are independent of to-be-encoded material. The combination of measuring the same paradigm in MEG and iEEG provides the possibility to investigate these effects on a whole brain scale in MEG data and on a more local scale using iEEG.

# MAIN FINDINGS, LIMITATIONS AND OPEN QUESTIONS

## OSCILLATORY FINGERPRINTS OF MEMORY ENCODING

### *OSCILLATORY ACTIVITY VARYING WITH ENCODING TASK AND MATERIAL*

One of the main findings of the presented studies is that alpha and beta activity vary with to-be-encoded material and also with the encoding task. In study 1, alpha/beta power decreases were specifically related to semantic encoding, whereas more elaborative survival encoding was related to increases in long-range alpha/beta phase synchrony. In study 4 in which we contrasted encoding of words and faces, alpha/beta decreases were localized to areas typically involved in processing words and faces. Furthermore, alpha/beta decreases during word processing and for word SMEs were equally located in left sided areas typically related to semantic processing (Pulvermuller, 2013): left IFG, left temporal and left temporo-parietal areas. Alpha/beta decreases during face processing showed a conjunction with face SMEs in the right ventro-occipito-temporal stream, an area specifically related to process visual features and also faces (Kanwisher & Yovel, 2006). Alpha/beta oscillations therefore seem to track cortical information processing during memory formation. Alpha/beta decreases were specifically involved in semantic processing (see also Hanslmayr et al. (2014); Hanslmayr et al. (2009)): Decreases during successful encoding of words were stronger than during encoding of faces, possibly indexing the higher use of semantics for encoding words than faces (Winograd, 1981). Encoding effects for faces were stronger in the gamma range, possibly related to the higher importance of encoding visual features for encoding faces. Concluding from these findings, alpha/beta decreases and gamma increases vary with encoding type and material and therefore seem to be specific fingerprints of cortical information processing networks involved in memory encoding.

### *OSCILLATORY ACTIVITY INDEPENDENT OF MATERIAL AND ENCODING TASKS*

In contrast to alpha/beta decreases and gamma increases, theta oscillatory SMEs did not vary depending on encoding task (study 1 and study 2) and material (study 3). In study 1, prestimulus increases in theta power were related to successful memory encoding for both encoding tasks. Note, that these memory unspecific theta increases in study 1 might also index attentional orienting. The reported theta increases were centered to the cue onset and not to the stimulus presented 1 sec after the cue, therefore and according to the following studies, these

theta increases might be connected to attentional processes and not directly to processing involved in memory encoding. In study 2 and 4 pre- and poststimulus theta decreases were found during successful memory formation irrespective of encoding task and material. In study 2 these theta decreases were equally found during a spatial as well as during a non-spatial associative encoding strategy and co-occurred with MTL BOLD increases. In study 4 material independent theta decreases were found in MEG data source localized to a widespread cortical network including the MTL. These MTL related theta decreases occurred independently of cortical information processing, therefore follow the assumptions of a processing independent memory binding process.

### *COGNITIVE MODEL BASED VIEW OF MEMORY ENCODING*

According to Tulving's model of memory encoding, every information has to pass two stages of processing before it can be encoded into episodic memory: first information has to be processed in the perceptual system, followed by the semantic system and then it can be encoded into episodic memory (see Figure 1, original model by Tulving (2001)). This division of memory encoding sub-processes is very much in line with the presented findings. Local gamma power increases were found in the visual ventral stream involved in processing complex visual features, and therefore might index sensory feature representations. Alpha/beta decreases are reported especially during semantic encoding processes (Hanslmayr et al., 2014; Hanslmayr et al., 2009; Hanslmayr et al., 2011) and were located in semantic hubs (see study 4). Theta decreases were found to index memory encoding independently of cortical processing demands (study 2 & 4), were localized in the MTL (study 2 & 4) and did co-occur with MTL BOLD activity (study 2).

Alpha/beta oscillations have been consistently reported in memory encoding using semantic processing (Fellner, Bauml, & Hanslmayr, 2013; Hanslmayr et al., 2009; Hanslmayr et al., 2011). Alpha/beta oscillations might serve a crucial function in semantic processing by enabling interaction between gamma related perceptual representations (Fries, 2009; Fries et al., 2007). Alpha/beta oscillations have been shown to enable widespread cortical communication (Popov, Miller, Rockstroh, & Weisz, 2013; Weisz et al., 2014) and are generally considered to be involved in cortical top down processes (Buffalo et al., 2011; Donner & Siegel, 2011; Jensen et al., 2015). These findings render alpha/beta oscillations are very plausible mechanism for the integration of widespread cortical activity into a semantic representation (Patterson et al., 2007; Pulvermuller, 2013).

Theta oscillatory activity has consistently been linked to MTL activity and memory like processes in rodents (Buzsaki, 2005; Buzsaki & Moser, 2013). In study 2 we demonstrated a link

between theta oscillatory power decreases and the MTL during a highly associative memory encoding irrespective of encoding task. In study 4, again, processing independent theta activity was found in a widespread cortical network including the MTL. These theta decreases therefore might index the integration of widespread semantic representations into a complex spatio-temporal episodic memory trace. Similar accounts of cortical representations and MTL based integration are part of several models of memory (Bird & Burgess, 2008; Hasselmo & Stern, 2006; Mcclelland, Mcnaughton, & Oreilly, 1995; Nadel, Samsonovich, Ryan, & Moscovitch, 2000). Note, that this presented model based view in Figure 1 is a mere heuristic of encoding processes. For example, in the model presented by Tulving (2001) the semantic processing step is a necessary prerequisite for encoding into episodic memory. However, if indeed semantic processing is truly a necessity for episodic encoding cannot be answered by the present data.

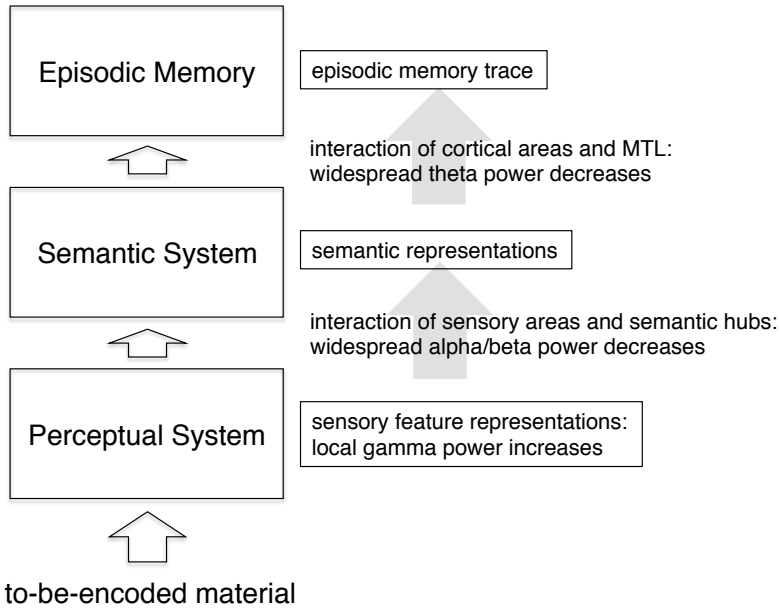


**Figure 1: Model-based view of memory encoding.** In order to successfully encode into episodic memory to-be-encoded material first has to be represented in a perceptual code and secondly represented in a semantic code to be finally encoded into episodic memory. The presented findings suggest that representations of sensory features are related to gamma power increases. Alpha/beta power decreases are involved in the formation of semantic representations, which then are encoded into episodic memory via theta power related MTL memory binding processes.

### *OPEN QUESTIONS AND LIMITATIONS: INTERPLAY OF OSCILLATIONS AND REPRESENTATIONAL CODE*

The main limitation of the present findings in respect to the proposed cognitive model is how these separated systems represent information and functionally interact with each other. In the presented studies the focus was mainly on oscillatory power effects, which seem to map quite well to the sub-processes outlined above. However, it remains an open question how these processes interact with each other. An additional open question is how communication within the proposed networks is facilitated. It has been proposed that phase synchrony facilitates communication between distributed cortical areas during memory encoding (Fell & Axmacher, 2011) and a previous study has shown that interactions between MTL and cortex during memory retrieval are reflected in coherent theta networks (Watrous, Tandon, Conner, Pieters, & Ekstrom, 2013). Therefore phase synchrony might be a possible mechanism. Indeed, in study 1, encoding using an especially efficient encoding task led to increases in alpha/beta phase synchrony. Another possible index of encoding related networks might be inter-areal correlation of power, for example common fMRI resting state networks are reflected by inter-areal power-to-power correlations (Brookes et al., 2011; Hipp & Siegel, 2015). These possible mechanisms of interaction in the proposed alpha/beta and theta networks remain to be investigated.

A possible candidate for interaction between these perceptual, semantic and episodic systems might also be correlations between frequencies, for example a correlation of alpha/beta decreases and theta decreases or in the form of amplitude-phase coupling (Canolty et al., 2006). Coupling of theta phase with local gamma power has been reported in context memory in rodents (Tort, Komorowski, Manns, Kopell, & Eichenbaum, 2009) and humans (Staudigl & Hanslmayr, 2013). Furthermore, phase-power relationships have been postulated as a special coding principle. A theta-gamma code has first been proposed in working memory and MTL functions (Lisman & Idiart, 1995; Lisman & Jensen, 2013). Extensions of this low frequency phase to high frequency gamma power code have been hypothesized for alpha and gamma in visual processing (Jensen, Gips, Bergmann, & Bonnefond, 2014; Roux & Uhlhaas, 2014) and across several frequency combinations as a general code of cortical representations and memory encoding (Watrous et al., 2015). The presented results suggest a relation of local gamma power and alpha/beta decreases and additionally an interaction between cortical alpha/beta oscillations and MTL based theta oscillations. These possible interactions between the proposed networks remain to be investigated.

## LOW FREQUENCY DECREASES AS MARKER OF NEURAL ACTIVITY

Another interesting pattern in the presented data is the observation of low frequency, i.e. theta, alpha and beta power decreases in areas usually showing fMRI BOLD increases. In study 1 we found alpha/beta decreases during semantic encoding, a task that previously has been related to left IFG increases (Kapur et al., 1994; Otten & Rugg, 2001b). In study 2, theta power decreases were found in areas that showed BOLD increases during the same paradigm. Additionally, increases in alpha/beta power were related to decreases in BOLD, suggesting a general negative relationship of low frequency oscillatory power and BOLD signals. In study 4, again, alpha/beta decreases were found related to face and word processing in areas that typically exhibit BOLD activity increases. Also, theta power decreases were found during memory formation localized to areas matching fMRI encoding networks. This pattern of results demonstrates that low frequency power decreases might be generally related to activity increases in the brain, which also been demonstrated in previous studies (Hermes et al., 2014; Mukamel et al., 2005; Niessing et al., 2005; Scheeringa et al., 2011; Zumer, Scheeringa, Schoffelen, Norris, & Jensen, 2014). This general match of power decreases and BOLD activity suggest a vital role of reduced oscillatory power/ amplitudes in the low-frequency range for cortical processing.

### *OPEN QUESTIONS AND LIMITATIONS: FUNCTIONAL RELEVANCE OF LOW FREQUENCY POWER DECREASES*

An open question remains: How are power decreases related to neural processing? Considering power increases, there seems to be an easy connection to cortical processing: increases in neural synchrony synchronize neural firing and thereby enhance information transfer between two cortical regions (Fries, 2005; Varela et al., 2001). This synchronized firing strengthens synaptic connections and thereby a durable memory trace is encoded (Fell & Axmacher, 2011). The functional relevance of power decreases eludes such a simple explanation. However, first and foremost, communication through power increases might be rather inflexible, considering that thousands of neurons need to spike in synchrony to produce a power increase on scalp level (Hämäläinen, Hari, Ilmoniemi, Knuutila, & Lounasmaa, 1993). In a quite intuitive manner we argued in a recent review that a desynchronized firing pattern from a information theoretic view is able to code more information than synchronized firing pattern (Hanslmayr, Staudigl, et al., 2012). The idea of a temporal correlated oscillatory code in neural systems has been criticized since its inception (Shadlen & Movshon, 1999). For example, the impact of a spiking neuron in the absence of spiking of other neurons transfer more information than numerous neurons spiking synchronized (Schneidman et al., 2011).

Another assumption is that power decreases measured by using the available measurement methods ranging from EEG to intracranial recordings might only represent an epiphenomenon and not a functional important neural computation principle. However, even if these power decreases are only the "dark side of the moon", these decreases still have been proven a stable marker of neural activity, in the presented studies and in other studies. For instance, fMRI BOLD activity is by definition only an epiphenomenon of neural activity and albeit this "mere" epiphenomenal relationship to neural activity, fMRI studies have contributed crucially to the knowledge we hold today about the human brain functions.

However, the wealth of studies reporting correlations of behavior and cognition with oscillations and theoretical considerations (Buzsaki & Draguhn, 2004) speak against the notion that brain oscillations are a mere epiphenomenon without functional value. However, initial hypotheses especially about the function of power increases during memory formation might have been incorrect, as indeed at least in the low frequency range power decreases are correlated with neural activity, as for example measured by fMRI (Hermes et al., 2014; Mukamel et al., 2005; Niessing et al., 2005; Scheeringa et al., 2011; Zumer et al., 2014).

A major open question is still how desynchronization can enable neural communication, the basic mechanism need for encoding information (Hebb, 1949). One possibility is that decreases in power are needed in order to form fine-grained connected networks capable of representing specific representations. For example the sparse coding of information in the MTL, where single neurons can represent very specific modality independent information (Quiroga, Kreiman, Koch, & Fried, 2008; Quiroga, Reddy, Kreiman, Koch, & Fried, 2005), shows that specific neurons seem to receive very specific input from widespread areas from across the cortex. It has been shown that alpha power decreases are related to increased long range phase synchrony (Popov et al., 2013; Weisz et al., 2014), a mechanism that might enable such specific input. Considering theta power decreases, such a relationship remains to be shown. Such a relationship of power and long range connectivity increases might yielding a balance between cortical integration and separation (Deco, Tononi, Boly, & Kringelbach, 2015) and thereby provide a flexible mechanism of neural representation and computation.

## THE CONCEPT OF THE SUBSEQUENT MEMORY EFFECT

### *LIMITATIONS OF SUBSEQUENT MEMORY EFFECTS*

A more general critique of the presented data is the encoding-centric view of subsequent memory analyses. By definition successful memory encoding at least encompasses encoding *and* retrieval and also the processes in between. Subsequent remembrance is not exclusively depending on processing during encoding, for example also the match of the retrieval context to the encoding context is important (Godden & Baddeley, 1975; Morris, Bransford, & Franks, 1977; Staudigl & Hanslmayr, 2013; Tulving & Thomson, 1973) and consolidation processes between encoding and retrieval can shape memory (Nadel & Moscovitch, 1997; Nadel et al., 2000). However, as the presented work is focused on encoding processes and the correlates of manipulating encoding, these effects are not considered in the present studies. Other studies have focused on the overlap in encoding and retrieval and reported reactivation of encoding related activity during memory retrieval (Jafarpour, Fuentemilla, Horner, Penny, & Duzel, 2014; Jafarpour, Horner, Fuentemilla, Penny, & Duzel, 2013; Staudigl et al., 2015; Wimber, Maass, Staudigl, Richardson-Klavehn, & Hanslmayr, 2012). In regard to this line of research the presented results are also an important contribution to research on reactivation, as the presented studies yield a more precise definition of encoding related activity that possibly might be reactivated. Namely, the presented results of material and encoding dependent alpha/beta effects suggest that reactivation effects are most likely to be found in the alpha/beta frequency range. Indeed, previous studies have reported alpha/beta decreases depending on the encoded material during retrieval (Khader, Heil, & Rosler, 2005; Waldhauser et al., 2012).

Subsequent memory effects are also limited by the subtraction logic: memory formation equals later remembered minus later forgotten activity. As mentioned above, subsequent memory is not only dependent on encoding operations but also determined by retrieval. For example, the context during retrieval, general attention level or individual response biases influence retrieval performance (Yonelinas, 2001). Furthermore, the measurement of successful retention is an additional problem. In the presented studies, recognition tests and free recall tests were used as memory measures. Free recall and recognition tests measure in some respects different memory processes (Ranganath, 2010; Tulving & Thomson, 1973; Yonelinas, 2001). Also recognition tests are not "process-pure". For example, in recognition tests, items might be correctly labeled as seen before because of familiarity and not because of a detailed autonoetic episodic memory trace. A previous study has reported differences in oscillatory SMEs between recognition tests and free recall (Merkow, Burke, Stein, & Kahana, 2014). However, note that in

the presented studies comparable correlates of memory encoding were found in recognition (study 1 & 4) and free recall (study 2). Albeit, the impact of the retrieval test on material and processing dependent SMEs was not explicitly investigated and remains an open question.

### *ARTIFACTUAL MEMORY ENCODING EFFECTS IN EEG-FMRI*

In study 3, spurious SMEs in simultaneous EEG-fMRI are reported. Small event-related motion was correlated with successful remembering. The magnetic field of the MR scanner can be considered as an amplifier of the effects of such small movements on EEG by the physical principle of electromagnetic induction. Those specific effects are therefore limited to the scanner environment and probably do not affect non-simultaneously recorded data. However, one of most probable causes of this effect is respiration phase locked to stimulus presentation. A similar stronger phase locking of respiration to subsequently remembered in contrast to later forgotten trials has been reported before in fMRI (Huijbers et al., 2014). Such a relationship between physiological signals and performance is nothing new. For example, eye movements have been shown to index memory retrieval (Hannula & Ranganath, 2009). Cardiac activity has been shown to predict visual detection performance and also to correlate with MEG activity (Park, Correia, Ducorps, & Tallon-Baudry, 2014). Although to date still highly speculative, it might be wrong to neglect correlations between cognitive performance, physiology and neural activity. Emerging theories propose that these neural-physiological correlations might have a vital role in neural processing (Klimesch, 2013; Park & Tallon-Baudry, 2014). Especially, memory formation as a process that depends on how the internal state of the system encodes sensory information might be especially prone to be affected by the physiological state of the system.

# CONCLUSION

In the present work the influence of encoding tasks and material on oscillatory memory encoding effects have been investigated. Reliable spectral fingerprints of memory encoding have been found. Decreases in alpha/beta power and increase in gamma power during memory formations have been demonstrated to vary with encoding task and material and are potential linked to semantic processing and representations of specific features. Decreases in theta power co-occur with MTL activity increases and index memory encoding irrespective of to-encoded material and encoding tasks. These theta decreases therefore do reflect specific memory related binding processes. These results demonstrate that oscillatory activity during memory encoding indexes activity in separable neural networks. An open question remains how these systems interact in order to form a durable memory trace.

# STUDY 1: BRAIN OSCILLATORY SUBSEQUENT MEMORY EFFECTS DIFFER IN POWER AND LONG-RANGE SYNCHRONIZATION BETWEEN SEMANTIC AND SURVIVAL PROCESSING

Memory crucially depends on the way information is processed during encoding. Differences in processes during encoding not only lead to differences in memory performance but also rely on different brain networks. Although these assumptions are corroborated by several previous fMRI and ERP studies, little is known about how brain oscillations dissociate between different memory encoding tasks. The present study therefore compared encoding related brain oscillatory activity elicited by two very efficient encoding tasks: a typical deep semantic item feature judgment task and a more elaborative survival encoding task. Subjects were asked to judge words either for survival relevance or for animacy, as indicated by a cue presented prior to the item. This allowed dissociating pre-item activity from item-related activity for both tasks. Replicating prior studies, survival processing led to higher recognition performance than semantic processing. Successful encoding in the semantic condition was reflected by a strong decrease in alpha and beta power, whereas successful encoding in the survival condition was related to increased alpha and beta long-range phase synchrony. Moreover, a pre-item subsequent memory effect in theta power was found which did not vary with encoding condition. These results show that measures of local synchrony (power) and global long range-synchrony (phase synchronization) dissociate between memory encoding processes. Whereas semantic encoding was reflected in decreases in local synchrony, increases in global long range synchrony were related to elaborative survival encoding, presumably reflecting the involvement of a more widespread cortical network in this task.

## INTRODUCTION

Memory is crucially shaped by the way information is processed during encoding (Craik & Lockhart, 1972). This impact of varying encoding tasks on later memory performance has been known for decades and is a defining part of several theoretical and functional frameworks of memory (Craik & Lockhart, 1972; Fuster, 1997; Morris et al., 1977; Tulving & Thomson, 1973). However, little is known about the underlying neural mechanisms of successful memory formation in different encoding tasks. The neural correlates of successful memory formation can be investigated with the so-called Subsequent Memory Paradigm. In this paradigm, neural activity during encoding is contrasted between items that are later remembered and items that are later not remembered. Subsequent Memory Effects (SMEs) have been investigated by numerous fMRI, ERP, and brain oscillation studies (Hanslmayr, Staudigl, et al., 2012; Paller & Wagner, 2002), but only few have investigated the impact of different encoding tasks on SMEs. In line with the process view of memory encoding, several neuro-cognitive studies found dissociable SMEs in different encoding tasks (Hanslmayr et al., 2009; Otten & Rugg, 2001a, 2001b; Schott et al., 2013).

However, the interpretation of the results is to some degree limited as these studies typically contrast a shallow encoding task, usually focused on some alphabetical or phonological feature, with a deep, semantic encoding task, that requires the processing of an item in regard to a single semantic feature (e.g. animacy). These tasks do not only differ in their amount of phonological or semantic processing, but also in other respects, for example in encoding efficiency. As semantic encoding leads to higher subsequent memory than shallow encoding, the reported effects may not specifically reflect semantic feature processing, but also efficient memory processing. To clarify this issue, SMEs elicited by semantic feature processing have to be contrasted with SMEs elicited by other equally efficient, or even more efficient encoding tasks. Encoding strategies that promote higher memory performance than semantic feature judgment are usually intentional tasks, that involve usage of more complex strategies like organizing material, mental imagery or mnemonic systems (for review of effective encoding strategies Worthen and Hunt (2008).

An incidental encoding task (i.e. the subjects do not know of a later memory test) that promotes very high memory performance and involves a similar judgment procedure as typical semantic encoding tasks, is the survival processing task (Nairne et al., 2007). During survival encoding, subjects are asked to imagine being stranded in a foreign land without basic supplies and their task is to rate presented items for relevance in such a scenario. Judging items for their

survival value results in superior memory compared to several other efficient encoding tasks, including semantic processing (Nairne & Pandeirada, 2008). Survival processing was first introduced as an effective encoding strategy based on special adaption of memory to survival related information (Nairne et al., 2007). Following research suggested that the effectiveness of survival processing can be explained by the utilization of several proximate encoding mechanisms (Howe & Otgaar, 2013). Survival processing is regarded to rely less on semantic item-specific processing, but more on relational processing of the items (Burns et al., 2011). Further, it has been shown that survival processing also relies on the richness and distinctiveness of the encoding context (Kroneisen & Erdfelder, 2011). On a neural level this elaborative encoding process might be reflected in increased engagement of widespread cortical networks.

A measure of cortical communication in cortical networks is brain oscillatory activity (Fries, 2005). Brain oscillations are assumed to be involved in memory formation as they enable communication within local and distant cortical cell assemblies and thereby shape synaptic plasticity (Buzsaki & Draguhn, 2004; Fell & Axmacher, 2011). Oscillatory activity recorded by scalp electrodes is a tool to measure memory related changes in local and global communication. Thereby, phase synchrony between electrodes indicates synchrony between distant cell assemblies enabling more global communication, whereas oscillatory power presumably reflects the amount of local synchrony in a cell assembly measured by an electrode (Lachaux, Rodriguez, Martinerie, & Varela, 1999; Varela et al., 2001).

Several studies investigated changes in oscillatory power related to successful memory formation (Axmacher, Mormann, Fernandez, Elger, & Fell, 2006; Duzel et al., 2010; Hanslmayr, Staudigl, et al., 2012; Klimesch, Freunberger, Sauseng, & Gruber, 2008). The typical findings in these studies are positive theta (4–8 Hz) and gamma (>40 Hz) power SMEs, i.e., increases in power for subsequently remembered compared to subsequently forgotten items during item processing (Klimesch et al., 1997; Osipova et al., 2006; Summerfield & Mangels, 2005). A different picture arises in the alpha (8–12 Hz) and beta (12–30 Hz) frequency range in which negative SMEs are usually observed, i.e., decreases in alpha and beta power for remembered vs. forgotten items (see Hanslmayr, Staudigl, et al. (2012); for a review).Recently, successful memory encoding has not only been related to effects during item presentation, but also to oscillatory activity preceding item presentation. For instance, positive pre-stimulus theta SMEs have been reported before the successful encoding of an item (Fell et al., 2011; Gruber, Watrous, Ekstrom, Ranganath, & Otten, 2013; Guderian et al., 2009). In addition to these memory related

changes in power, several studies found a positive relationship between long range phase synchronization in different frequency bands and memory encoding (Bauml, Hanslmayr, Pastotter, & Klimesch, 2008; Fell et al., 2001; Hanslmayr, Volberg, et al., 2012; Summerfield & Mangels, 2005; Weiss & Rappelsberger, 2000).

Whether and how these brain oscillatory SMEs vary with encoding tasks is still unknown. To the best of our knowledge, only one prior study compared brain oscillatory SMEs in a shallow, alphabetical task, and a deep, semantic feature judgment task (Hanslmayr et al., 2009). The results showed that the negative SMEs in alpha and beta power were specifically obtained in the semantic feature condition, but not in the shallow encoding condition (Hanslmayr et al., 2009). In contrast, positive SMEs in theta power were specifically obtained in the shallow, but not in the semantic encoding condition, suggesting that alpha/beta power decreases specifically reflect semantic feature memory encoding. However, as explained above, semantic and non-semantic encoding tasks differ not only in the level of semantic processing, but also in encoding efficiency. Therefore these results could also reflect efficient encoding instead of semantic encoding.

To investigate the question of whether two efficient encoding tasks lead to dissociable brain oscillatory SMEs and to further elucidate the role of global and local synchrony in memory formation, the present study compares brain oscillatory SMEs elicited by a classical semantic encoding task with the more elaborative survival processing task. Subjects judged words during encoding either for survival relevance (survival task) or for animacy (semantic task). A colored fixation cross was presented 1000 ms before item presentation as encoding task cue (Fig. 1A) to dissociate item-related encoding processes from pre-item encoding processes. If alpha/beta power decreases specifically reflect semantic feature processing, and not efficient encoding in general, similar results as reported by Hanslmayr et al. (2009) should arise when comparing semantic feature processing with the more efficient survival encoding. The putative more complex processing during the survival judgment might engage a more widespread cortical network, which should be reflected by increases in long range phase synchrony between distant electrodes (PLV). In addition, we aimed to replicate the positive SME in theta power preceding item presentation, and to clarify whether this pre-item effect dissociates between the two encoding tasks (Gruber & Otten, 2010; Otten, Quayle, Akram, Ditewig, & Rugg, 2006).

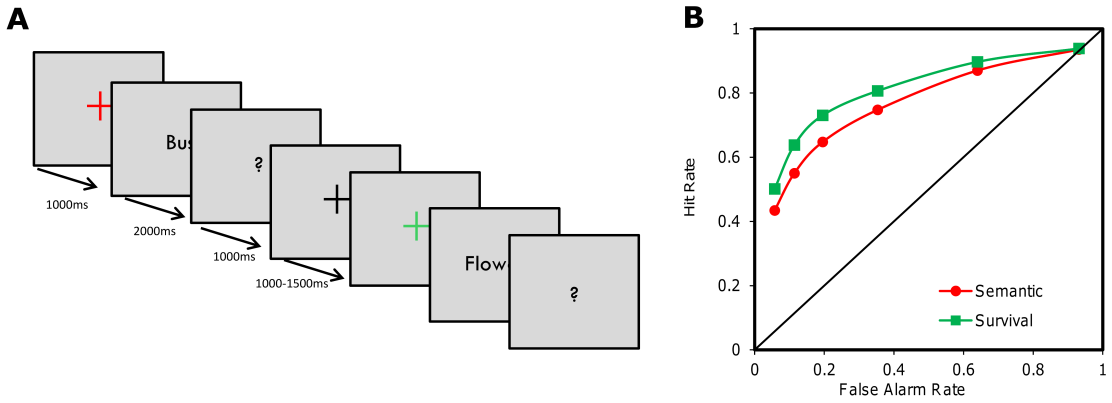


**Figure 1**. (A) Experimental procedure: Subjects performed an incidental encoding task judging words randomly intermixed for survival relevance and animacy on a scale from 1 to 6. Which encoding task should be performed, was indicated by a colored fixation cross preceding the item, allowing dissociating pre-item task related activity from item-related activity. (B) Memory performance for both conditions is shown by means of item recognition ROCs. Hit (y-axis) and false alarm rates (x-axis) are depicted for the semantic and survival condition. Hit and false alarm rates were obtained by cumulating responses over confidence ratings, starting with the sure old confidence rating. Recognition performance was significantly higher for words encoded in the survival condition than in the semantic condition.

## MATERIAL AND METHODS

### *SUBJECTS*

18 healthy volunteers participated in the experiment. Data from two subjects were excluded because total trial number was less than 14 trials in one of the conditions. All of the 16 participants included in data analysis were students aged between 20 and 28 years (M = 23.75, SD = 2.24). Five of them were male and one of them was left-handed. They reported no history of neurological or psychiatric diseases, had normal or corrected to normal vision and were native German speakers. All subjects received 20 € compensation or course credit for participation. Participants signed informed consent at the beginning of the experiment.

### *MATERIAL*

All items were randomly chosen from CELEX Database (Baayen, Piepenbrock, & van H, 1993). Words were neither specifically related to animacy nor survival. Three word lists containing 150 words each were constructed. Across lists the words were matched according to word frequency, word length and for survival and animacy relatedness. Across subjects word material was counterbalanced, as each list was used equally often in the semantic encoding condition, survival encoding condition and as new words during recognition. Sequence of words and conditions was randomized for each subject. Additionally, twenty randomly chosen words were used during the practice phase.

### *PROCEDURE*

Each subject was tested individually in a quiet surrounding seated in front of a PC screen. The experiment consisted of an encoding phase, a distractor phase and a recognition phase.

At the beginning of the encoding phase participants received a printed instruction containing the semantic and survival task instructions. In the semantic task condition they were instructed to judge words if they are animated or are related to something animated. Subjects were instructed to give subjective ratings on a six point scale. This graded response was applicable as some words were not specifically animated or unanimated (e.g. harmony). The survival task instruction was a German translation of the survival processing strategy proposed by Nairne et al. (2007): "In this task we would like you to imagine that you are stranded in the grasslands of a foreign land, without any basic survival materials. Over the next few months, you'll need to find steady supplies of food and water and protect yourself from predators. We are going to show you a list of words, and we would like you to rate how relevant each of these

words would be for you in this survival situation. Some of the words may be relevant and others may not — it's up to you to decide."

They received no information about the following memory test and they received no instruction to memorize the words. Participants were especially reminded to switch between encoding conditions and to give a response on each trial. The experiment started with a practice phase consisting of twenty items to familiarize the participants with the judgment and response process and to check if the subjects had understood the instructions. During encoding participants judged 150 items for survival value and 150 items for animacy. The sequence of semantic and survival trials was randomized. Each trial started with a fixation cross presented for a variable time (1000–1500 ms) followed by a colored fixation cross, the encoding task cue, presented for 1000 ms, indicating whether the following item should be judged for animacy or survival. The color of the encoding task cue was counterbalanced across subjects. After the cue, the to-be-judged word was presented for 2000 ms. Subjects were instructed not to respond until a question mark appeared after 2000 ms to avoid contamination of movement related activity. Subjects then indicated their survival or animacy judgment using a one to six scale on a computer keyboard in front of them. The assignment of the keys was counterbalanced across subjects. The whole encoding phase lasted for ca. 25 min with a variable pause after half of the trials.

The encoding phase was followed by a distractor task in which subjects discriminated high and low tones for ten minutes. Afterwards participants received the instructions for the surprise recognition test. During the recognition phase 300 words, which were shown in the encoding phase, were presented again, randomly mixed with 150 new words. Subjects gave recognition confidence judgments using the same response buttons from 1 to 6 as during the encoding task. Subjects were instructed to use the extreme points of the scale for very sure old and very sure new judgments and the intermediate points as varying levels of uncertainty. Subjects were especially reminded to use the whole scale according to their subjective recognition and to answer on each trial. A trial during recognition consisted of a fixation cross presented for variable duration (1000–1500 ms) and the word presented for 2000 ms, followed by a question mark requesting a response. The recognition phase lasted for about 35 min.

### *ELECTROPHYSIOLOGICAL RECORDING*

During encoding, distractor and recognition phase, the EEG was recorded from 61 equidistant active electrodes (ActiCAP, Montage 10, Brain Products, Gilching, Germany). Impedances were kept below 20 kΩ. Signals were recorded with a sampling rate of 500 Hz and

amplified between 0.15 and 100 Hz with a notch filter at 50 Hz to remove line noise (BrainAmpMR plus, BrainVision Recorder, Brain Products, Gilching, Germany). The EEG was initially recorded against a reference electrode placed at FCz and was later rereferenced against average reference.

### *BEHAVIORAL DATA*

Behavioral data was analyzed utilizing a modeling approach to obtain bias free measures of memory strength. A single process unequal variance model was used, as it provided a good fit to recognition data in other studies (Dunn, 2004; Spitzer & Bauml, 2007; Wixted, 2007).

This model assumes that recognition is based on a single process, which represents memory strength. Memory strength can be modeled using signal detection theory (for details, see Macmillan and Creelman (1991). It is assumed that the probabilities of old and new words eliciting a certain memory strength can be modeled using normal distributions, with the distribution of new words set to N(0,1) and the mean d′ and standard deviation **σ** of the distribution of the old items varying freely according to the data. d′ in this model can be interpreted a measure of memory performance. The model assumes that subjects respond with a certain confidence rating i, whenever their subjective memory strength exceeds a certain criterion ci (see supplemental figure 1). The parameters (d′, c1–c5, **σ**) were estimated from the data utilizing a maximum likelihood procedure. This procedure also yields a $\chi$2-distributed G2 statistic to test the goodness of fit of the assumed model (for more details and specific equations see Spitzer and Bauml (2007). For each condition and each subject parameters were estimated separately. In order to compare recognition performance, nonparametric Wilcoxon signed-rank tests were used to compare d′ in the semantic and survival condition.

### *EEG*

Data was analyzed using MATLAB (The Mathworks, Inc., Munich, Germany), in-house MATLAB scripts, and FieldTrip (http://www.ru.nl/neuroimaging/fieldtrip), an open-source Matlab toolbox developed at the Donders Institute for Brain, Cognition, and Behaviour (Nijmegen, The Netherlands) Oostenveld, Fries, Maris, and Schoffelen (2011).

Hits and misses were classified using the recognition confidence ratings. In contrast to binary yes/no ratings, confidence ratings provide a more fine grained scale of memory performance that allow classifying hits and misses independent of individual response bias. To enhance signal to noise ratio for analyzing SMEs only words receiving the highest confidence

rating were classified as hits (Otten et al., 2006; Otten & Rugg, 2001a, 2001b) for a similar trial definition).

To classify misses, the same signal detection theory approach was used as for analyzing behavioral memory performance. For each subject single process unequal variance models were fitted irrespective of encoding condition to obtain individual criterion measures ci for each confidence rating i. The location of these criteria ci relative to the neutral criterion represents the response bias of a certain rating i. The neutral response criterion represents the criterion with zero bias. A criterion ci that is lower than the neutral criterion indicates that rather low memory strength is necessary for a subject to use this rating i. The assumed underlying memory strength of such a rating i is more likely elicited by a new word than old word. Consequently an old word receiving such a rating i elicits a feeling of remembering similar to a completely new word and thus it can be assumed that most words receiving this rating i were not successfully encoded (the underlying model is illustrated in supplemental figure 1). Accordingly, misses were classified by the relative position of the estimated criterion ci of the given confidence rating i to the neutral response criterion.

The location of this neutral criterion was calculated for each subject. A rating i was classified as miss if the corresponding estimated criterion ci was less than the criterion nearest to the neutral criterion (the same approach was used by Hanslmayr et al. (2009). This approach is further illustrated in the supplementary material (see supplemental figure 1). For seven subjects the ratings from 3 to 6 were classified as misses, for another seven subjects ratings from 4 to 6 and for two subjects' ratings from 2 to 6. This procedure was utilized to enhance signal to noise ratio, as misclassification of misses is minimized. We showed this by calculating SMEs using a fixed criterion for the classification of misses instead of individual one. Using a fixed criterion effectively reduced the number of miss trials for 9 subjects. This led to a decrease from on average 41 miss trials to 35 trials per condition. All effects and topographies remained qualitatively similar (see supplemental figure 2). However, the effects were slightly decreased showing that a fixed criterion decreased the signal-to-noise ratio of the oscillatory memory effects.

Before analysis the EEG was segmented in epochs from 2500 ms preceding word onset to 2500 ms after word onset. The EEGs were corrected for blinks and eye movements, using Independent Component Analysis. Remaining artifacts, due to muscle activity or poor EOG correction, were excluded by careful visual inspection. Mean trial number for semantic hits was

61 (ranging from 25 to 117), for semantic misses 48 (ranging from 26 to 83), for survival hits 70 (ranging from 23 to 129), and for survival misses 36 (ranging from 14 to 73).

For time–frequency power analysis the EEG epochs were subjected to a Gabor transformation, which transforms a signal into a complex time–frequency signal, from which the power information can be extracted. The data were filtered in a frequency range of 1–30 Hz and for 30–100 Hz. The filter parameter for time–frequency resolution (gamma) was set to 1 for the lower frequencies and to 2pi for the higher frequencies, to accommodate for the different time frequency characteristics in the lower and higher frequency bands. Power values were calculated for each single trial, and averaged across trials within the four conditions (later remembered, later forgotten for semantic and survival processed items). These power values were then baseline corrected using a 500 ms baseline interval preceding task cue onset. The resulting power values represent percentage signal change with respect to that baseline (Pfurtscheller & Aranibar, 1977).

For long range phase synchrony analysis the EEG epochs were first current source density transformed and then phase locking values (PLV; see Lachaux et al. (1999) for details) were calculated for each possible electrode pair, but excluding neighboring pairs, in time–frequency bins of 50 ms and 1 Hz using FieldTrip. Current source density transformation was carried out to diminish the effect of volume conduction on phase synchrony (Lachaux et al., 1999; Nunez et al., 1997). High PLVs indicate a high consistency in phase differences between an electrode pair across trials. Hence PLV is a measure of global synchronization and global communication. As unequal trial numbers influence phase measures, PLVs were calculated on a subsample of trials containing as many trials as the condition with the least trials. E.g., if one subject had only 20 semantic misses, then PLVs for all other conditions for this subject were calculated only for a randomly selected subsample of 20 trials. In order to not produce a bias because of the random selection of such a subsample of trials, PLVs for each condition were calculated for 100 randomly selected sets of trials (e.g. 100 times 20 trials were randomly selected) for each condition and then averaged.

For statistical analysis of time–frequency data and PLVs a nonparametric two stage randomization process was used to minimize influences from outliers and to account for multiple testing (Blair & Karniski, 1993). At a first level, Wilcoxon signed rank tests were used to assess, which and how many electrodes/electrode pairs exhibit a significant difference between conditions for a time–frequency window of interest. The threshold for significance was set to 0.05 for power values and to 0.005 for PLVs. A higher threshold was used for PLVs

because of the high number of statistical comparisons. Then, to correct this result for multiple comparisons a permutation test was used. The test used 1000 permutation runs shuffling the assignment of the conditions randomly for each subject. After each run a Wilcoxon signed rank test was calculated returning the number of electrodes/ electrode pairs showing a significant difference between the randomly assigned conditions. After 1000 permutation runs this procedure yields a distribution of the number of significant electrodes in a sample with randomly assigned conditions. This distribution then constitutes an approximation of the probability distribution under the null hypothesis. A significant difference between conditions is indicated, if the number of electrodes/electrode pairs showing a significant difference between the two conditions is less likely than pcorr = 0.05 according to the generated distribution. This procedure therefore effectively controls for type-I errors due to multiple testing and was applied in several previous studies from our lab, investigating power (Hanslmayr et al., 2009) and phase synchrony (Hanslmayr et al., 2007; Hanslmayr, Volberg, et al., 2012).

To assess if subsequent memory effects (hit–miss) differed significantly between semantic and survival encoding, differences of hits and misses for power values and PLVs were calculated in both conditions. These differences were then compared using the same nonparametric randomization procedure for the time–frequency windows in which SMEs were found in one of both conditions. This comparison is equivalent to a two-way ANOVA interaction analysis.

## RESULTS

### *BEHAVIORAL RESULTS*

For the ROC analysis the hit and false alarm rates were cumulated over the five criterion points, starting with the highest confidence rating. By plotting cumulated false alarm rates against cumulated hit rates ROC curves are obtained, which illustrate recognition performance. The closer the ROC curve is to the left upper corner of the graph, the higher is the recognition performance. ROCs for both encoding conditions are presented in Fig. 1B. Single process unequal-variance signal detection models were fitted to the data for every subject and every condition to obtain individual memory performance parameters. In order to evaluate the goodness of fit to our data $\chi 2$-tests were carried out. The signal detection model fit the data of all subjects adequately as indicated by non significant maximum likelihood tests (all ps > 0.28). Recognition performance d′ in both conditions was very high. However, in the survival

condition d′ was significantly higher than in the semantic condition (d′: 2.03 vs. 1.57; $Z = -3.15$; $p < 0.005$).

To control for rating during encoding as potential confounding factor, the mean ratings for hits and misses for each condition were calculated. A two-way ANOVA was carried out on the mean ratings with the factors encoding condition (semantic vs. survival) and subsequent memory (hit vs. miss). A significant main effect for subsequent memory ($F(1,15) = 6.36$, $p<0.05$) was obtained, which was due to subsequent hits receiving higher ratings during encoding than misses. However, and most importantly, no main effect of encoding condition ($F(1,15) = 0.01$, $p > 0.9$) and no significant interaction effect between encoding conditions and subsequent memory emerged ($F(1,15) = 1.07$, $p > 0.3$). This shows that differences found in SMEs between conditions are not confounded by differences in ratings during encoding.

Additionally, reaction time data during encoding was analyzed. Subjects were not allowed to respond until 2 s after word presentation onset (see Fig. 1A). Thus, to analyze reaction time the median reaction time between rating button press and question mark presentation was calculated for each subject and condition. A two-way ANOVA was carried out on the mean RTs with the factors encoding condition (semantic vs. survival) and subsequent memory (hit vs. miss). A significant interaction effect was found ($F(1,15) = 4.99$, $p < 0.05$). This interaction effect was due to a significant difference between hits and misses in the semantic condition (482 ms vs. 538 ms, $T = -2.35$; $p < 0.05$), that was not evident in the survival condition (493 ms vs. 487 ms, $T = 0.56$). There was no significant main effect of encoding condition ($F(1,15) = 1.52$, $p > 0.2$).

### *OSCILLATORY POWER*

Following previous work (Hanslmayr et al., 2009), time frequency data was analyzed in the theta (5–8 Hz), alpha (8–12 Hz), beta1 (15– 19 Hz) and beta2 (23–28 Hz) frequency range. In a first step, significant differences between hits and misses (SMEs) were identified for each condition separately. Then, differences between these SMEs were contrasted for time frequency windows, in which SMEs were found. The time–frequency diagrams of SMEs averaged over all electrodes are depicted in Fig. 2, separately for the two encoding conditions, showing clusters of significant time–frequency bins in the theta, alpha, and beta frequency range. SMEs were also analyzed in the gamma frequency range (30–100 Hz). However, no significant effects were found in this frequency band.

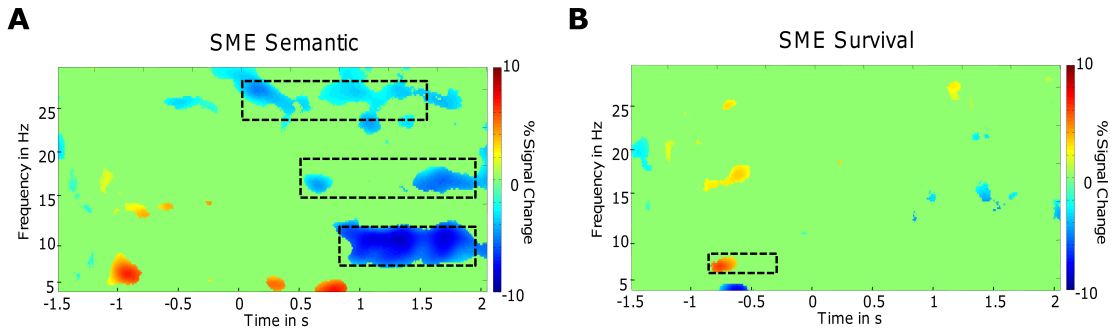


**Figure 2.** Time-frequency plots of oscillatory SMEs averaged across all electrodes for (A) semantic encoding and (B) survival encoding. Time-frequency bins showing no significant differences as obtained by non-parametric Wilcoxon tests comparing hits and misses for each time-frequency bin are masked in green. Red/blue indicates more/less power for hits than misses, respectively. Time-frequency windows, in which significant SMEs were found, are highlighted in dashed boxes.

In the semantic encoding condition, SMEs were found after item presentation in the alpha, beta1, and beta2 frequency range (see Fig. 2A). Semantic hits were related to a more pronounced alpha power decrease than semantic misses (800–2000 ms, 8–12 Hz, pcorr < 0.001, see Fig. 3A). This effect showed a widespread topography involving frontal, parietal, and occipital electrodes. Successful later remembering was also related to a beta1 power decrease (300–2000 ms, 15–19 Hz, pcorr < 0.05, see Fig. 3B) at central and posterior electrodes, and a decrease in beta2 power (0–1500 ms, 23–28 Hz, pcorr < 0.001, see Fig. 3C) at posterior electrodes.

In the survival encoding condition, a significant difference between hits and misses was only found related to the task cue in the theta frequency range −900 to −300 ms before item presentation (5–8 Hz, pcorr < 0.05, see Figs. 2B and 3D) at central and left parietal electrodes. Later remembered survival processed words elicited a stronger theta power increase than later forgotten words in this pre-item interval. Significant SMEs after item presentation were not evident in any frequency band.

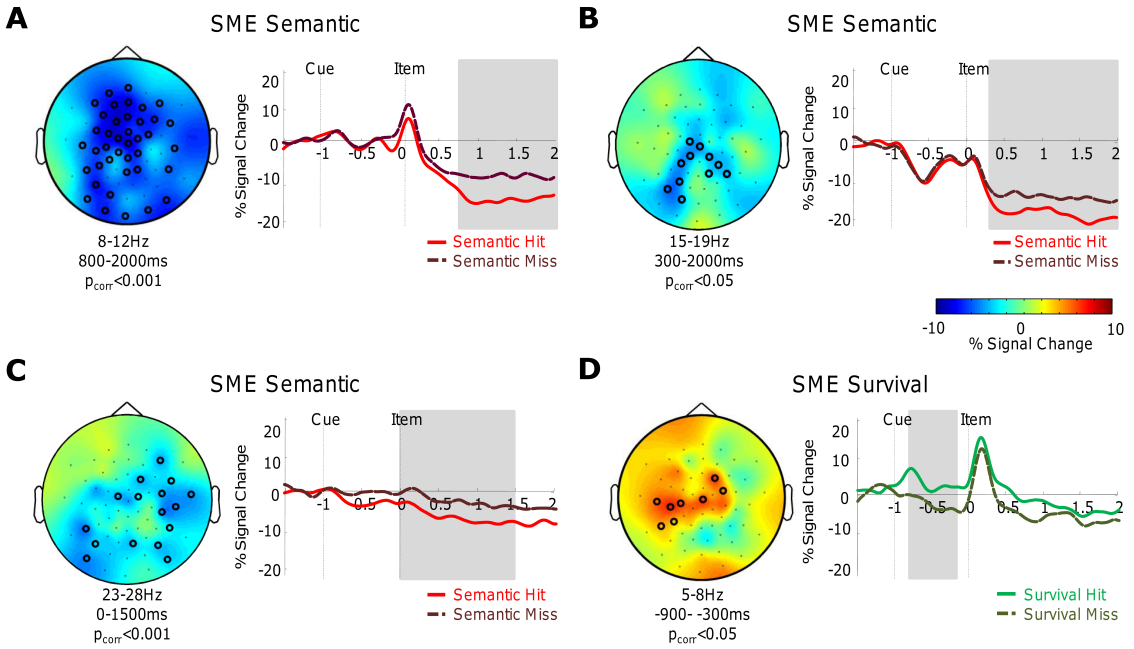


**Figure 3.** Oscillatory power subsequent memory effects (SMEs) are shown for both conditions separately. (A) In the semantic processing condition a negative SME was found in alpha power (8-12Hz) from 800-2000 ms post item presentation; (B) in beta1 power (15-20Hz) 300-2000 ms post item presentation, and (C) in beta2 power (23-29Hz) 0-1500 ms post item presentation. (D) In the survival encoding condition subsequently remembered words were associated with a theta power (5-8Hz) increase in the pre-item interval (-900-300ms). Circles in the topography plots highlight significant electrodes. Red/blue indicates more/less power for hits than misses, respectively. Time courses of power increases/decreases for hits and misses collapsed across all electrodes that showed significant SMEs are depicted on the right for the respective time-frequency window. Time windows of significant SMEs are highlighted by grey boxes.

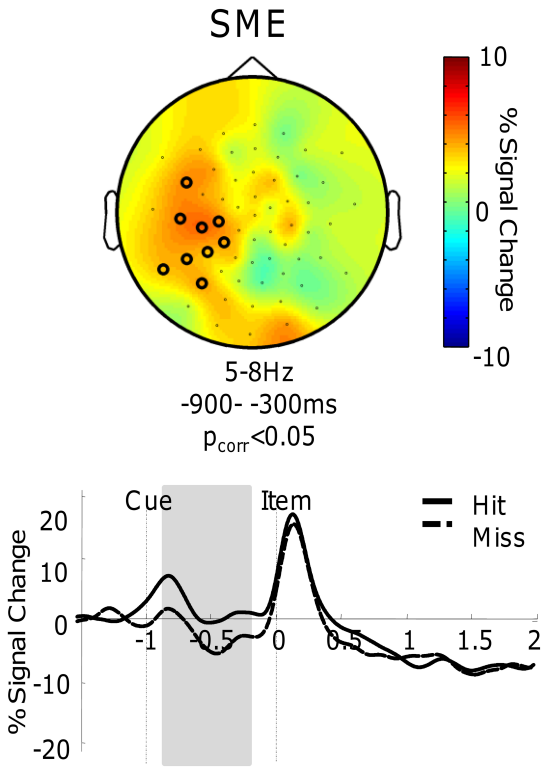


**Figure 4.** Pre-item theta SME (5-8Hz, 900-300ms before item presentation) irrespective of encoding condition. The pre-item theta effect showed no interaction of subsequent memory and encoding condition. However, pooled for hits and misses of both conditions a significant main effect of subsequent memory was obtained. Circles highlight significant electrodes in the topography plots and red indicates more power for hits than misses. Time courses of power depict average power collapsed across all electrodes that showed a significant SME in the respective time-frequency window.

To investigate differences in SMEs between semantic and survival processing, differences between hits and misses for the two conditions were compared. This was done for time–frequency windows in which significant SMEs were found in one of the two conditions. SMEs for survival and semantic processing did not differ for the pre-item theta SME ( −900 to −300 ms before item presentation, 5–8 Hz). This was confirmed by an additional analysis, which revealed a significant main effect of subsequent memory for pre-item theta power comparing hits and misses irrespective of encoding condition (Fig. 4). This can also be seen in Fig. 5D, showing a comparable positive theta SME in both conditions. Concerning alpha power, the SMEs differed significantly between the two encoding conditions (800–2000 ms, 8–12 Hz, pcorr < 0.05, Fig. 5A), demonstrating a significantly stronger SME at fronto-central electrodes in the

semantic than in the survival condition. The beta2 SME (0–1500 ms, 23–28 Hz, pcorr < 0.05, Fig. 5C) was also significantly stronger for the semantic condition than the survival condition at posterior electrodes. A similar tendency, yet not quite significant, was found for beta1 power (300–2000 ms, 15–19 Hz, pcorr < 0.1, Fig. 5B) at left posterior electrodes. This picture is also evident for the mean over all electrodes (Fig. 5D).

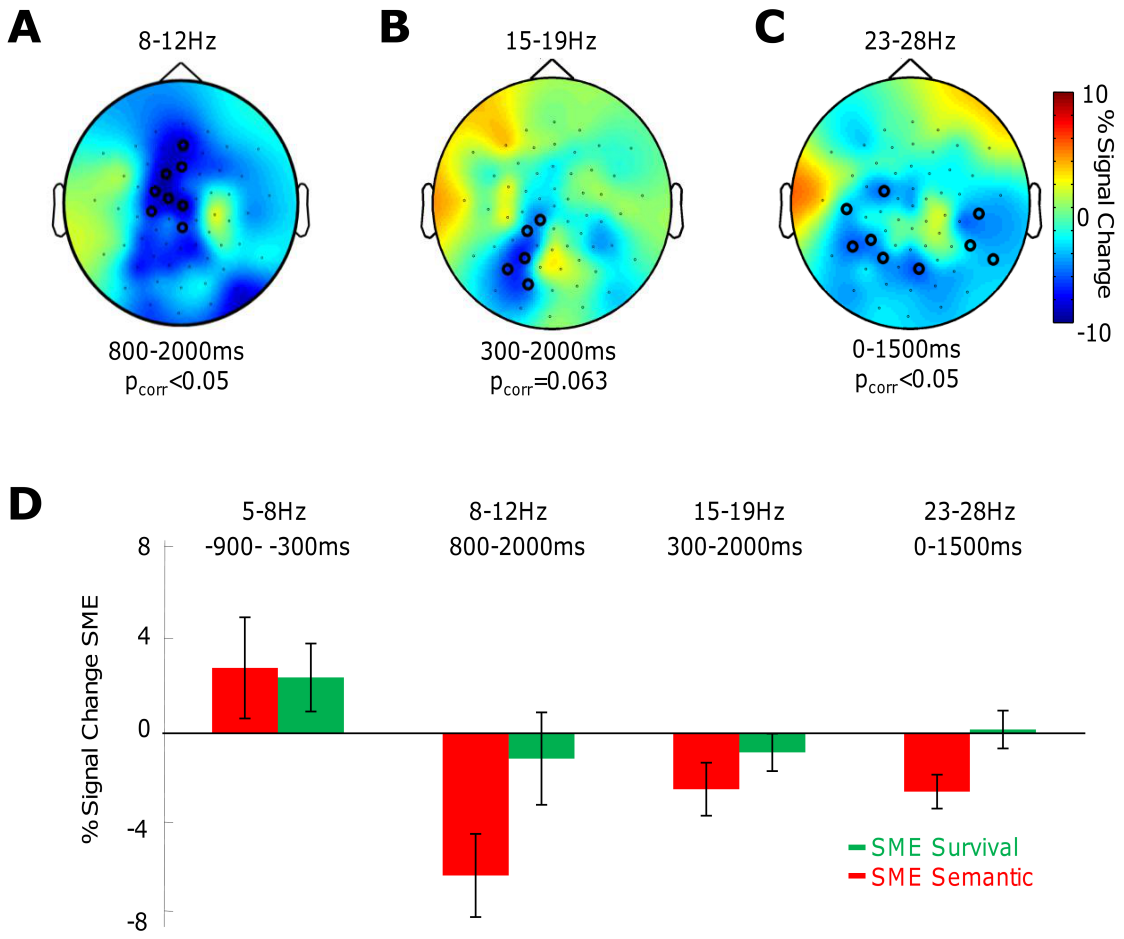


**Figure 5.** Differences between power SMEs are shown for both conditions. (A) SMEs for survival and semantic processing differed significantly in alpha power (8-12 Hz, 800-2000 ms), with the semantic condition eliciting a stronger negative SME than the survival condition. (B) SMEs in beta1 power (15-19 Hz, 300-2000 ms) showed a marginally significant difference between the two encoding conditions. (C) SMEs in beta2 power (23-28 Hz, 0-1500 ms) also differed significantly between both encoding conditions. Blue indicates stronger negative SMEs for the semantic encoding conditions, circles in the topography plots highlight significant electrodes. (D) Mean power of hit–misses collapsed across all electrodes for the respective time windows and frequency bands. Error bars indicated standard errors.

To investigate whether differences of SMEs arose because of generally higher or lower power levels in one of the encoding tasks, hits for both conditions were compared with each other for the time frequency windows in which SMEs were found. No differences were found in power between semantic hits and survival hits in those time–frequency ranges (all pcorr > 0.3).

### *PHASE SYNCHRONY*

Phase synchrony SMEs were analyzed for the frequency bands in which oscillatory power SMEs were found, albeit in differing time windows. As a measure of phase synchrony, the phase locking value (PLV) was calculated for each electrode pair excluding neighboring pairs. PLVs between hits and misses in each condition were contrasted in time bins of 500 ms in the same frequency bands in which power SMEs emerged. The identical frequency bands were analyzed, because both encoding conditions are hypothesized to differ in the amount of local and global synchrony, but not in the involvement of differing frequency bands. Effects were analyzed in consecutive, non-overlapping bins of 500 ms, as the time course of local and global effects might differ. Additionally, comparing PLVs in 500 ms time windows allows obtaining stable effects lasting several cycles of an oscillation and reduces the total number of tests. If a significant effect was found in two consecutive 500 ms time bins, the time windows were merged.

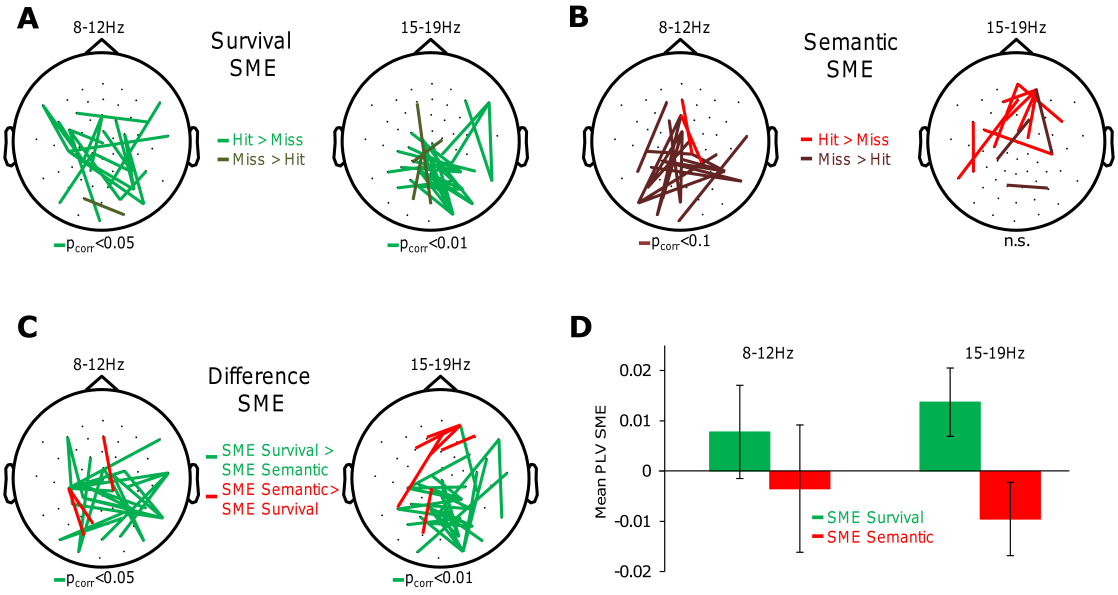


**Figure 6.** Results of the phase synchronization analysis. SMEs in phase synchrony were compared for frequency bands in which significant power SMEs were obtained. (A) Long range synchrony in the alpha band (8-12 Hz, 500-1000 ms) and beta1 band (15-19 Hz, 0-1000 ms) increased significantly for subsequently remembered words compared to forgotten words in the survival condition. (B) In the semantic condition this effect was not evident. In the alpha band there was even a non-significant tendency (8-12 Hz, 500-1000 ms) of a negative semantic phase synchrony SME. (C) The alpha and beta1 phase synchrony SMEs differed significantly between survival and semantic encoding. (D) Mean phase locking values for the respective time windows and frequency bands are shown for hits and misses of both conditions, collapsed across all electrodes showing a significant interaction. Error bars indicated standard errors.

In the survival condition, significant phase synchrony SMEs were found in the alpha frequency range (500–1000 ms, 8–12 Hz, 21 significant pairs, pcorr < 0.05, Fig. 6A) and in the beta1 frequency range (0–1000 ms, 15–19 Hz, 28 significant pairs, pcorr < 0.01, Fig. 6A). Survival hits showed an increase in alpha and beta1 PLV compared to survival misses. No significant SMEs were evident in the theta frequency band and in the semantic condition. In the same time window in which the positive survival alpha phase synchrony SME was observed, a marginally significant negative SME (a decrease in PLV for hits compared to misses) was obtained in the semantic condition (500–1000 ms, 8–12 Hz, 18 significant pairs, pcorr < 0.1, Fig. 6B). Comparing the phase synchrony SMEs in the time–frequency windows of the alpha and beta1 survival SMEs with semantic SMEs revealed significant differences between phase

synchrony SMEs. The encoding related increase in alpha and beta1 phase synchrony SMEs was significantly larger in the survival condition than in the semantic condition (500–1000 ms, 8–12 Hz, 23 significant pairs, pcorr < 0.05, 0–1000 ms, 15–19 Hz, 28 significant pairs, pcorr < 0.01, Fig. 6C). This pattern of results is also evident in the mean PLVs averaged over all electrode pairs showing a significant difference in SMEs between conditions (Fig. 6D).

## DISCUSSION

In the present study, we investigated whether brain oscillatory activity related to successful memory encoding differs between two highly efficient encoding tasks, a semantic feature processing and a survival judgment task. Indeed, SMEs in both encoding tasks were dissociable. Successful encoding in the semantic processing condition was characterized by a decrease in alpha and beta power, whereas successful encoding in the survival processing condition was related to an increase in long range phase synchrony in the alpha and beta1 frequency bands and to a higher recognition performance. These results replicate prior findings (Hanslmayr et al., 2009). Going beyond prior work this study shows that two highly efficient encoding tasks differing in processing complexity lead to dissociable SMEs in local and global synchrony measures.

This specific relationship of alpha/beta power decreases to successful encoding in a semantic task across two studies further corroborates the close relationship between semantic encoding and alpha/ beta power decreases. These specific beta power decreases in the semantic condition are also consistent with findings linking negative beta power SMEs to BOLD signal increases in the left inferior prefrontal gyrus (Hanslmayr et al., 2011), a brain region that is reliably activated during encoding (Kim, 2011) and semantic processes (Binder & Desai, 2011) and has been shown to support semantic memory encoding (Otten & Rugg, 2001b).

Encoding in the survival processing condition was associated with increases in alpha and beta long range phase synchronization. Phase synchronization has been generally proposed as a mechanism facilitating communication between distant cortical areas (Fries, 2005; Varela et al., 2001) and especially alpha and beta phase synchrony has been related to cortico–cortical communication (Buffalo et al., 2011; Donner & Siegel, 2011; von Stein et al., 2000). The phase synchrony SMEs found specifically in the elaborative survival condition might therefore indicate communication in large cortical networks involved in the different processes underlying the survival task. Increases in phase synchronization related to memory formation

have been reported by several other studies in various frequency bands. Weiss and Rappelsberger (2000) reported increases in global synchronization related to encoding success in several frequency bands. Other studies specifically related increases in theta synchronization to item context binding (Summerfield & Mangels, 2005) and alpha phase synchrony to binding mechanisms in episodic memory (Bauml et al., 2008). In intracranial recordings phase synchronization in the gamma and theta frequency was found to support episodic memory encoding (Burke et al., 2013; Fell et al., 2001). The results of local synchrony SMEs in the item feature based semantic task, and global synchrony SMEs in the more elaborative survival task, suggests that encoding in the survival task relied on a more widespread cortical network. Potentially, this increase in cortical communication indexes the concurrent processing of the items in regard to several dimensions (e.g. Is the item eatable/drinkable/useful as a tool/weapon?, images of using the item in different survival situations) that lead to the encoding of a contextual rich episodic memory and consequently to a higher chance of successful later retrieval (Craik & Tulving, 1975; Klein & Saltz, 1976).

As survival processing also requires semantic processing of the items, it was surprising that no SMEs in alpha or beta power were found. To investigate if alpha/beta power generally differed between tasks or only between SMEs, power for semantic hits and survival hits was contrasted in the time–frequency windows of the SMEs. No differences in alpha/beta power were evident between hits of both encoding conditions. Alpha and beta power therefore do not generally differ between semantic and survival judgments, but differ in whether they predict later remembrance of the item in that condition. Assuming that decreases in local alpha/beta synchronization indexes information processing (Hanslmayr, Staudigl, et al., 2012) this indicates that in both tasks a similar amount of semantic processing is employed. However, only in the animacy condition does this semantic processing shape later memory, whereas in the survival condition these item feature related processes did not influence subsequent memory to the same extent.

In contrast to the alpha power decrease and phase synchronization SMEs, the pre-item theta SME for survival processed words did not differ between conditions. As can be seen in Fig. 5D, the increase in theta power for hits compared to misses was very similar for both conditions, and pooling both conditions yielded a significant SME (Fig. 4). These results replicate previous findings, demonstrating that pre-item theta power does not differ between deep and shallow encoding tasks (Guderian et al., 2009). Therefore, the prestimulus theta SME seems not connected to task specific processing, but may rather reflect motivational preparatory processes

as reported by (Gruber et al., 2013). This unspecificity for content also resembles results during retrieval showing that theta power does not vary during retrieval of different kinds of materials, whereas alpha and beta power varies material specific (Khader & Rosler, 2011).

Importantly, the reported dissociable SMEs are not confounded by task related differences in reactions times or ratings during encoding. To check for possible differences, reaction times and ratings were contrasted for hits and misses in both conditions. There was an effect of ratings being higher for later remembered words, but this effect did not vary with encoding condition. Reaction times of the survival condition and semantic condition did not differ. However, reaction times for semantic hits were slightly faster than for semantic misses (~50 ms). No such difference was evident in the survival condition. Since this difference was evident approximately 2500 ms after word presentation and therefore at least 500 ms after the reported SMEs, it presumably did not influence the reported memory effects.

The present results show that two tasks, which are classically labeled as "deep encoding tasks" elicit dissociable SMEs. Interestingly, both encoding tasks elicited SMEs in the alpha/beta and theta frequency range. Whereas theta power effects have been reported in several memory studies and are generally thought to be related to contextual episodic memory encoding (Axmacher et al., 2006; Nyhus & Curran, 2010), beta effects have only been reported in some studies (Hanslmayr et al., 2009; Hanslmayr, Staudigl, et al., 2012; Hanslmayr, Volberg, et al., 2012; Hanslmayr et al., 2011). However, beta oscillations have been connected to semantic and language processes (for a review see Weiss and Mueller (2012), which are processes presumably underlying both encoding tasks. The differences in local/global beta synchrony between both tasks presumably indexes the size of networks involved in the task reflecting the task complexity. This parallels findings that increasing long-range phase synchrony is related to more demanding working memory tasks (Cashdollar et al., 2009; Sauseng et al., 2005). The present findings in the alpha/ beta band also fit the theory that alpha and lower beta oscillations reflect operations in a very broadly defined knowledge system (Klimesch, 2012; Klimesch, Freunberger, & Sauseng, 2010). Semantic and survival processing lead to information processing indexed by alpha/beta power decreases (Hanslmayr, Staudigl, et al., 2012), but survival processing might involve a stronger interaction between different cortical areas.

The present results also have implications for the ongoing debate concerning the nature of the survival processing advantage. (Nairne & Pandeirada, 2008) claimed that this encoding advantage arises from the fact that our brains have been shaped by evolution and that this particular encoding scenario makes use of these old, evolutionary modules that are tuned to

process survival related information (see also e.g. Aslan and Bauml (2012)). The need for this evolutionary explanation is much debated (Howe & Otgaar, 2013). Several studies show that the survival advantage is based on more proximate mechanisms such as novelty, contextual, relational or schematic processes (Butler, Kang, & Roediger, 2009; Kroneisen & Erdfelder, 2011; Kroneisen, Erdfelder, & Buchner, 2013; Soderstrom & McCabe, 2011). These processes might best be subsumed as elaborative encoding processing. As the semantic feature judgment task and the survival task differ not only in the alleged evolutionary importance of the task but also in processing complexity and many other respects, the present study is clearly not designed to reveal a potential evolutionary survival module underlying the survival processing task. However, increases in phase synchrony related to successful encoding have also been found in studies that did use mere intentional encoding strategies (Weiss & Rappelsberger, 2000). Therefore increases in alpha/beta phase synchrony do not seem to reflect activation of a special survival module.

## CONCLUSION

The present study compared a semantic encoding task with a survival processing task. Both tasks are classically considered as "deep" encoding tasks. However, the present study shows that encoding related activity is significantly different in both tasks. This pattern of results supports the process view of memory illustrated by several cognitive theories of memory. The dissociation of global and local synchrony SMEs related to a semantic feature and an elaborative encoding task indicate the potential dissociable role of local and global synchrony measures in memory formation. Additionally, these results emphasize the important role of encoding strategies usage on SMEs. Consequently, task instructions in memory encoding studies have to be considered as important contributing factors.

## ACKNOWLEDGMENTS

This research was supported by a grant from the Deutsche Forschungsgemeinschaft (Project HA 5622/1-1) awarded to S.H. We thank Sebastian Frank for help in data collection and Bernhard Spitzer for helpful advice regarding ROC analysis.

# STUDY 2: SPATIAL MNEMONIC ENCODING IS RELATED TO THETA POWER DECREASES AND MEDIAL TEMPORAL LOBE BOLD INCREASES

fMRI studies consistently demonstrate medial temporal lobe (MTL) activity in episodic memory formation and spatial navigation, while electrophysiological studies have emphasized the important role of theta oscillations (3-8Hz) in these tasks. How MTL activity is linked to theta oscillatory EEG power, however, is unknown. We recorded EEG and fMRI while participants used two memory encoding strategies: the spatial Method of Loci and the non-spatial Pegword Method. The spatial mnemonic requires participants to mentally navigate and associate items to waypoints on a well-known path, thus engaging the two core cognitive processes assumed to rely on the MTL. In contrast the Pegword Method, is equally associative but lacking the spatial component. Surprisingly, the more effective spatial mnemonic induced a pronounced theta power decrease in the left MTL compared to the non-spatial associative mnemonic strategy. This effect was mirrored by BOLD increases in the MTL. This pattern of results implies that theta oscillations in the MTL are negatively related to BOLD increases, extending the well-known negative relation of alpha/beta oscillations and BOLD signals in the cortex to theta oscillations in the MTL. The results also demonstrate that decreases in theta power index memory encoding and MTL involvement.

## INTRODUCTION

The formation of episodic memories relies crucially on the medial temporal lobes (MTL), as demonstrated by lesion (Scoville & Milner, 1957) and fMRI studies (Paller & Wagner, 2002). In rodents the predominant rhythm in the hippocampus is the theta oscillation (Buzsaki, 2005; Watrous, Fried, & Ekstrom, 2011; Watrous, Lee, et al., 2013), which is a crucial element in influential models of memory (Burgess et al., 2007; Hasselmo & Stern, 2014; Lisman & Jensen, 2013). Consequently, a link between theta oscillations in the MTL and memory formation has been proposed (Klimesch, 1996; Nyhus & Curran, 2010). However, there is still an ongoing debate about the functional relationship of theta oscillations and MTL activity. In the cortex, decreases in alpha/beta oscillations are typically related to increased neural activity (Scheeringa et al., 2011; Zumer et al., 2014). Whether this negative relationship extends to theta oscillations in general, and specifically in the MTL, remains to be investigated (Lisman & Jensen, 2013).

MTL and theta oscillation are not only involved in memory processes. Especially in animals, but also in humans, MTL and theta oscillations are involved in spatial processing and navigation (Burgess, Maguire, & O'Keefe, 2002; Ekstrom et al., 2005; Vanderwolf, 1969; Watrous, Lee, et al., 2013), with the finding of place and grid cells as evidence of the existence of a spatial code within the MTL (Buzsaki & Moser, 2013; Ekstrom, 2014; Moser & Moser, 2013). It is hypothesized that specifically the formation of associations in episodic memory involves similar mechanisms (Buffalo, 2015; Buzsaki & Moser, 2013; Ekstrom, 2014), reflected in the commonly found increase in MTL BOLD activity during successful encoding of associations into long term memory (Davachi & DuBrow, 2015; Staresina & Davachi, 2009; Uncapher, Otten, & Rugg, 2006). The relation between memory formation and theta oscillations, however, is less clear. Whereas most studies agree that theta oscillations in the MTL are involved during memory and play a specific role for binding single items into complex episodes (Buzsaki & Moser, 2013; Ranganath, 2010) conflicting results have been reported as to whether increases or decreases in theta power reflect MTL engagement (for a review see, Hanslmayr and Staudigl (2014). For instance several studies report increases in theta power during memory formation to reflect MTL involvement (Klimesch, Doppelmayr, et al., 1996; Nyhus & Curran, 2010). In contrast other studies found decreased theta activity to be related to successful memory encoding. Importantly, the latter finding has been shown in several intracranial EEG datasets directly recording from MTL regions (Burke et al., 2013; Greenberg et al., 2015; Long et al., 2014; Sederberg et al., 2007). Consequently, the relation between MTL BOLD signal and theta power during memory formation is not at all clear. We here address this issue in a new way,

utilizing a memory strategy that is specifically tailored to drive the MTL's spatial and memory processes and related theta oscillations.

Summed up previous findings predict that MTL structures should be maximally driven during memory tasks that combine associative and spatial processing (Bird & Burgess, 2008). Investigating correlates of memory formation during such a task might shed light on the relationship between MTL BOLD signal and theta power dynamics. Indeed, a mnemonic strategy, which has been used since ancient times - the Method of Loci - involves exactly such associative and spatial processing. This method, being an efficient mnemonic (Roediger, 1980) and the preferred method of memory athletes (Maguire, Valentine, Wilding, & Kapur, 2003), relies on imagining to-be-memorized material on a familiar route. We here investigate neural processes engaged during memory encoding, while participants used either the Method of Loci or the pegword method, a similarly associative but non-spatial mnemonic (see Fig 1). Recording EEG and fMRI data during the same paradigm, we predicted a higher MTL BOLD signal during spatial encoding, and our main interest was how theta power changes mirror these MTL effects. EEG and fMRI were recorded using the exact same paradigm, but different participants (see Singh (2012) for a discussion of the validity of this approach and Materials and Methods for reasons why recorded simultaneous EEG data are not reported here).

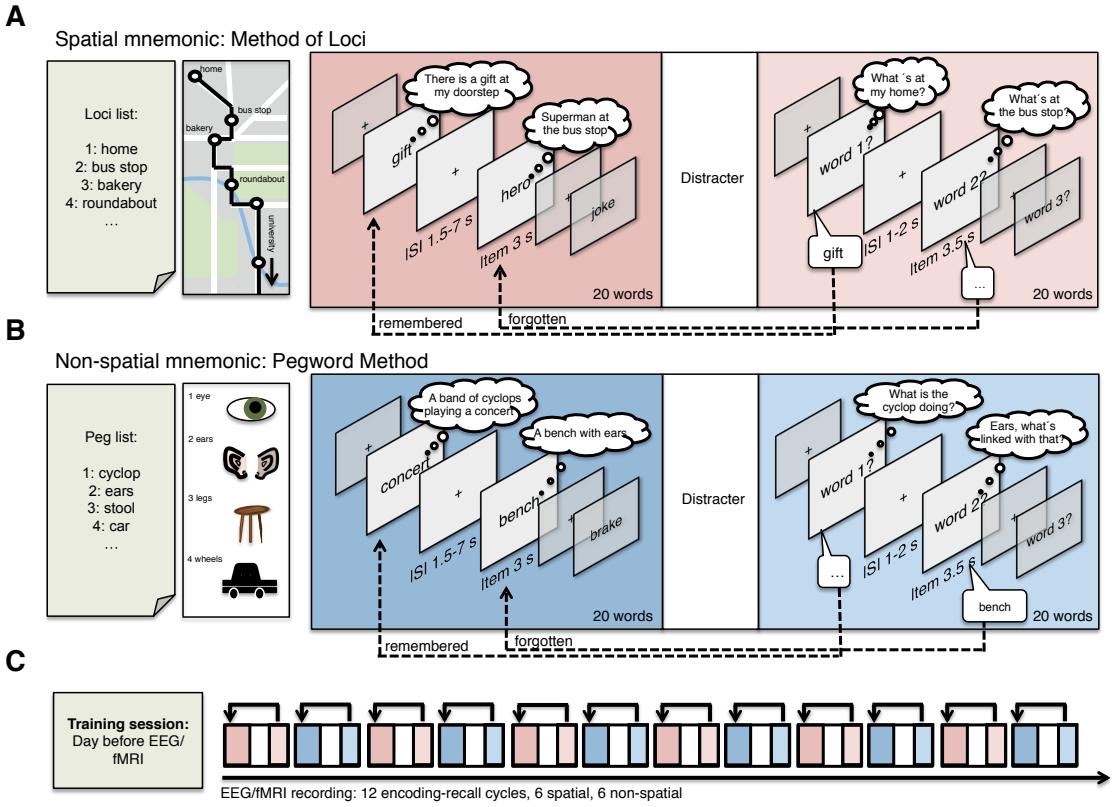


**Fig 1: Memory encoding paradigm.** Participants were trained to use two mnemonic encoding strategies: the spatial Method of Loci (A) and the non-spatial pegword method (B). In both methods participants have to link internal cues, which are either familiar way points or semantic associations to numbers, to items presented during the encoding phase. During each encoding phase, lists of 20 words were presented sequentially followed by a distracter task and a free recall phase. The whole experiment (C) entailed a training phase the day before and 12 encoding- recall cycles during EEG or fMRI recordings

## MATERIALS AND METHODS

### *SUBJECTS AND RECORDING SESSIONS*

Two separate groups of participants underwent testing with the same paradigm, one group participating in the EEG recording, the other group in the fMRI experiment. During fMRI scanning, simultaneous EEG was recorded. However because of major MR scanner induced EEG artifacts, especially in the theta frequency range, prevented reliable analysis of the simultaneously recorded EEG. This issue will be discussed in a separate publication focused on spurious effects in simultaneous EEG-fMRI recordings (Fellner et al, submitted).

Twenty-five participants took part in the fMRI study and thirty participants took part in the EEG study. The fMRI datasets of two participants had to be excluded because of a missing structural scan in one dataset and a poor task performance in another dataset (memory performance two standard deviations below the average) resulting in a sample of 23 datasets. In the EEG dataset nine participants had to be excluded because of low trial numbers in one of the conditions after excluding EEG artifacts (>15 trials) resulting in a sample of 21 datasets. The age of the remaining participants ranged from eighteen to thirty-six years (M=22.9, 15 female) in the fMRI sample, and from eighteen to twenty-four years (M=20.19, 12 female) in the EEG sample. All subjects spoke German as their native language, reported no history of neurologic or psychiatric disease, and had normal or corrected to normal vision. All participants gave their written informed consent, and the experimental protocol was approved by the local ethical review board.

### *TASK DESIGN*

Participants performed the same paradigm in the MR scanner as during EEG recording. Participants were instructed to utilize a spatial and a non-spatial mnemonic strategy: the Method of Loci and the pegword method. Both mnemonics entail linking to-be-learned items to internal cues, waypoints in the case of the Method of Loci, and number related pegs in the case of the pegword method (Fig 1 A&B). Before entering the scanner, participants had been trained extensively in the use of both methods (see below). In the scanner, during the encoding phase, only to-be-learned words were presented sequentially, and participants were instructed to associate each word with the corresponding cue in the loci or pegword sequence. They were instructed to visualize to-be-learned items (e.g. first item gift) at the respective waypoint while using the Method of Loci (e.g. first loci cue home), thus participants might imagine a nicely wrapped gift at their doorstep (Fig 1A). During the pegword method, they were asked to focus on semantic relations between the item (e.g. first item concert) and the respective pegword (e.g.

first pegword cyclop), such that a possible association could be "A band of cyclops playing a concert" (Fig 1B). During recall, participants were told to use the pegword and loci way points as retrieval cues to recall the words in the same sequence as during the encoding phase.

A training session took place one day before fMRI or EEG recording to ensure that all participants were able to employ both mnemonic encoding strategies. Before entering training, participants already had received information about the Method of Loci and the pegword method and were instructed to prepare 20 waypoints on a highly familiar path (e.g.. for most participants this was the way to the university as participants were mostly university students), and to memorize the 20 pegword cues. The training session then consisted of 3 parts: First, the experimenter ensured that all participants had memorized the loci and pegword cues. Second, participants had to encode a list of 20 words in a self-paced manner, telling the experimenter how they linked the to-be-learned items to the loci or pegword cues. If the chosen associations did not fit with the task instruction, the training session was restarted. The training session ended with a trial run of the paradigm consisting of 4 encoding-recall-cycles with the same timing and settings as during the EEG/fMRI recordings.

The fMRI- or EEG-recorded part of the experiment consisted of 12 repeated memory encoding and recall cycles, with each encoding-recall block consisting of an encoding phase, a visual detection task, a free recall memory test and a short rest period (see Fig 1C). Each experiment was split into 4 consecutive recording sessions to keep file sizes manageable; the MR image acquisition was thus stopped after every third encoding-recall cycle. Participants in each cycle memorized 20 words using either the Method of Loci or the pegword method. Encoding methods were alternated between encoding cycles and word material was counterbalanced across subjects. During the encoding phase, each to-be-encoded word was presented for 3 sec followed by a fixation cross presented with an exponential jitter from 1.5-7 sec to increase design efficiency for fMRI analysis. The encoding phase was followed by a visual detection task (ca. 2.5 min) serving as a distracter task in order to avoid short term memory effects on later recall. Participants had to detect contours in a field of Gabor patches and indicate their answer by buttons presses (similar task as in Hanslmayr, Volberg, Wimber, Dalal, and Greenlee (2013)). The distracter was followed by a memory test, in which subjects were asked to speak aloud words memorized prior to the visual detection task in their original encoding order, whenever the screen showed a "word no. x" cue. Recall performance was used to classify trials during the encoding phase as subsequently remembered or subsequently forgotten. Only words recalled in the corrected order were labeled as hits. In-scanner verbal responses were recorded using an

fMRI-compatible microphone (MRconfon). Scanner noise was removed from the resulting audio files using the free software package Audacity (http://audacity.sourceforge.net/). For two participants, data from one of the 4 fMRI sessions had to be discarded because of missing microphone recordings. During the out-of-scanner EEG experiment, recall performance was scored manually by the experimenter. Each encoding-recall cycle ended with a 20 sec rest period in which participants were told to relax to be prepared for the next cycle. During EEG recordings participants were sitting upright in front of a computer screen instead of in supine position in the MR scanner, where stimuli were projected on a screen in the scanner bore, visible to the participants on a mirror attached to the head coil.

As study material, 360 words were drawn from the MRC Psycholinguistic Database (Coltheart, 2007), translated into German and separated into 16 lists with 20 words each. Six lists were used during the training session; the other 12 lists were used during the EEG and fMRI recordings. Each of these 12 lists was matched according to average word frequency (M=61.98; SEM=1.58), number of letters (M=5.59; SEM=0.04), syllables (M1.84; SEM=0.02), concreteness (M=375.65; SEM=2.17), and imageability (M=414.21; SEM=2.83). Lists were counterbalanced across participants and encoding tasks. Word order in each list was randomized.

### *FMRI RECORDING*

Imaging was performed using a 3 Tesla MR head scanner (Siemens Allegra). During fMRI scanning, 2475-2480 whole-brain images, consisting of 34 axial slices, were continuously acquired using an interleaved, standard T2*-weighted echo-planar imaging sequence (repetition time TR=2000 ms; echo time TE=30 ms; flip angle=90°; 64x64 matrices; in-plane resolution: 3x3 mm; slice thickness: 3 mm). High-resolution (1mm isotropic voxel size) sagittal T1-weighted images were acquired after the functional scans, using a magnetization-prepared rapid gradient echo sequence (TR=2250 ms; TE=2.6 ms) to obtain a 3D structural scan. Extra padding was placed surrounding the head of the subject to minimize head movements.

### *FMRI PREPROCESSING*

Image preprocessing and statistical analysis was performed using SPM8 (Wellcome Department of Cognitive Neurology, London: UK, www.fil.ion.ucl.ac.uk/spm), running on MATLAB (Version 2012b, The MathWorks, Natick, MA). After discarding the first two images of each session, time series were corrected for differences in slice acquisition time, spatially realigned to the first image of the session, and unwarped. The mean functional image was co-registered to the structural image. Global effects in the functional time series within each session and voxel were removed using linear detrending (Macey, Macey, Kumar, & Harper, 2004). All

functional images were then normalized to MNI space (Montreal Neurological Institute, www.mni.mcgill.ca) using the normalization parameters determined from segmentation of the structural image. As a last step images were smoothed with a Gaussian kernel of 8 mm (FWHM).

### *FMRI ANALYSIS*

Scans of all four session were concatenated in first level GLMs. Activity related to subsequent memory and encoding task was modeled by event related stick regressors for each condition (loci-remembered, loci-forgotten, pegword-remembered, pegword-forgotten) convolved with the canonical first order hemodynamic response function. Further regressors of no interest were modeling the rest periods, free recall periods (separately for each encoding condition), and the distracter task. Session-specific regressors, linear drifts within each session, and movement parameters determined during realignment were also included in the model. T-contrasts capturing encoding effects for the 4 conditions of interest were calculated in each single participant, and combined in a 2 (task) x 2 (subsequent memory) full factorial random effects model on a group level.

As a first step, a ROI analysis on MTL effects was carried out using small volume correction on bilateral MTL defined by Wake Forest University WFU pick atlas (https://www.nitrc.org/projects/wfu_pickatlas/, parahippocampal cortices plus hippocampi using TD atlas). Small volume corrected effects are reported using a $p<0.001$, cluster size>10 voxels. An additional whole-brain analysis was carried out using a threshold of $p<0.001$ uncorrected, cluster p-level, family-wise error corrected <0.05. Marsbar (http://marsbar.sourceforge.net) was used to extract parameter estimates of significant clusters. Results are plotted on the mean normalized structural scan of all subjects.

### *EEG-RECORDING*

The EEG was recorded from 63 channels in an equidistant montage, (EasyCap, Herrsching, Germany, BrainampMR). Recordings were referenced to Fz and later re-referenced to average reference. Impedances were kept below 20 kΩ. The signals were amplified between 0.1–250 Hz. The EEG data were sampled at 500 Hz with an amplitude resolution of 0.5μV

### *EEG PREPROCESSING*

All EEG data analyses were carried out using custom MATLAB scripts and fieldtrip (http://www.fieldtriptoolbox.org, (Oostenveld et al., 2011)). For analysis of memory encoding effects data were epoched in trials -2.5 to 3.5 sec around each item onset during encoding. Data

was visually inspected, trials with idiographic artifacts (channel jumps, muscle artifacts, noisy channels) were excluded from further analysis. Noisy channels were excluded (in 4 datasets up to 3 electrodes were excluded). Infomax independent component analysis was applied to correct for residual artifacts (e.g. eye blinks, eye movements, or tonic muscle activity). The maximum number of independent components was estimated, equating the number of channels in a dataset (59 to 62 ICs). On average 3.8 ICs were discarded (range: 1-8 ICs), and remaining ICs were back projected to channel level. Data was again visually inspected for remaining artifacts. In datasets with rejected electrodes prior to ICA, these missing channels were then interpolated using neighboring electrodes. On average 62.9 spatial/remembered trials (range 33-96), 45.7 non-spatial/remembered trials (range 23-74), 34.7 spatial/forgotten trials (range 19-61), and 49.7 non-spatial/forgotten trials (range 22-81) passed artifact corrections.

Data was filtered to obtain oscillatory power between 2 Hz and 30 Hz using wavelets with a 5 cycle length. Resulting data was z-transformed to respective mean and standard deviation of power across the time dimension i.e. across all trials of each frequency band and channel. For each subject and condition (remembered, forgotten, loci, pegword) all trials were averaged and smoothed with Gaussian kernel (FWHM 200ms and 2 Hz) to control for inter-individual differences and to control for the time-frequency resolution trade-off across frequencies.

### *EEG ANALYSIS*

For statistical analysis of the frequency band of interest, i.e. the theta frequency range (~3-8 Hz) a non-parametric cluster permutation test was run restricted to 2-10 Hz as implemented in fieldtrip (Maris & Oostenveld, 2007). As a first step summed t-values of three dimensional clusters (time x frequency x electrodes) were contrasted in the data to a distribution of summed t-values obtained by randomizing conditions, which effectively controls for type-I errors due to multiple testing.

To identify time-frequency clusters showing significant differences between conditions across all lower frequencies (1-30 Hz) in a more explorative manner a sliding window cluster permutation test was used (for details Staudigl and Hanslmayr (2013)). This procedure was used to analyze memory encoding effects, and for comparing trials from the spatial and non-spatial task. A cluster permutation test as implemented in fieldtrip was calculated for each 300 ms x 1 Hz time-frequency bin, clustering only across electrodes and averaging across time and frequency bin, and thus returning a p-value for each time-frequency bin. The Monte Carlo method involving 1000 random permutations was used and Monte Carlo cluster p-values below

0.05 (two-tailed testing) were considered significant. To check if significant time clusters revealed in this analysis showed continuous scalp topography, a second cluster permutation test was performed on the respective time-frequency bin of the cluster.

Source analysis was carried out using a linearly constrained minimal variance (LCMV) beamformer (Van Veen, van Drongelen, Yuchtman, & Suzuki, 1997), calculating a spatial filter based on the whole length of all trials, with each trial bandpass filtered in the frequency range of interest. Data were bandpass filtered between 1-12 Hz for theta source reconstruction and bandpass filtered between 8-40 Hz for sources of activity in the alpha/beta frequency range. For all subjects, a standard source model with a grid resolution of 12 mm based on the Montreal Neurological Institute (MNI) brain and standard electrode positions realigned to the MNI MRI was used. The source time-course for each grid point was calculated and subjected to a wavelet analysis and z transformed the same way as the electrode level data. Results of the source localization are plotted on a MNI single subject template file.

# RESULTS

## *BEHAVIORAL RESULTS*

Memory performance across both experiments and conditions was reasonably high. Memory performance i.e. hit rates (Fig 2) in both datasets was significantly higher during the spatial encoding condition than during the non-spatial encoding task (fMRI: $t(22)=6.26$, $p<0.0001$, EEG: $t(20)=10.23$, $p<0.0001$). This was a very robust effect, which was visible in almost every single subject, demonstrating the power of the Method of Loci as a mnemonic (Roediger, 1980).

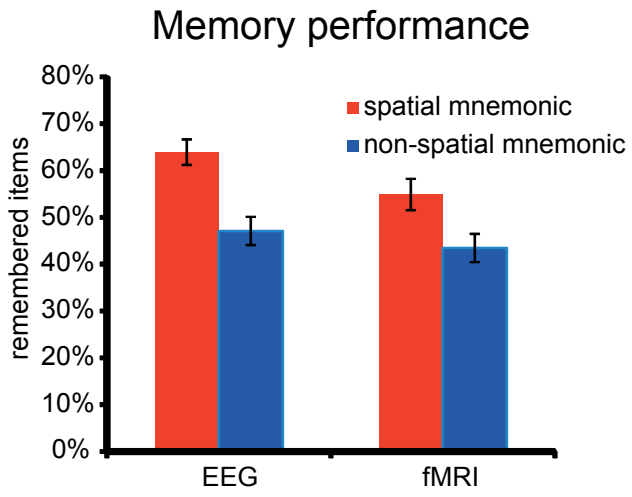


**Fig 2: Memory performance.** Percent of recalled words in the spatial and non-spatial encoding condition separately for the EEG experiment and fMRI experiment. In both datasets memory performance was higher using the spatial Method of Loci mnemonic. Error bars show standard error of the mean

## *FMRI. RESULTS*

As a first step we investigated if MTL BOLD activity is increased during spatial processing and memory encoding. To this end, a region of interest (ROI) analysis on anatomically predefined MTL regions was carried out (Fig. 3A & Table 1). BOLD activity increased significantly in bilateral parahippocampal regions during the spatial processing task in contrast to the non-spatial task. Positive SMEs were found in the left MTL, i.e. BOLD signal increases were evident in left parahippocampal gyrus during subsequently remembered in contrast to subsequently forgotten trials (Fig 3A & Table 1). In line with our hypotheses, these results suggest that spatial processing and successful memory formation both drive hemodynamic MTL activity.

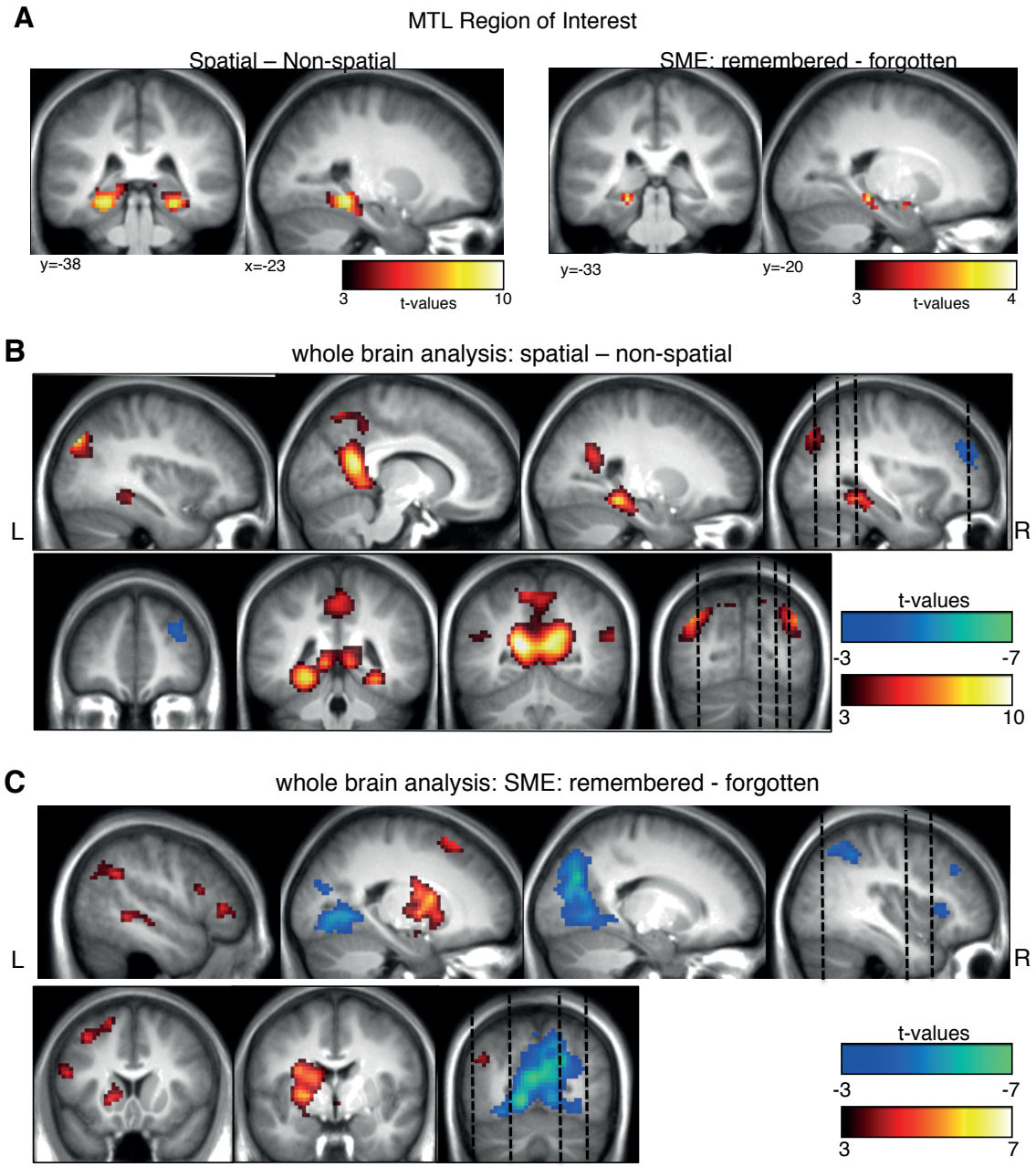


**Fig 3: fMRI results for spatial vs. non-spatial contrasts and memory effects.** A region of interest analysis was carried out for MTL regions revealing increases in activity for the spatial mnemonic and successful memory formation (A, $p<0.001$, cluster size>10). An exploratory whole brain analysis revealed additional effects in typical spatial cortical networks (i.e. retrosplenial cortex, bilateral MTL, B) and memory related regions (i.e. left inferior frontal gyrus C) ($p<0.001$, all $p<0.05$ FWE cluster level). Warm colors indicate higher BOLD signal for spatial processing and later remembered items, cold color indicate higher BOLD signals for non-spatial processing and subsequently forgotten items.

**Table 1:** Locations of peak activation revealed in MTL ROI analysis

Spatial > Non-spatial

| | hs | BA | size | x | y | z | t |
|---|---|---|---|---|---|---|---|
| Parahippocampal gyrus | L | 36 | 197 | -24 | -40 | -11 | 9.67 |
| | L | | | -9 | -46 | 1 | 7.28 |
| Parahippocampal gyrus | R | 36 | 156 | 27 | -37 | -14 | 8.54 |
| Parahippocampal gyrus | R | | 20 | 12 | -46 | 1 | 6.83 |

positive SME: remembered > forgotten

| | hs | BA | size | x | y | z | t |
|---|---|---|---|---|---|---|---|
| Parahippocampal gyrus | L | | 14 | -27 | 2 | -14 | 4.07 |
| | L | 28 | | -15 | -10 | -17 | 4.00 |
| Parahippocampal gyrus | L | 35 | 18 | -21 | -34 | -11 | 3.79 |
| | L | 35 | | -24 | -28 | -20 | 3.38 |

An additional exploratory whole brain analysis (Fig 3 B&C & Table 2) was carried out to investigate which other regions are involved in spatial processing and memory formation. Regions typically associated with spatial processing (Burgess et al., 2002; Epstein, 2008) showed BOLD signal increases during spatial compared to non-spatial processing (Fig 3B): bilateral retrosplenial cortex (posterior cingulate cortex, BA30), and lateral temporal areas of the angular gyrus (BA 39). In contrast the right middle frontal gyrus (Fig 3B) showed relative increases in activity during non-spatial processing, potentially related to enhanced control processes during non-spatial cue retrieval (Schott et al., 2005). Positive subsequent memory effects (SMEs) (Fig 3C), irrespective of task, were found in the left hemisphere in inferior frontal gyrus, an area typically involved in memory encoding of verbal material (Kim, 2011). Additional memory related activity was evident in striatal areas (putamen, caudate body), left superior and middle temporal gyrus. Relative decreases in BOLD signals during remembered words contrasted to forgotten words, i.e. negative SMEs, were evident in bilateral occipital areas (cuneus, lingual gyrus) and right lateralized parietal and frontal regions (Fig 3C).

**Table 2:** Locations of peak activation revealed in the whole brain analysis

| Spatial > Non-spatial | | | | MNI coordinates | | | |
|---|---|---|---|---|---|---|---|
| | hs | BA | size | x | y | z | t |
| Posterior Cingulate | L | 30 | 1999 | -15 | -58 | 16 | 12.64 |
| Parahippocampal Gyrus | L | 36 | | -24 | -40 | -11 | 9.67 |
| Posterior Cingulate | R | 30 | | 12 | -52 | 16 | 9.56 |
| Superior Occipital Gyrus | L | 19 | 186 | -36 | -76 | 34 | 8.78 |
| Superior Temporal Gyrus | L | 22 | | -45 | -55 | 22 | 3.91 |
| Middle Temporal Gyrus | L | 39 | | -54 | -67 | 22 | 3.59 |
| Parahippocampal Gyrus | R | 36 | 206 | 27 | -37 | -14 | 8.54 |
| Middle Temporal Gyrus | R | 39 | 215 | 42 | -73 | 34 | 6.89 |
| Superior Temporal Gyrus | R | 39 | | 57 | -58 | 22 | 5.19 |
| Middle Temporal Gyrus | R | 39 | | 48 | -67 | 25 | 4.92 |
| Non-spatial > Spatial | | | | | | | |
| Middle frontal gyrus | R | 9 | 102 | 30 | 47 | 28 | 4.23 |
| | R | 9 | | 45 | 29 | 22 | 3.76 |
| positive SME: remembered > forgotten | | | | | | | |
| Insula | L | 13 | 608 | -30 | -7 | 19 | 5.77 |
| Caudate Body | L | | | 21 | 5 | 13 | 5.68 |
| Putamen | L | | | -24 | -4 | 1 | 5.58 |
| Middle frontal gyrus | L | 6 | 141 | -24 | 23 | 52 | 4.83 |
| | L | 6 | | -28 | 17 | 58 | 4.61 |
| | L | 6 | | -36 | 17 | 46 | 4.49 |
| Middle temporal Gyrus | L | 22 | 86 | -51 | -43 | -2 | 4.56 |
| | L | 21 | | -60 | -19 | -5 | 4.01 |
| Superior Temporal Gyrus | L | 22 | | -48 | -25 | -5 | 3.77 |
| Middle Temporal Gyrus | L | 39 | 114 | -42 | -73 | 31 | 4.44 |
| Superior Temporal Gyrus | L | 39 | | -48 | -52 | 31 | 4.41 |
| Inferior Frontal Gyrus | L | 44 | 135 | -51 | 14 | 19 | 4.37 |
| | L | 13 | | -45 | 32 | 1 | 4.36 |
| | L | | | -45 | 47 | -5 | 3.93 |
| negative SME: forgotten > remembered | | | | | | | |
| Lingual Gyrus | L | 18 | 2237 | -12 | -70 | -2 | 7.25 |
| Posterior Cingulate | L | 30 | | -3 | -70 | 16 | 6.98 |
| Cuneus | R | 18 | | 9 | -73 | 25 | 6.67 |
| Inferior Parietal Lobule | R | 40 | 355 | 42 | -46 | 46 | 4.94 |
| Superior Parietal Lobule | R | 7 | | 33 | -52 | 49 | 4.41 |
| Supramarginal Gyrus | R | 40 | | 57 | -43 | 37 | 4.41 |
| Middle Frontal Gyrus | R | 10 | 96 | 30 | 62 | 13 | 4.36 |
| | R | 8 | | 39 | 35 | 34 | 4.08 |
| Superior Frontal Gyrus | R | 9 | | 27 | 53 | 34 | 3.67 |
| Insula | R | 13 | 68 | 36 | 26 | 1 | 4.36 |

To elucidate if memory encoding related activity differs between the spatial and non-spatial mnemonic strategies, interaction effects were calculated. No significant differences in memory encoding effects between encoding strategies (i.e. no interaction effects between condition and memory) were found in the ROI analysis or in the whole-brain analysis ($p<0.001$, cluster size > 10). The reported results support our hypothesis of increases in hemodynamic MTL activity being related to spatial processing and associative memory formation.

### *EEG SENSOR LEVEL RESULTS*

Similar to the fMRI analysis we first investigated the effects of interest focusing on the theta frequency range (i.e. from 2 to 10 Hz), as the primary question of the study was how theta power is related to spatial processing and memory formation. Contrasting the spatial with the non-spatial encoding strategy a significant theta cluster was found spanning the whole trial epoch (-1.5 to 2.5 sec, $p_{corr} < 0.005$). This effect was driven by a robust theta power decrease in the spatial compared to the non-spatial task, and does not appear to be triggered by the onset of the to-be-encoded words. Decreases in theta power were also related to successful memory formation as revealed by negative SMEs. A significant cluster was evident from around stimulus onset lasting until the end of the trial (0-2.5 sec, $p_{corr}<0.05$). The extent of the clusters is shown in Fig 4A (left for spatial vs. non-spatial; right for SMEs), showing the number of electrodes belonging to the cluster at a certain time-frequency bin in order to visualize the extent of the three-dimensional cluster in the time-frequency dimensions.

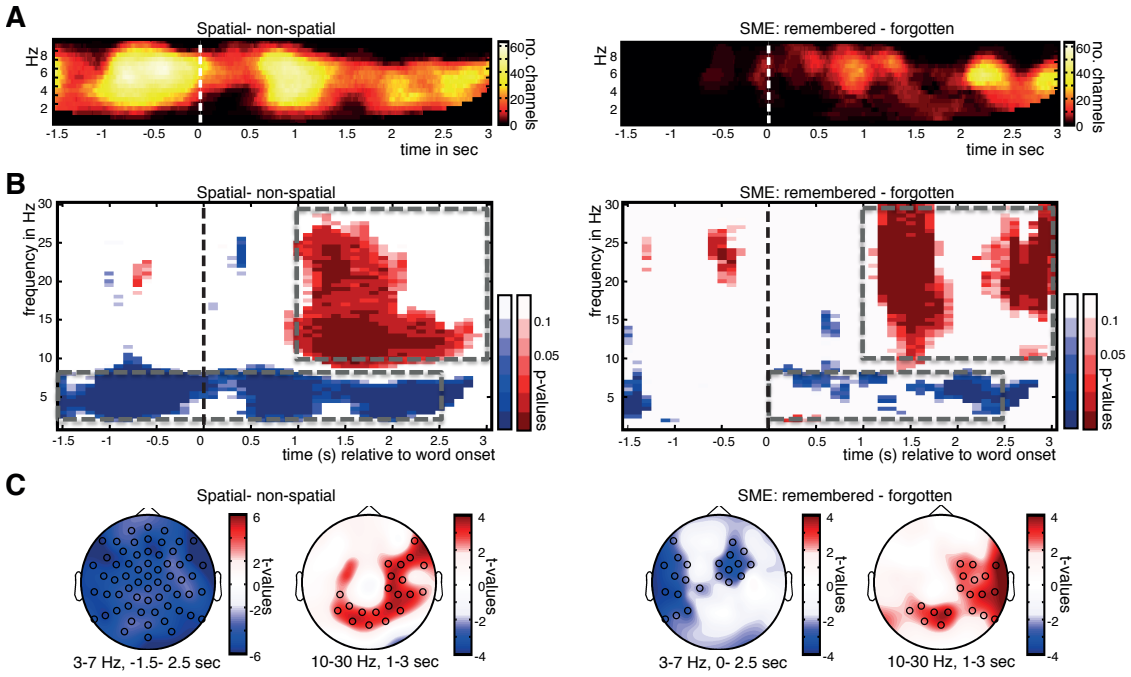


**Fig 4: EEG sensor level results.** A cluster permutation statistic restricted to the theta frequency range revealed ongoing decreases in theta oscillatory power for spatial mnemonic processing in contrast to non-spatial processing, and item related theta power decreases correlating with successful memory formation (A). Additional increases in alpha/beta power during spatial encoding and memory formation were evident after word presentation; time frequency plots show p-values of separately calculated cluster permutation tests of each time-frequency bin (B). Topographies of theta and alpha/beta power effects for the time-frequency windows in which effects were present highlighted in (B, dashed boxes) are plotted below, circle highlight electrodes belonging to a significant cluster (C). Warm colors in (B) & (C) indicate increases in power for spatial processing and successfully encoded items, cold colors indicate decreases in power for spatial processing and successfully encoded items in contrast to non-spatial processing and subsequently forgotten items, respectively.

An additional sliding cluster permutation statistic was carried out on all lower frequency bands (1-30 Hz, Fig 4B) to reveal effects outside of the frequency band of interest. In addition to the effects in the theta range, significant effects were also obtained in the alpha/beta range (10-30Hz), where a stronger power increase was evident after stimulus presentation (1-3 sec) during spatial compared to non-spatial processing. In the same time window a positive SME for alpha/beta power was observed, i.e. higher power for later remembered compared to later forgotten items.

For a first identification of potential sources of EEG effects, topographies of the time windows of significant effects are shown in Fig 4C. The decrease in theta power related to spatial processing showed a widespread topography with the strongest effects over lateral electrodes ($p_{corr}<0.001$). Increases in alpha/beta power related to spatial processing were found over parietal electrodes ($p_{corr}<0.005$). Theta power decreases related to memory encoding were evident in left lateral and right frontal regions (two separate clusters: $p_{corr}<0.001$, $p_{corr}<0.05$, respectively). Memory related alpha/beta power increases showed a similar posterior and right lateralized topography as spatial processing related effects in two separate clusters (both $p_{corr}$'s$<0.05$).

The pattern of results reveals that a stronger ongoing decrease of theta power was indicative of the spatial processing task, and that a stimulus-related decreases in theta power reflected successful memory formation. To investigate potential differences of encoding effects between the spatial and non-spatial mnemonic strategies, interaction effects were calculated by contrasting SMEs of both conditions. No significant clusters were found in a cluster analysis in the theta frequency range (2-10 Hz, c.f. Fig 4A), an additional sliding cluster statistic including all lower frequencies (2-30 Hz) revealed no coherent effects exceeding a size of 8 time-frequency bins, suggesting that successful encoding with both mnemonic strategies similarly relies on theta power decreases.

### *EEG SOURCE ANALYSIS RESULTS*

To link the EEG results with the fMRI results, we investigated the sources of the oscillatory EEG effects by means of a source localization analysis utilizing LCMV beamforming (Van Veen et al., 1997). Analyzing the differences in power at the source level revealed that the theta power decreases for spatial processing compared to non-spatial processing were strongest in the left anterior MTL ($p_{corr}<0.0001$, peak MNI coordinate: x=-32, y= -18, z= -31, parahippocampal gyrus, BA 36; Fig 5A). Memory formation related theta power decreases were strongest in left lateral temporal lobe areas ($p_{corr}<0.05$, peak MNI coordinate: x= -56,y= -43, z= 5, middle temporal gyrus, BA22; Fig 5A). In contrast, source localization of alpha/beta power increases during spatial processing and memory formation revealed effects in occipital areas and right lateralized regions (spatial-non-spatial: $p_{corr}<0.05$, peak MNI coordinate: x= -20,y= -67, z= -8, lingual gyrus, BA19, SME: $p_{corr}<0.05$, peak MNI coordinate: x= 27,y= -92, z= 28, cuneus, BA19; Fig 5B). Note the high overlap between the estimated sources of theta power decreases, and the medial temporal and lateral temporal BOLD increases revealed by the fMRI analyses (cf.

Fig 5A & Fig 3). Similarly, alpha/beta increases overlap with BOLD decreases during successful memory formation (cf. Fig 5B & Fig 3C).

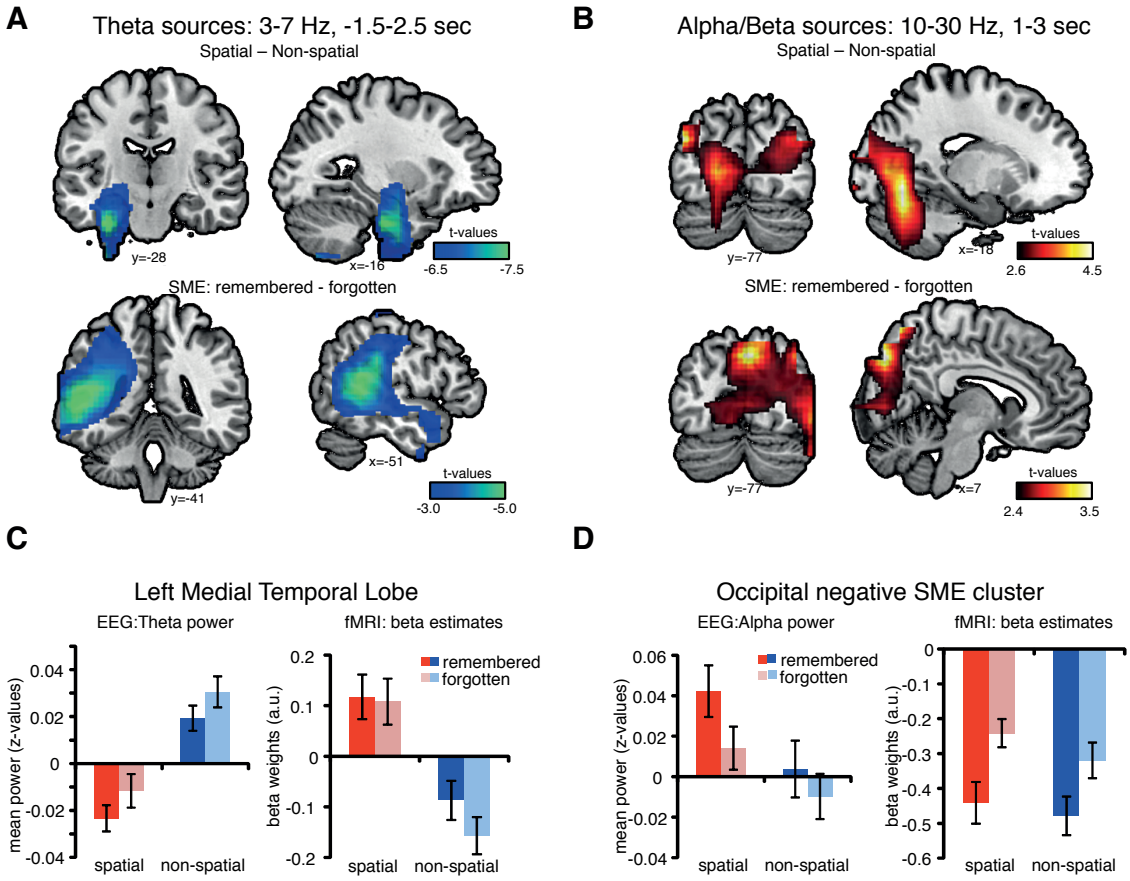


**Fig 5: EEG source localization results.** Peaks of t-values are shown for the comparison between spatial and non-spatial, and remembered vs. forgotten theta power (A) and alpha/beta power (B) data are shown. Decreases in theta power for spatial processing were strongest in anterior MTL areas (peak MNI coordinate: -32, -18, -31, parahippocampal gyrus, BA 36), theta power decreases during successful memory formation were strongest in left temporal areas (peak MNI coordinate: -56, -43, 5, middle temporal gyrus, BA22) (A). Alpha/beta power increases were strongest in occipital areas, for spatial vs. non-spatial processing (peak MNI coordinate: -20, -67, -8, lingual gyrus, BA19) and during memory formation (peak MNI coordinate: 27, -92, 28, cuneus, BA19) (B). Mean EEG power and fMRI beta weights of MTL and occipital areas are plotted in (C & D, respectively). Theta power decreases show the reversed pattern of BOLD increases in left MTL regions (C); alpha/beta increases in occipital areas also mirrored by BOLD increases in occipital areas (D). Error bars show standard error of the mean.

To further illustrate the relationship between the fMRI and EEG results, average EEG power and the corresponding fMRI beta estimates are plotted in Fig 5C & D. Source localized theta power, as well as mean BOLD signal estimates (beta weights) were extracted from the anatomically defined left MTL ROI used in the fMRI analysis (Fig 5C). Decreases in theta power mirror fMRI effects insofar as decreases in theta power are strongest for spatially processed and remembered trials, the condition that also exhibited the highest MTL BOLD signal increase. Additionally source localized alpha/beta power was extracted of the source voxels overlapping with the occipital negative fMRI SME (cf. Fig 3C, Table 2). Alpha/beta power increased in occipital cortex during successfully encoded trials, which again was mirrored by BOLD signal decreases in this region during memory formation (Fig 5D).

## DISCUSSION

Brain oscillations in the theta range and hemodynamic activity in the medial temporal lobe have been suggested as the core neural correlates of successful memory formation in electrophysiological and functional imaging studies, respectively. We here addressed the question of how theta power and MTL BOLD signals are functionally related a memory encoding task. To this end we measured EEG and fMRI during an associative, spatial mnemonic strategy, the Method of Loci, which is a task that we assumed to maximally rely on the MTL and the theta oscillations therein. Indeed, during usage of the spatial (vs. non-spatial) mnemonic we observed a prominent theta decrease concurrent with an increase in MTL BOLD signal, suggesting a negative relation between theta power and MTL activity. A negative relationship between theta power and MTL activity was also found during successful (compared with unsuccessful) memory formation, and these negative theta SMEs and positive MTL BOLD SMEs were equally pronounced during the spatial and non-spatial encoding task suggesting that these processes benefit memory irrespective of the current task. Theta decreases and MTL BOLD increases were not only co-occurring during spatial processing and memory formation but were also co-localized in the same anatomical regions: the strongest sources theta effects were evident in the left lateral temporal lobe and in the left MTL, areas overlapping with positive fMRI-BOLD effects. Together, these findings provide strong evidence for negative relationship between theta power, memory formation, spatial processing, and MTL BOLD signal.

The present study was specifically tailored to examine theta oscillations during a spatial memory task that maximally drives the MTL. The Method of Loci recruits almost all cognitive

processes that have been linked to MTL functions, i.e. scene construction, spatial processing, imagery, memory encoding and retrieval, and building new associative links (Bird & Burgess, 2008). Our results, maybe surprisingly, demonstrate that this specific task elicits strong theta power decreases in the MTL alongside BOLD signal increases. Importantly, theta decreases were not only found to be paralleled by lateral and medial temporal BOLD increases (Fig 5C) but were also source localized to the left MTL, further strengthening the argument of task related theta power decreases in the MTL.

While intracranial studies directly recording electrophysiological activity from the MTL have reported similar theta decreases (Burke et al., 2013; Greenberg et al., 2015; Long et al., 2014; Sederberg et al., 2007), previous M/EEG (Klimesch, Doppelmayr, et al., 1996; Osipova et al., 2006; Staudigl & Hanslmayr, 2013), have reported increases in theta during memory formation. Specifically, our findings are in conflict with a previous MEG study, which found increased theta power during active spatial navigation and memory formation (Kaplan et al., 2012). This discrepancy is likely driven by a difference in the task, which in our case involved mental navigation, i.e. passive spatial processing in cognitive space, as opposed to active navigation in the environment. Indeed, studies in rodents found that theta power relatively decreases in passive compared to active navigation (Terrazas et al., 2005) Therefore, theta power effects during memory encoding and building association in cognitive space might exhibit a different pattern as during active movement.

FMRI effects during spatial encoding closely followed previously reported effects relating to the usage of mnemonic strategies (Maguire et al., 2003) and spatial processing in general. The spatial mnemonic exhibited increases in BOLD signal in bilateral MTL and retrosplenial cortex, regions typically involved in imagining scenes and retrieving familiar landmarks (Burgess et al., 2002; Epstein, 2008). The Method of Loci task entails retrieving familiar waypoints and constructing spatial scenes linking the to-be-learned items to these familiar landmarks. Constructing such complex visual scenes crucially involves MTL structures (Addis, Wong, & Schacter, 2007; Hassabis & Maguire, 2007) and retrosplenial cortex has been conceptualized as a buffer of such imagined constructions (Bird & Burgess, 2008; Vann, Aggleton, & Maguire, 2009). The greater involvement of this spatial network in forming associations in cognitive space, which also serves a central function in human memory (Hassabis & Maguire, 2007), might be in part responsible for the higher memory performance during the spatial mnemonic and the efficiency of the Method of Loci in general (Roediger, 1980).

Interestingly, activity related to successful memory encoding (i.e. SMEs), in both mnemonics did not differ depending on the spatial or non-spatial nature of the mnemonic, neither in EEG nor in fMRI. Memory formation during both tasks was related to activity in left MTL, consistent with the notion that the human MTL is involved in building item-cue associations (Buzsaki & Moser, 2013; Ranganath, 2010), regardless of whether these associations involve spatial or non-spatial cues. The lack of an interaction between successful encoding and mnemonic is also interesting since SMEs have been shown to differ depending on encoding tasks and to-be-encoded material (Fellner et al., 2013; Hanslmayr et al., 2009; Kim, 2011; Otten & Rugg, 2001b). The similarity of SMEs in this study suggests that theta power decreases and MTL BOLD increases are a general mechanism of associative encoding, irrespective of strategy or content. Successful formation of associations in imagined space and in semantic space thus seems to rely on similar mechanisms. This pattern of similar encoding effects for both encoding strategies supports the idea that humans use similar MTL mechanisms in spatial processing and in episodic memory encoding (see (Buffalo, 2015; Buzsaki & Moser, 2013; Ekstrom, 2014)).

In addition to decreases in theta power, increases in alpha/beta power were found during spatial processing and memory formation. These increases in alpha/beta power were mirrored by BOLD signal decreases during successful memory formation in occipital regions. A similar negative relation between occipital alpha power and BOLD signals has been reported during various tasks including visual attention (Scheeringa et al., 2011; Zumer et al., 2014). Furthermore, similar occipital alpha power increases have also been reported to predict long term memory formation during working memory maintenance, i.e. internal processing of the memory material (Khader et al., 2010; Meeuwissen et al., 2011), which relates to our study, as both encoding tasks involve constructing complex mental associations during memory formation. Therefore, during the formation of these internal scenes the occipital cortex might be actively inhibited to prevent task-interfering visual input (Jensen & Mazaheri, 2010; Klimesch et al., 2007). Arguably such an inhibition of posterior processing regions would be reflected by decreases in BOLD activity accompanied by alpha/beta power increases in the occipital cortex, consistent with the pattern observed in the present study.

Comparing EEG and fMRI task related activity, an overall consistent pattern emerges of a negative relationship between low frequency power and BOLD signals: theta power decreases match lateral and medial temporal BOLD signal increases, alpha power increases match occipital BOLD decreases. This fits with the general pattern of negative correlations between low frequency power and BOLD signals, reported by most studies investigating relationships of low

frequency EEG or LFP power and BOLD signals (Conner, Ellmore, Pieters, DiSano, & Tandon, 2011; Hermes et al., 2014; Khursheed et al., 2011; Magri, Schridde, Murayama, Panzeri, & Logothetis, 2012; Mukamel et al., 2005; Niessing et al., 2005). Decreases in low frequency power seem to be generally related to increases in neural activity as measured with the BOLD signal. Considering alpha power this is a widely accepted concept (Jensen & Mazaheri, 2010; Klimesch et al., 2007)

The present results suggest that this negative relationship of power and neural activity indeed also extends to theta oscillations and specifically theta oscillations in the MTL during memory encoding (Lisman & Jensen, 2013). The resemblance of low frequency power decreases during memory encoding in iEEG to positive SMEs in fMRI has been noted before (Burke et al., 2013) albeit no study before has shown this overlap in scalp EEG. Recording EEG and fMRI in the same paradigm, the present results support a strong functional link between theta power decreases and MTL BOLD increases, showing that these neural processes not only occur in the same regions, but also co-vary with the same task conditions.

The important question that remains is how, physiologically, we can link theta power decreases to increases in neural activity, and why these power decreases are predictive for successful memory formation. Traditionally, theta power increases have been hypothesized to relate to hippocampal-cortical feedback loops (Klimesch, 1996; Nyhus & Curran, 2010). However, theta power might not be very well suited to capture the connectivity between MTL regions and cortical areas. For instance, studies using intracranial recordings during memory formation reported decreases in low frequency power, including theta power decreases in the MTL along with increases in long-range phase synchrony (Burke et al., 2013). A similar relationship of local power decreases and global synchrony increases has been shown for alpha oscillations in sensory networks (Popov et al., 2013; Weisz et al., 2014). This relationship of local and global synchrony in alpha power might extend to other regions and lower frequency bands, i.e. to MTL regions and theta. Theta oscillations which are dominant in the MTL and retrosplenial cortex during rest and movement (Ekstrom, Suthana, Millett, Fried, & Bookheimer, 2009; Foster & Parvizi, 2012; Watrous, Lee, et al., 2013), might desynchronize during active tasks (Halgren, Babb, & Crandall, 1978; Mitchell, Sundberg, & Reynolds, 2009), for example memory encoding and spatial processing, in order to flexibly form fine grained cortical networks connecting cortical regions to specific MTL sub-regions (Watrous, Tandon, et al., 2013) The EEG records a spatially smoothed attenuated sum of LFPs (Buzsaki, Anastassiou,

& Koch, 2012), therefore fine grained long range synchronizations of specific individual cortical-MTL networks might appear as power decreases in scalp EEG and iEEG recordings.

A direct mapping of EEG power effects onto BOLD signals is not straightforward; both modalities correlate with LFPs (Buzsaki et al., 2012; Logothetis, Pauls, Augath, Trinath, & Oeltermann, 2001) but do not necessarily reflect the same neural processes (Ekstrom, 2010). Adding to the differences of physiological correlates between EEG and fMRI, both modalities differ substantially in their temporal and spatial resolution. Considering these constraints in spatial and temporal resolution, our EEG localization and fMRI results exhibited a relatively good fit. The present ongoing theta power decreases and MTL BOLD effects were largely overlapping in both modalities (see Fig 5C). In contrast, alpha/beta power and negative BOLD effects only closely matched for SMEs. Task related increases in alpha/beta power in EEG were evident during spatial processing and memory formation, overlapping with the negative occipital BOLD effects, which were only evident during memory formation (i.e. no such BOLD decreases were found during spatial processing, see Fig 5D). A possible reason for this discrepancy might be that alpha/beta power increases were more transient compared to the sustained theta power decreases, therefore these short lived effects might not have been picked up by event-related fMRI to the same extent as by EEG. Another difference is that the theta power decreases during spatial compared to non-spatial processing were localized to the left MTL, whereas the corresponding BOLD effect was bilateral. This result might be driven by a limitation of the beamforming technique, which has a tendency to suppress the weaker of two sources if their activity is correlated (Dalal, Sekihara, & Nagarajan, 2006; Van Veen et al., 1997). Indeed the BOLD signal difference between spatial and non-spatial processing was qualitatively stronger in the left compared to the right MTL as indicated by higher t-values in left MTL (see table 1 & 2).

A limitation of the present study is that an analysis of simultaneously recorded theta oscillations during fMRI was not feasible due to strong artifacts induced by the MR scanning environment (see Materials and Methods). Therefore EEG and fMRI were measured separately in independent subject samples, preventing calculation of EEG-fMRI correlations. Nevertheless, the same paradigm was used in both datasets and the same behavioral pattern of results was found across the two datasets. Therefore we can assume that, on average, the same cognitive processes were driving the EEG and fMRI effects in the two datasets (Singh, 2012).

## CONCLUSION

In summary, present results show that decreases in theta oscillatory power in the MTL - similar to other cortical low frequency oscillations (i.e. alpha/beta) – co-occur with neural activity as reflected in fMRI-BOLD signals. MTL activity in memory tasks might therefore map onto decreases in EEG/MEG theta power and not, as often suggested, to increases in theta power. MTL and theta effects were more pronounced during the Method of Loci mnemonic, which indicates that navigating cognitive space might be a particularly efficient encoding strategy by maximally driving the neural processes crucial for spatial processing and episodic memory. The reported theta decreases located to MTL BOLD increases are an important contribution to debate how theta oscillations are linked to MTL BOLD activity.

# STUDY 3: SPURIOUS CORRELATIONS IN SIMULTANEOUS EEG-FMRI DRIVEN BY IN-SCANNER MOVEMENT

Simultaneous EEG-fMRI provides an increasingly attractive research tool to investigate cognitive processes with high temporal and spatial resolution. However, artifacts in EEG data introduced by the MR-scanner still remain a major obstacle. This study employs a standard analysis pipeline and shows that head motion, one overlooked major source of artifacts in EEG-fMRI data, can cause plausible EEG effects and EEG-BOLD correlations. Specifically, low frequency EEG (<20 Hz) is strongly correlated with in-scanner movement. Thereby, minor head motion (<0.2 mm), induce spurious effects in a twofold manner: Small differences in task correlated motion elicit spurious low frequency effects, and, as motion concurrently influences fMRI data, EEG-BOLD correlations closely matched motion-fMRI correlations. We demonstrate these effects in a memory encoding experiment showing that obtained theta power (~3-7 Hz) effects and theta-BOLD correlations reflect motion in the scanner. These findings highlight an important caveat that needs to be addressed by future EEG-fMRI studies.

## INTRODUCTION

Simultaneous EEG and fMRI recordings provide an immensely useful neuroimaging technique as they offer the unique possibility to non-invasively record neural activity at highest temporal and spatial resolution (Debener, Ullsperger, Siegel, & Engel, 2006). Such rich multidimensional datasets allow for numerous ways of merging EEG and fMRI data (Huster, Debener, Eichele, & Herrmann, 2012) with the most popular approach being EEG-informed fMRI analysis. Here, EEG parameters of interest are used to create a model of the BOLD responses. BOLD signals can be correlated with ERP components (Debener et al., 2005), resting state alpha power (Goldman, Stern, Engel, & Cohen, 2002) or task-related oscillatory power changes (Hanslmayr et al., 2011). Resulting spatial maps provide regions in which BOLD signal changes correlate with EEG parameters indicating a common generator of BOLD and EEG signals.

However the biggest restraining factor in simultaneous recordings is still the quality of the EEG data. Usually two types of artifacts are considered: the gradient and ballisto-cardiographic (BCG) artifacts (Allen, Polizzi, Krakow, Fish, & Lemieux, 1998; Debener, Mullinger, Niazy, & Bowtell, 2008; Liu, de Zwart, van Gelderen, Kuo, & Duyn, 2012; Mullinger, Havenhand, & Bowtell, 2013; Niazy, Beckmann, Iannetti, Brady, & Smith, 2005). Another major source of artifact, spontaneous movement, is rarely discussed. Motion is a general problem for simultaneous recordings, since movement of any conductive material (i.e. EEG electrodes and wires) in a static magnetic field (as in an MR scanner) causes electromagnetic induction and consequently an artifactual EEG signal. Therefore, even very minor head motion on a sub-millimeter level severely affects the EEG, as for example the tiny movements related to every heartbeat are visible in the EEG data as BCG (Debener et al., 2008; Mullinger et al., 2013). Most researchers employing EEG-fMRI accept that these artifacts remain to some extent in their data, even after careful preprocessing, implicitly assuming that those artifacts are mainly decreasing the signal to noise ratio but not introducing spurious effects. This logic fails when head motion is correlated with the task parameters of interest (i.e. paradigm, behavioral performance, BOLD signals). Since it is well known that fMRI-BOLD signals are correlating with motion (voluntary or physiologically driven), BOLD-motion correlations might be a serious concern for EEG-fMRI correlations (Birn, Bandettini, Cox, & Shaker, 1999; Friston, Williams, Howard, Frackowiak, & Turner, 1996; Murphy, Birn, & Bandettini, 2013; Power et al., 2014).

We here present data measuring EEG data inside and outside an MR-scanner. EEG and simultaneous EEG-fMRI data were recorded during a memory paradigm where we focused on

theta oscillations and their relation to BOLD signals (Figure 1A). The memory relevant aspects of this dataset will be reported in detail elsewhere (Fellner et al., in prep) and are only in so far relevant for this study as motion induced spurious "memory-like" effects. Specifically, we demonstrate that: (i) In-scanner EEG data is highly dominated by motion related artifacts. (ii) Task related motion in-scanner can cause spurious task related EEG power effects that are in stark contrast to artifact-free out-of-scanner data. (iii) In scanner motion can drive spurious, but neurophysiologically plausible EEG-BOLD correlations.

## METHODS

### *PARTICIPANTS*

The same memory encoding paradigm was measured in two different setups: in one group of twenty-five participants simultaneous EEG-fMRI was recorded (in-scanner data), whereas another group of thirty volunteers participated in an EEG only study (out-of-scanner data). In-scanner data from three participants had to be excluded because of poor data quality, one participant had to be excluded because of a missing structural scan and data from another two participants did not provide enough items in one of the memory conditions, i.e. not enough items either remembered or forgotten resulting in a sample of nineteen in-scanner datasets (mean age=22.95, 12 female). In out-of-scanner data eight participants had to be excluded because of low trial numbers resulting in twenty-two out-of-scanner datasets (mean age=20.23, 12 female). All participants spoke German as their native language, reported no history of neurologic or psychiatric disease, and had normal or corrected to normal vision.

### *PARADIGM*

Participants in both datasets participated in the identical experiment. The experiment consisted of twelve repeated memory encoding-recall cycles including an encoding phase, a distractor phase, a free recall memory test and a short rest period (see Figure 1). In each encoding phase the participants' task was to memorize 20 words. During free recall participants were asked to verbally recall items of the preceding encoding phase. Recall performance was used to classify encoding trials as subsequently remembered or forgotten. Each encoding-recall cycle ended with a 20 sec rest period in which participants were allowed to relax (blink etc). During encoding participants were instructed to use two differing mnemonic strategies: The method of loci and the pegword method. Both encoding conditions are cognitive demanding and call for high levels of attention. Both conditions showed no difference in spurious

oscillatory activity and movement pattern and therefore data was merged for the presented analysis. Each to-be-encoded word was presented for 3 sec followed by fixation cross presented with an exponential jitter from 1.5-7 sec to improve design efficiency for event-related fMRI analysis. The encoding phase was followed by a visual detection task serving as distractor task for the memory paradigm. Participants were asked to detect contours in a field of Gabor patches and to indicate their answer by buttons presses (similar task as reported in Hanslmayr et al., 2013). In the following free recall phase participants were asked to recall all 20 words as presented during the preceding encoding phase. In scanner, verbal responses were recorded using an fMRI-compatible microphone (MRconfon). Scanner noise was removed from the resulting audio files using the free software package Audacity (http://audacity.sourceforge.net/). In out-of-scanner EEG recordings recall performance was scored manually by the experimenter. Each experiment was split into 4 consecutive recording sessions to keep file sizes manageable.

Different word material was used for each study-test cycle counterbalanced across participants and between conditions. Participants remembered on average 48.7% (std= 0.12) of the words in the in-scanner dataset and 55.5% (std=0.13) in the out-of-scanner datasets, revealing a non significant tendency of higher recall rates out-of-scanner ($T(39)=1.757$, $p=0.087$).

### *EEG DATA-RECORDING*

The in-scanner EEG data were recorded from 63 channels in an equidistant montage, (EasyCap, Herrsching, Germany). An MR compatible amplifier (BrainAmp MR, Brain Products, Gilching Germany) together with the Syncbox device (Brain Products) was used to synchronize EEG recordings to the MR scanner clock. Recordings were referenced to Fz and later rereferenced to average reference (which excluded any noisy channels). Impedances were kept below 20 kΩ. ECG was recorded by an electrode placed below the left scapula. The signals were amplified between 0.1–250 Hz and a software filter with a low cutoff of 0.3Hz and high cutoff of 70Hz applied during acquisition. The EEG data were sampled at 5 kHz with a resolution of 0.5μV. Cables connecting cap and amplifiers were fixated by adhesive tape to prevent any additional movement-related artifacts. The same EEG amplifier and caps were used in both experiments (in-scanner and out-of-scanner). The only differences in recording between the two datasets concerned specific settings for simultaneous recordings: in the out-of-scanner data no syncbox was used, data was sampled at 500 Hz with a resolution of 0.5μV, no software filters were set and no ECG was recorded. During out-of-scanner recordings participants were sitting upright in front of a computer screen instead of in supine position in-scanner, where

stimuli were presented on a mirror. Changes in body position have been shown to affect resting state EEG in higher frequencies (>30 Hz), but not task related changes in lower frequency bands (Rice, Rorden, Little, & Parra, 2013; Thibault, Lifshitz, Jones, & Raz, 2014).

### FMRI DATA RECORDING

After EEG preparation participants were placed in the scanner. Extra padding was placed surrounding the head of the participants to suppress head movements and discomfort caused by the EEG cap. Imaging was performed using a 3-Tesla MR head-only scanner (Siemens Allegra). During fMRI scanning, 2475-2480 whole-brain image volumes, consisting of 34 axial slices each, were continuously acquired using a standard T2*-weighted echo-planar imaging (EPI) sequence (repetition time TR=2000 ms; echo time TE=30 ms; flip angle=90°; 64x64 matrices; in-plane resolution: 3x3 mm; slice thickness: 3 mm, interleaved slice acquisition). High-resolution sagittal T1-weighted images were acquired after the functional scans, using a magnetization-prepared rapid gradient echo sequence (TR=2250 ms; TE=2.6 ms; 1 mm isotropic voxel size) to obtain a 3D structural scan. To prevent EEG artifacts caused by the helium pump and internal ventilation of the scanner, both were switched off during the recordings.

### EEG DATA PREPROCESSING

The first preprocessing step for in-scanner EEG data was to reduce scanner-induced gradient artifacts. The EEGLAB plug-in FMRIB (www.sccn.ucsd.edu/eeglab, (Niazy et al., 2005) was used to reduce gradient artifacts. Synchronisation of scanner clocks by the syncbox ensured accurate sampling of the gradient artifact. BCG artifact correction involved two steps: heartbeat detection and BCG correction. At first, each heartbeat was identified by detecting QRS complexes in the ECG recording. Heartbeat detection was carried out using the FMRIB implemented method or AMRI-eegfmri-toolbox (https://amri.ninds.nih.gov/cgi-bin/software, Liu et al. (2012)). For all but one dataset, the AMRI method provided a higher QRS detection performance revealed by average QRS-triggered-ECG ERPs and visual single trial inspection. OBS method was used to reduce the BCG artifact (Niazy et al., 2005).

For analysis of memory encoding effects, encoding phase data from both datasets, in-scanner and out-of-scanner, were epoched into trials -2.5 to 3.5 sec around item onset to provide sufficiently long epochs for wavelet analysis. The epoched data was visually inspected, and trials containing residual scanner artifacts and other idiographic artifacts (channel jumps, muscle artifacts, noisy channels) were excluded from further analysis. Noisy channels were excluded in 4 datasets recorded out-of-scanner and in 3 datasets in-scanner, maximally 3

electrodes were excluded in each of these datasets. Infomax independent component analysis as implemented in Fieldtrip (www.ru.nl/fcdonders/fieldtrip, (Oostenveld et al., 2011) was applied to correct for residual artifacts (e.g. remaining gradient and BCG artifacts, eyeblinks, eye movements, or tonic muscle activity). The maximum number of independent components was estimated, equaling the number of channels in a dataset (59 to 62 ICs). On average 11.8 ICs were rejected owing to these residual artifacts in the in-scanner dataset (range: 9-17 ICs), 3.8 ICs were rejected in the out-of-scanner data (range:1-8 ICs). Remaining ICs were back projected to channel level. Data was again visually inspected for remaining artifacts and then subjected to further analysis. In in-scanner data, on average 62.05 hit trials (range 28-113) and 65.21 miss trials (range 34-115) passed the artifact corrections. Out-of-scanner consisted of an average of 107.55 hit trials (range 56-170) and 82.55 miss trials (range 41-142). Finally, for datasets with rejected electrodes prior to ICA, those channels were interpolated using neighboring electrodes.

### FMRI DATA PREPROCESSING

Image preprocessing and statistical analysis was performed using SPM8 (Wellcome Department of Cognitive Neurology, London: UK, www.fil.ion.ucl.ac.uk/spm). After discarding the first images of each session, time series were corrected for differences in slice acquisition time, and spatially realigned to the first image of the session. The realignment parameters obtained in this preprocessing step were used to quantify movement in the latter analyses. The mean functional image was coregistered with the structural image, and all images were then normalized to the MNI brain (Montreal Neurological Institute, www.mni.mcgill.ca) using the normalization parameters determined from segmentation of the structural image. As a last step, images were smoothed with a Gaussian kernel of 8 mm FWHM.

### EEG DATA ANALYSIS

For time frequency analysis, data were subjected to a wavelet transform as implemented in Fieldtrip (www.ru.nl/fcdonders/fieldtrip,). Data were filtered to obtain oscillatory power between 2 Hz and 30 Hz using wavelets with a 5 cycle length. Resulting data was z-transformed to the mean power and standard deviation across all trials of each respective frequency band and channel.

To identify time-frequency clusters showing significant differences between conditions, a sliding window cluster permutation test was used (for details, see Staudigl and Hanslmayr (2013)). This procedure was used to analyze memory encoding effects (Figures 4 A&B) and to analyze power differences between high and low motion encoding trials (Figure 4 C). For each 300 ms x 1 Hz time bin a cluster permutation test, as implemented in Fieldtrip, was calculated

(Maris & Oostenveld, 2007), which returned a p-value for each bin. To check if significant time clusters revealed in this analysis, show continuous scalp topography, another cluster permutation test was performed on the respective time-frequency bin of these clusters.

### MOVEMENT MEASURE

A movement measure was calculated using fMRI realignment parameters. In the realignment procedure absolute displacement in 6 directions (*x, y, z* translations and 3 rotations: pitch, yaw and roll) of every MR volume relative to the first MR volume is estimated. Realignment parameters represent absolute shifts in position relative to the first volume acquired in a given session. Those absolute position measures can be used to calculate a relative motion measure for each 2 s (TR) period by subtraction of realignment parameters of consecutive scans. We combined realignment parameters to a single normalized motion measure:

(MATLAB code: *motion_parameter= zscore(sum((diff(zscore(realignment_parameters)).^2),2))*), Both motion types, rotation and translation, exhibited highly similar time courses (Figure 1B). Albeit theoretically head rotations should cause the biggest artifact by cutting the magnetic flux, natural human head motion rotation co-occur with translations explaining the similarity between both measures. Therefore movement collapsed across all 6 motion parameters was used for all subsequent correlative analyses. To more closely identify the motion patterns related to the spurious correlations, we additionally report mean relative differences of each realignment parameter between consecutive scans. This measure is more easily comparable to outputs of standard SPM analysis pipelines and is referred to as relative translation or relative rotation (Figure 5).

### MOVEMENT ANALYSIS OF EEG DATA

To investigate the relationship of oscillatory power and in-scanner motion, irrespective of condition, the continuous artifact corrected EEG recording was epoched in 2-second trials relative to each volume trigger. Trials were epoched from -500 ms to 2500 ms relative to each volume trigger in order to provide a sufficiently long epoch for wavelet analysis. The resulting 2-second trials are temporally matched to a certain fMRI volume (i.e. realignment parameter and motion parameter). The out-of-scanner data was epoched into arbitrary consecutive 2-second epochs to create a comparable dataset. Those epochs were subjected to time frequency wavelet analysis specified above. The *z*-transformed mean power for each 2-s scan interval was calculated for 5 frequency bands (delta: 2-3Hz, theta 4-8Hz, alpha: 9-12Hz, beta1: 13-16Hz, beta2: 17-20Hz).

For in-scanner data Spearman's rank correlation coefficients were calculated between EEG power and in-scanner motion for each participant, electrode, and frequency band. Spearman's correlations were used to prevent outlier driven correlations; furthermore trials with extreme power values, *z* larger than 2, were excluded from this analysis. To test, if group level correlations significantly exceeded zero, and to investigate the scalp topographies of those correlations, correlation coefficients were first Fisher z-transformed, and then subjected to a two-stage permutation approach. In a first step Wilcoxon sign-ranked tests were carried out for each electrode testing if correlation coefficients are different from zero. Then, to correct this result for multiple comparisons across electrodes a permutation test was employed. The test used 1000 permutation runs shuffling the sign of the correlation coefficient randomly for each subject and electrode. After each run, a Wilcoxon-signed-rank test was calculated returning the number of electrodes showing a significant effect in a randomly distributed dataset. After 1000 permutation runs this procedure yields test distribution of the probability of a given number of significant electrodes in a sample with random correlations. This distribution was used to calculate the corrected p-value henceforth referred to a $p_{corr}$.

### FMRI: POWER AND MOVEMENT CORRELATIONS

To investigate correlations of BOLD signals with motion and EEG power several random-effects GLMs were set up. In EEG-fMRI GLMs theta power was added as a regressor either throughout the scanning session (GLM-alltheta) or only during encoding trials that passed stringent artifact correction criteria (GLM-cleantheta). Realignment parameters were added as regressors of no interest only to GLM-cleantheta. In all other models we strived to identify effects of motion in the data and therefore omitted realignment parameters from the GLMs. In each GLM event-related regressors modeling remembered and forgotten trials for each encoding condition, task block regressors modeling rest periods, free recall periods for each encoding condition and the distracter task, and session-specific block and drift regressors were included. GLMs differed only in the specific theta/motion regressor added.

In GLM-alltheta, a theta power regressor was added based on theta power across the whole experiment including theta power during high motion recall phases. Power irrespective of motion or other artifacts (after the standard cleaning methods outlined above) was convolved with the canonical HRF and downsampled to match the 2 s TR and orthogonalized to regressors modeling task epochs and remembered and forgotten events. In GLM-allmotion a motion regressor was added based on the combined motion parameter across the whole recording period. To construct the allmotion regressor the combined movement parameter was z-

transformed, convolved with the HRF, and orthogonalized to task regressors to avoid regressor correlations. For GLM-cleantheta, a theta regressor was built by averaging z-transformed power of all electrodes showing the positive theta encoding effect (see Figure 4A) of all artifact free encoding trials. These power time courses were concatenated and zeros were added for trials that did not pass artifact correction. Data during epochs outside of encoding was not considered (i.e. replaced with zeros). This time series was then convolved with the canonical HRF, downsampled to match the TR and mean centered to avoid regressor correlations. GLM-smallmotion was designed to capture only correlations of small motion with BOLD signals. A motion regressor was added with only motion parameters of scans in which none of the relative translational movements exceeded 0.2 mm. The analysis was restricted to those small movements, as those match the small movements that occur during encoding trials (see Figure 5). Motion parameters of those scans were *z*-transformed and motion parameters with larger movements were replaced with zeros. The time series were then convolved with the HRF, and orthogonalized to task regressors to avoid regressor correlations

GLM-cleanalpha and GLM-cleanbeta were matching GLM-cleantheta, except, that in these models average alpha and beta power respectively was averaged across all electrodes, convolved and added to the GLM. Non-convolved models were matching GLM-alltheta, GLM-cleantheta and GLM-allmotion and GLM-small motion except that in the non-convolved (no convolution with HRF) version of the theta power or motion model were added to the GLM.

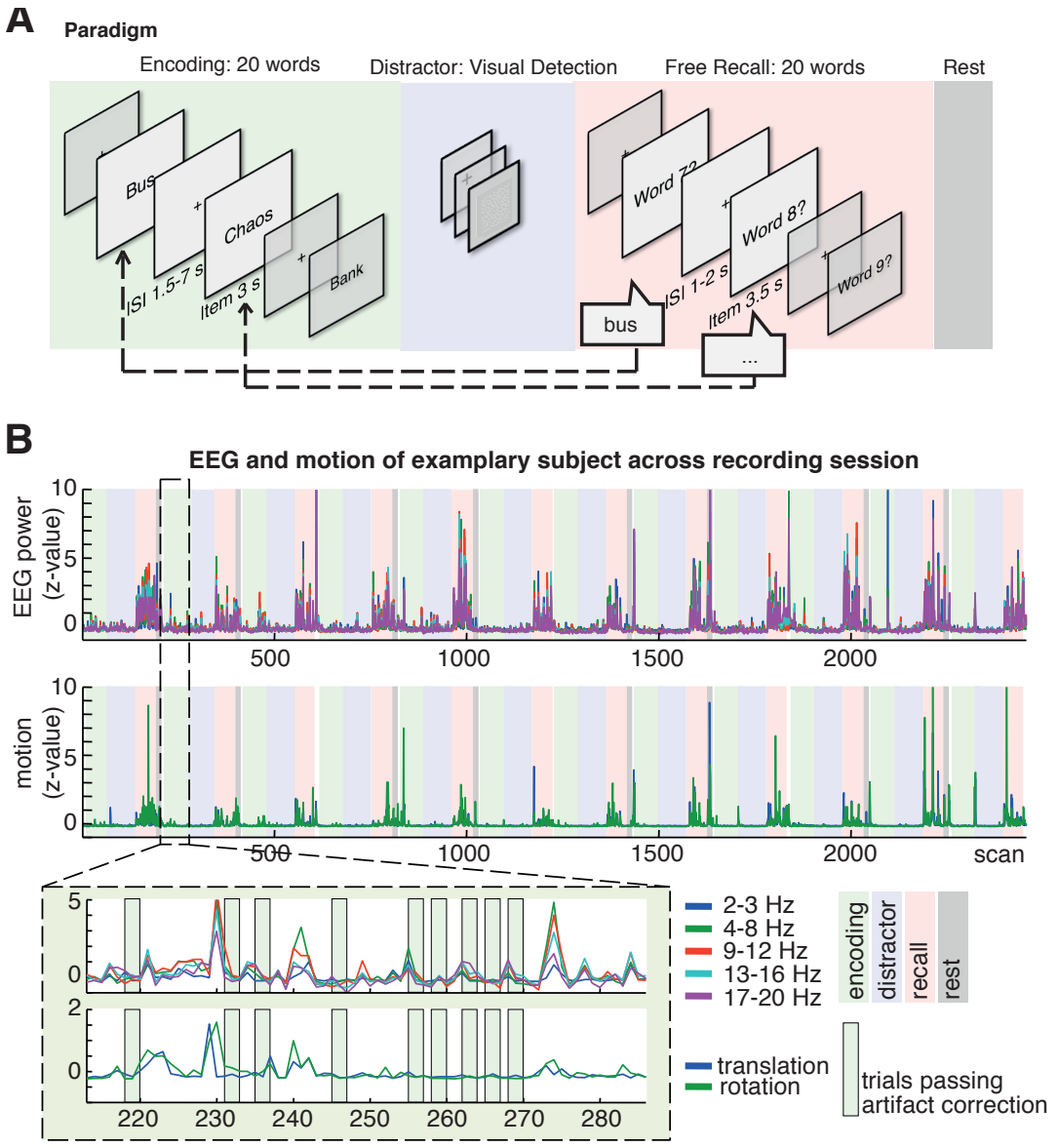


**Figure 1: Paradigm and exemplary oscillatory power and motion timecourses** (A) The experiment consisted of 12 study-recall cycles, each of these cycles consisted of an encoding phase, a visual detection task, which served as a memory distracter, a free recall phase and a short rest period, in which participants were allowed to relax, move and close their eyes. During recall participants verbally recalled items presented in the previous encoding phase. Items during encoding were classified as later remembered or forgotten according to those responses. (B) Power time courses of different frequency bands and motion during the whole scanning session of one exemplary participant. EEG closely resembles motion throughout all four task phases. Task phases are indicated by the shaded background colors matching coloring in (A). Epochs of interest in this experiment were encoding phases highlighted by green boxes. An exemplary encoding epoch is highlighted by dashed lines and shown in close-up. Encoding phases exhibited no exceedingly high motion and only low motion encoding trials that passed artifact correction highlighted by green boxes passed visual artifact inspection and were subjected to further encoding analyses.

## RESULTS

### *LOW FREQUENCY POWER AND MOTION IN SCANNER*

EEG power in-scanner is largely dominated by head motion throughout all four phases of the experiment (i.e. encoding, distracter, recall, and rest; see paradigm in Figure 1A). Figure 1B shows how EEG power in all lower frequency bands closely resembles translational and rotational head motion during the scanning session. This close relationship is especially evident during the free recall phase, which was not considered a period of interest, due to the high levels of movement generated by verbal recall. However, motion and power also co-varied during the low motion encoding phase (highlighted dashed box, Figure 1B). Not all encoding phase data was analyzed, but only relatively low motion trials that passed visual inspection during artifact correction (highlighted in light green in Figure 1B, also see Figure 5 for absolute motion values). Rotational and translational motion measures are closely related and consequently were combined into one motion parameter in all following analyses. In line with the above single-subject observations, analysis across all participants revealed that EEG power and motion are positively correlated across the whole experiment in all lower frequency bands (<20 Hz), even after exclusion of outlier trials with z-values of power exceeding z>2 (all frequency bands $p_{corr}$ <0.001) and also during the artifact free encoding phase trials, where correlations are smaller but still highly significant (all frequency bands $p_{corr}$ <0.001, Figure 2 shows the correlation topographies).

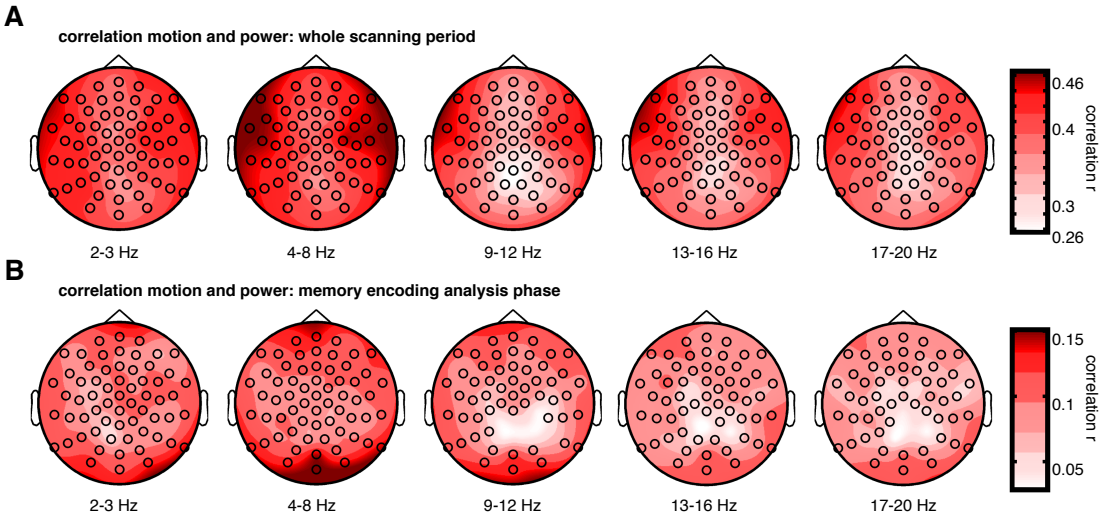


**Figure 2: Scalp topographies of motion power correlations across frequencies** Power and motion are significantly positively correlated in all lower frequency bands. (A) Topography plots of Spearman correlation coefficients throughout the scanning sessions (outlier corrected for power z>2). (B) shows correlation of power and motion for used encoding trials only. Note that topographies of correlations do not vary across frequency bands. Correlations were more pronounced on the outermost electrodes resembling a ring like pattern; circles highlight electrodes showing significant differences. All $p_{corr}$´s<0.001

As an assessment of data quality in- and out-of-scanner, mean raw EEG power in-scanner for all task phases was contrasted with out-of-scanner data. In-scanner data revealed amplitudes almost 10 times higher compared to out-of-scanner data (see Figure 3A). EEG power irrespective of frequency band was always highest for the rest and recall (high movement) conditions, whereas out-of-scanner data show frequency band specific variations across the task phases. This is especially apparent when controlling for the difference in scaling between measurements by normalization to the respective mean and standard deviation (Figure 3B). For example in data recorded out-of-scanner, alpha power (9-12Hz) during the distracter phase, a visual attention task, is more pronounced than during other phases. Also, during the free recall phase, when participants spoke, larger suppression of alpha and beta (9-20Hz) is evident presumably related to motor activity. In-scanner data is lacking these pronounced frequency specific effects. The differences between these two datasets show that the out-of-scanner EEG reflects general neurophysiological characteristics of the task whereas in-scanner EEG power across frequency bands and tasks seems to be largely driven by a common generator. A probable

common generator is motion, as mean EEG power in-scanner across phases (Figure 3B) closely resembles average relative motion across all task phases (Figure 3C).

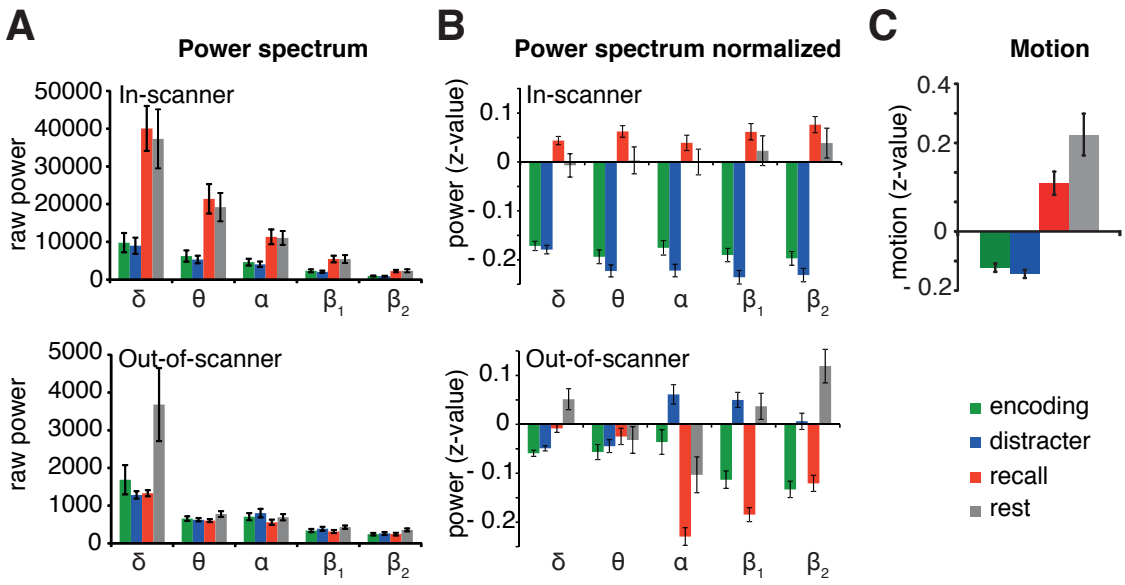


**Figure 3: Mean power and motion across task phases** EEG power is highly distorted in-scanner compared with out-of-scanner. (A) Mean absolute oscillatory power across the different phases of the experiment plotted for in-scanner and out-of-scanner data. There is a remarkable difference in scaling: power of inside scanner data is 10 times higher than outside scanner data (note the order-of-magnitude difference in ordinate scales for in-scanner and out-of-scanner data). (B) Z-transformed mean power of each task phase reveal that the frequency spectrum in the out-of-scanner data varies with experimental phase whereas in-scanner data show very little variation between phases. Mean motion per condition is shown in (C) and highly resembles mean power per condition in-scanner. Error bars show SEM.

### TASK-RELATED EEG EFFECTS: IN-SCANNER EEG CONTRASTED WITH OUT-OF-SCANNER EEG

In both datasets, in- and out-of-scanner, memory-encoding effects were analyzed by contrasting power in frequency bands from 2-20 Hz depending on subsequent memory performance. This contrast of later successfully remembered and later forgotten trials is usually termed subsequent memory effect (SME; (Paller & Wagner, 2002). For in-scanner data, a sliding cluster statistic revealed only positive SMEs, i.e. higher power for later remembered than for later forgotten trials (Figure 4A). In the theta band (4-7 Hz), two clusters of positive SMEs were evident from 500 ms before until 500 ms post word onset, and another cluster 1500 – 2500 ms after word onset (highlighted boxes and topographies in Figure 4A). Importantly, these theta SMEs in-scanner are in stark contrast to the effects found in the out-of-scanner dataset (Figure 4 B). In this dataset negative memory SMEs in the theta frequency range were found, i.e. less power for later remembered than later forgotten words. These negative SMEs were evident 500 – 1000 ms and 1500 – 2500 ms after word presentation (Figure 4B). As EEG data recorded outside the scanner is more reliable, i.e. free of any MR-related artifacts, the positive theta effect in-scanner seems to be related to artifacts caused by the scanning environment. Notably, negative as well as positive SMEs in the theta frequency range are in line with a host of recent EEG studies (see(Hanslmayr & Staudigl, 2014), for a recent review). Of note, the in-scanner theta effects seemed to be not limited to the theta frequency range but rather appeared to be part of a unselective power increase ranging from 2-20 Hz.

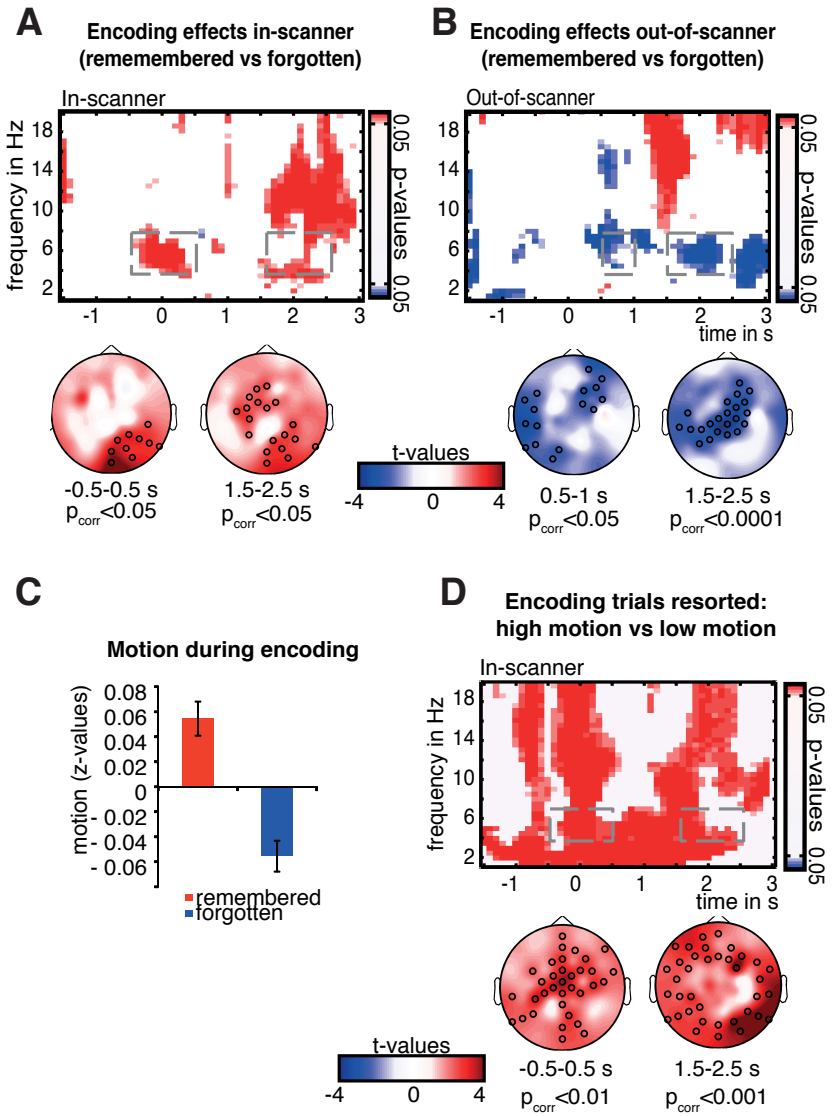


**Figure 4: Memory encoding effects and motion** (A) In-scanner data showed clusters of significant positive memory encoding effects. (B) In contrast, out-of-scanner data revealed positive and negative effects. Specifically, effects in the theta frequency range (~4-7 Hz) are reversed in-scanner compared with out-of-scanner: increases in theta power were found in-scanner, whereas decreases in theta power were evident out-of scanner to be related to successful memory formation. (C) Motion during later remembered trials was higher than during forgotten trials. (D) Resorting the same trials as in (A) not regarding memory performance, but regarding motion during the trials reveals significant power increases similar as for in-scanner memory effects. Topography plots in (A), (B) and (D) show theta effects highlighted in the time-frequency plots above with grey boxes; circles highlight electrodes showing significant differences. Time-frequency plot show p-values for time-frequency bin that reveal significant differences between remembered and forgotten trials. Warm colors indicate increases in power for remembered/high motion trials in contrast to forgotten/ low motion trials respectively. Error bars show SEM.

### SMALL EVENT-RELATED MOTION CAUSES SPURIOUS EVENT-RELATED OSCILLATORY EFFECTS

The above analyses show that EEG power in-scanner closely tracks motion artifacts suggesting motion as potential source of the artifactual task-related theta increases. However, correlation between motion and EEG power alone cannot explain the reversal of the theta effects related to task performance (i.e. subsequent memory) between the two datasets. For motion artifacts to drive task-related contrasts, motion needs to be correlated with memory formation, which might seem implausible at first. However, analysis of motion parameters showed that motion was indeed task related (Figure 4C). Specifically, the motion measure during those encoding trials that passed rigorous artifact rejection was z-transformed and contrasted dependent on memory performance. Surprisingly, participants very robustly exhibited more head motion during the encoding of words that were subsequently remembered compared to forgotten words ($T(18)=4.47$ $p<0.001$). Furthermore, in line with our other findings, splitting encoding trials into high and low motion trials and contrasting their EEG power, regardless of memory outcome, revealed that head motion and EEG power are indeed strongly related, with high motion relative to low motion trials inducing EEG power increases, especially in lower frequency bands (Figure 4D). Additionally, the time-frequency range of high vs. low motion effects was comparable to the positive SMEs obtained in scanner (comparing Figures 4A & 4D). The motion induced EEG power increases were present in all frequency bands. Especially in the theta band, this increase was continuous throughout the whole trial period (Figure 4D). Together, these analyses reveal that small task-related differences in motion can cause task-related effects in in-scanner EEG data.

### MOTION SHOWING TASK-RELATED DIFFERENCES

Event-related motion causing the spurious "subsequent-memory-effect" in each of the three translation and rotation dimensions is shown in Figure 5. Relative motion between consecutive realignment parameters are plotted to show the pattern of event- related motion in absolute mm and radians comparable to the typical realignment parameter output of fMRI preprocessing pipelines. In general, motion during encoding - even before excluding artifactual trials - was small (Figure 5A). Average motion in trials that passed visual inspection during preprocessing (Figure 5A, red and blue bars) is even lower than in trials before artifact inspection and rejection (Figure 5A, green bars) demonstrating that visual artifact correction of EEG data also implicitly reduces the magnitude of motion in the remaining data. Mean motion in each translation and rotation dimension is higher for successfully encoded trials in contrast to later forgotten trials (Figure 5A red compared with blue). To assess the statistical significance of

this effect, mean motion of *z*-transformed relative motion in each motion dimension was calculated for hits and misses and subjected to a repeated measurement ANOVA with factors motion direction and memory. The ANOVA showed no significant interaction ($F(1,18)=1.343$), no significant main effect of motion direction ($F(1,18)=1.250$) but a significant effect of memory ($F(1,18)=6.617$; $p<0.05$) indicating a memory effect for motion that was unspecific to any given movement direction. Albeit qualitatively the biggest memory related differences in motion were found to be related to a *z* translation (Figure 5A, red compared with blue). Figure 5B shows the distribution of this motion parameter (*z*-translation) for each participant and trial, which reveals that mean relative motion across all used trials and participants did not exceed 0.1 mm with the majority of movement being below 0.2 mm. This latter result shows that the task related effect was driven by movements that were small in magnitude but which consistently correlated with memory (as opposed to a few large movement outliers driving the effect). One would expect that motion increases across the recording session and that such an increase in motion across trials might explain the reported task related effect. Importantly, differences in motion between remembered and forgotten trials were not related to difference in position of the trials in the recordings. Indeed, the higher motion remembered trials tended to occur on average even earlier (M=1152 scan, std =180) than the lower motion forgotten trials (M=1199 scan, std=209), albeit this difference was not significant ($T(18)=-1.244$, $p>0.2$).

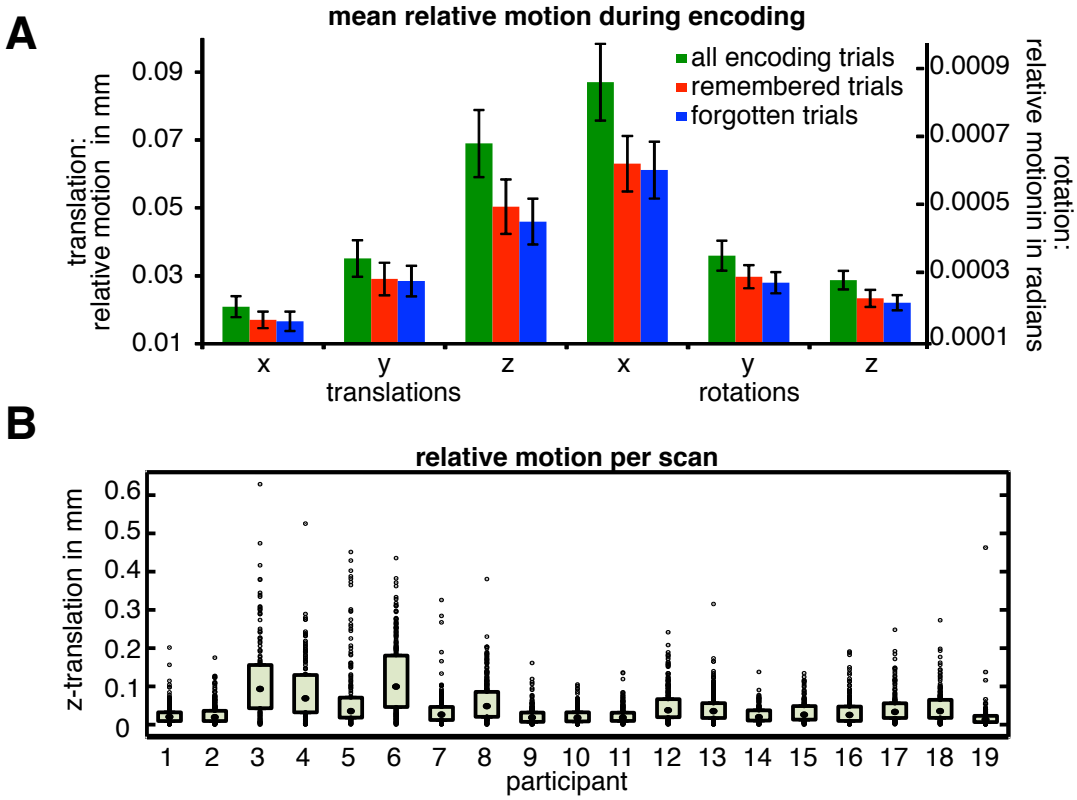


**Figure 5: Overview of the relative motion during encoding** (A) shows relative motion in all 6 motion dimensions (*x, y, z* planes for translation and rotation) during all of the encoding epochs (green bar) and for all trials used in memory effects analysis and EEG power-fMRI correlations (blue and red bars). To highlight memory related motion differences trials are split into remembered (red) and forgotten (blue) trials. (B) Distributions of relative translational motion in the *z* direction, the direction showing the largest relative movements. The median motion is highlighted in the center of the boxplots, borders of the rectangle signify the respective first and third quartile. Note that all relative motion is below 0.5 mm and all average motion is below 0.1 mm.

## MOTION CAUSES SPURIOUS EEG-FMRI CORRELATIONS

Next, we were interested in whether motion can also introduce spurious EEG-fMRI correlations. This is a highly relevant question given that EEG-BOLD correlations are the major motivation of most multimodal imaging studies (Hanslmayr et al., 2011; Mantini, Perrucci, Del Gratta, Romani, & Corbetta, 2007; Scheeringa et al., 2011). To this end EEG time courses are usually convolved with the HRF. Therefore it is important to elucidate if motion driven correlations with the fMRI data are also evident after convolution with the HRF. To test for this possibility, BOLD signals were separately correlated with convolved EEG power and convolved motion.

In a first step, we were interested in the general pattern of convolved motion-BOLD correlations including high motion task phases, and whether EEG-BOLD correlations follow the same pattern. For this analysis theta power and motion parameters throughout the scanning session were convolved and put as regressor of interest in two separate GLMs (GLM-alltheta and GLM-allmotion). Both continuous theta power and motion regressors showed widespread negative BOLD correlations in largely overlapping areas (Figure 6A, $p<0.001$, clustersize$\geq$10, see SI Table S1), especially in regions that are known to be susceptible to artifacts, like the ventricles and areas on tissue borders. However, strong negative correlations were also obtained in regions relevant to cognitive processes: medial frontal, medial- and lateral-parietal regions. This demonstrates that convolved EEG power and convolved motion indeed correlate with fMRI and that these correlations largely overlap.

These first BOLD-motion/EEG correlations identified similarities between motion and EEG correlations. However, including highly artifact loaded data (i.e. EEG data during the recall phase) does not resemble typical analysis pipelines. A more relevant question thus is if motion can also produce spurious correlations after stringent, state-of-the-art removal of data containing artifacts. A second set of GLMs was constructed to explore if the impact of motion on EEG and BOLD signals is large enough to also drive theta-BOLD correlation during a standard analysis pipeline. A theta GLM (GLM-cleantheta) was designed, including only convolved theta power of encoding trials that survived rigorous artifact removal. To further control for movement related artifacts, realignment parameters were added to the GLM-cleantheta. Matching this more conservative approach of correlating theta and BOLD signal, a second motion GLM was setup to investigate the correlation of small movements with the BOLD signal (GLM-smallmotion, only including motion not exceeding 0.2mm in any of the translational dimensions throughout the scanning session). The results of this analysis still revealed a similar motion driven pattern as the previous analysis (Figure 6B, Table S2). Theta power during encoding still correlated negatively with BOLD signal predominantly at medial locations (cyan areas, Figure 6B, $p<0.001$, clustersize$\geq$10), areas that also show a strong overlap with areas correlating with motion (Figure 4B, white areas). Lowering the statistical threshold to $p<0.005$ reveals that theta-BOLD correlations show a rim structure at frontal coronal slices and in axial slices (Figure 4B green areas) and exhibit larger overlap with motion-correlated areas (Figure 6B, yellow and white areas). Importantly, the correlations shown in green and cyan could easily pass as physiologically plausible correlates of medial frontal theta power (Cohen, 2014). Clusters showing positive correlations between motion and BOLD signals, and theta and

BOLD signals, are reported in Figure S1B. These positive correlations were predominantly found in areas related to voluntary movements such as the precentral gyrus and the cerebellum.

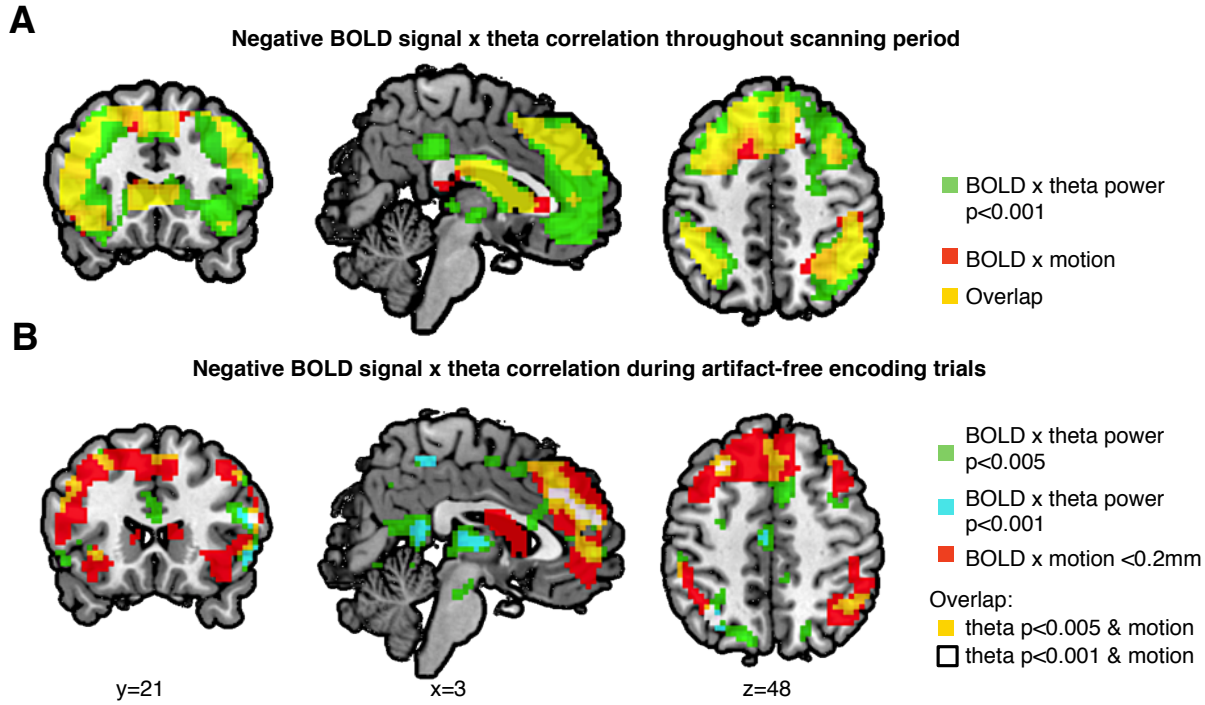


**Figure 6: Negative EEG-BOLD signal and negative motion-BOLD signal correlations.** Correlating convolved continuous theta power throughout the scanning session resulted in large overlap with areas correlating with convolved motion parameters throughout the recording, including high motion periods (A). Areas shown in green are significantly negatively correlated with theta power and areas shown in red are significantly negatively correlated with convolved motion regressor, areas in yellow indicate the overlap of these effects. (B) Correlations of convolved continuous theta power restricted encoding phase trials (different statistical threshold in cyan and green respectively) that passed artifact correction still showed an overlap (yellow) with areas exhibiting significant correlation with small movements (red). See figure S1 for unconvolved EEG-BOLD correlations, alpha/beta band EEG-BOLD correlations, and positive EEG/motion BOLD correlations.

Above we show that power across all frequency bands (<20 Hz) correlates with motion, therefore similar power-BOLD correlations were expected for alpha (8-12 Hz) and beta (13-20 Hz) frequency ranges. Accordingly, a GLM-cleanalpha and a GLM-cleanbeta were set up, matching the GLM-cleantheta. Indeed, the results of this analysis resembled the correlation patterns as obtained for theta (see Figure S1A, Table S3). Further control analyses investigated the nature of the convolved motion/power correlations by comparing models with convolved regressors to results of non-convolved models (Figure S1 C&D, Table S4 & S5). These models reveal that correlations with non-convolved regressors, including periods of large movements, match and exceed correlations with convolved regressors. This observation suggests that correlations observed with convolved regressors are, at least in part, due to a prolonged motion artifact. Likely spin history effects, induced during large movements cause a prolonged signal change in the EPI data appearing to be a BOLD signal change in the GLM with the convolved regressors (see Figure S1C). During small motion however, stronger correlations were found in convolved models, suggesting that correlation of power during small motion periods is only partially, if at all, linked to spin history MR motion related artifacts, but more related to neural activity that correlates with motion or physiological vascular correlates of motion (Bright, Whittaker, Driver, & Murphy, 2015), see Figure S1D, Table S5).

Finally, to demonstrate that the reported correlations are due to specific time-locked motion-BOLD and EEG power-BOLD correlations, as opposed to unspecific differences in motion or power, null models were set up resembling GLM-allmotion and GLM-alltheta with a randomized theta power and motion parameters timeseries convolved with the HRF. In these null models, no cluster exceeded a $p<0.001$, clustersize$\geq$10 threshold.

## DISCUSSION

This study demonstrates that movement related artifacts in simultaneous EEG-fMRI induce spurious effects in EEG data, but also spurious EEG-BOLD correlations. Movement in the MR scanner is positively correlated with amplitude increases in simultaneously recorded EEG, even during low motion epochs. This tight relationship between movement and EEG results in motion causing spurious EEG-fMRI effects in a twofold manner: in the magnetic field of the scanner, tiny differences in event-related motion between task conditions can (i) produce spurious task-related effects in EEG data that can be in stark contrast to task-related effects out-of-scanner, and (ii) elicit spurious EEG-BOLD correlations by introducing motion-related artifacts concurrently in EEG and fMRI data.

In our case, small task correlated differences in motion during a memory task introduced artifacts strong enough to reverse memory related theta effects (Figure 4). Furthermore, convolving theta power with an HRF before correlating it with the measured BOLD series, an analysis commonly carried out to reveal mutual generators of hemodynamic fMRI effects and electrophysiological oscillatory effects, exhibited results closely matching correlations of motion with BOLD signals. In the presence of even only small motion in the data, EEG-BOLD correlations do thus not reveal neural activity related to brain oscillatory power, but exhibit motion related changes present in EEG and fMRI. Importantly, these motion driven EEG-BOLD correlations were obtained using a standard analysis pipeline after convolving timecourses with the HRF, employing motion correction, and without exceedingly high motion in the data (mean relative motion below 0.05 mm, see Figure 5).

Alarmingly, the presented pattern of spurious motion related EEG-BOLD effects could easily pass as neurophysiological plausible results. The relationship of theta oscillatory power and successful memory formation remains controversial, as opposing effects are reported by recent studies (Hanslmayr & Staudigl, 2014). Only artifact free, out-of-scanner control data rendered the in-scanner theta effects and fMRI correlations implausible, and prompted us to conduct an in-depth analysis of motion during scanning which revealed the cause of this spurious theta power increase. BOLD-motion/power correlations were significant in areas typically thought to exhibit motion effects such as ventricles, regions at the rim of the cortex, but also in parietal cortex and in midline regions (Lemieux, Salek-Haddadi, Lund, Laufs, & Carmichael, 2007) (Figure 6). The spurious correlations between theta power and frontal midline regions we report do, however, fit with the hypothesis of medial frontal cortex generating theta oscillations (Cohen, 2014), which could easily lead to misinterpretation of our

data. Several published simultaneous EEG-fMRI studies investigating correlations of theta power and BOLD signals have reported similar negative correlations in frontal midline regions (Sammer et al., 2007; Scheeringa et al., 2009; White et al., 2013). The pattern of negative correlations of low frequency power with BOLD signals in several cortical areas, reported here, would also be in line with prior work suggesting a negative relationship of low frequency power and BOLD signals (Hermes et al., 2014; Mukamel et al., 2005; Zumer et al., 2014). This resemblance of spurious correlations with physiologically expected effects is a serious problem for simultaneous EEG-fMRI studies trying to unravel the relationship of BOLD signals and electrophysiological activity.

Even very small movements, generally not considered problematic in fMRI studies, correlate positively with increases in EEG amplitudes. During the encoding phase, task-related average motion differences smaller than 0.01mm between successfully encoded trials in contrast to forgotten trials (see Figure 5) caused spurious task related EEG power increases. An open question is: What kind of motion caused this effect? The very small magnitude of the motion during the encoding phase indicates that these effects might rather be related to physiological motion than voluntary head movements. Negative EEG-BOLD correlations even exceeded the negative motion-BOLD correlations in t-values and spatial extent, demonstrating that EEG can provide a more sensitive motion measure than the realignment parameters (Zotev, Yuan, Phillips, & Bodurka, 2012). Realignment parameters are considered to provide a very high spatial resolution up to 100 μm (Friston et al., 1996). However, they possess a very low temporal resolution (in the present case 2 seconds). Consequently, the combined motion measure as a derivative of the realignment parameter is insensitive to rapid, periodical movements, which would still produce artifactual increases in EEG power. Such a rapid, periodical movement for example is caused during each heartbeat, as each heartbeat causes a small nodding movement with velocities up to 0.5 mm per second (Mullinger et al., 2013).

This capacity of EEG to capture physiological motion of very small magnitude links the presented results to research focusing on the influence of physiological measures on fMRI. Several studies have shown that physiological noise related to respiration and heart-rate variability correlates with cognitive tasks (Birn et al., 1999; Birn, Murphy, Handwerker, & Bandettini, 2009; Ent, Braber, Rotgans, Geus, & Munck, 2014; Park et al., 2014; Vlemincx, Taelman, De Peuter, Van Diest, & Van den Bergh, 2011) and elicits prolonged negative correlations with BOLD signals - especially in midline areas (Birn et al., 2009; de Munck et al., 2008; Ent et al., 2014; Shmueli et al., 2007). Furthermore, task related changes in physiology can

produce BOLD signal changes in vascular networks mimicking neuronal network activations (Bright et al., 2015). An fMRI study, similarly focused on memory encoding as the present study, showed that respiration is phase-locked to item presentation (Huijbers et al., 2014). This respiration phase-locking was stronger for later remembered in contrast to later forgotten items. Interestingly, respiration also predominantly correlates with BOLD effects in midline regions (Birn, Diamond, Smith, & Bandettini, 2006; Huijbers et al., 2014), resembling the spatial pattern of motion-related correlations in the present results. Our results show that such small physiological motion, which in event related fMRI does not cause spurious activation (Birn et al., 1999), can dramatically drive effects in simultaneous EEG-fMRI. Future research needs to investigate respiration and other physiological measures (e.g. end-tidal $CO_2$) and measure head motion directly to reveal the source of these movements, thus inspiring development of methods to control for these artifacts.

At first glance it is surprising that negative motion-BOLD/EEG-BOLD correlations were obtained after convolving with the canonical HRF. Correlations of convolved motion with BOLD signals have been rarely reported (however, see (Jansen et al., 2012)). Commonly, one would expect that motion related artifacts immediately affect BOLD signals and therefore motion artifacts would be omitted by effectively delaying the response ~5sec by convolving the motion timecourse with the HRF. However, the effects of large motion are indeed prolonged enough to exhibit a similar, albeit weaker, correlation with BOLD signal after convolution. Negative correlations of non-convolved large motion shown in the supporting material (Figure S1C) reveal similar effects as after convolution in typical motion artifact prone regions. Similar widespread artifactual negative correlations between head motion and fMRI have consistently been found (Satterthwaite et al., 2013; Yan et al., 2013) and motion can induce artifacts lasting up to 10 sec (Power et al., 2014). Convolving power timeseries therefore does not prevent motion driven spurious correlations.

Correlations of convolved power and motion seem not only to be related to motion artifacts but are also found in regions involved in planning and executing motion like the motor cortices and the cerebellum. Those regions exhibit mainly positive correlations and in contrast to the motion artifacts are only evident after convolution (Figure S1B) and may reflect neural origins of motion, as previously suggested (Yan et al., 2013). Another striking pattern, which emerges especially when correlating power or motion during low movement phases, is an apparent resemblance with resting state networks (Fox & Raichle, 2007). Negative correlations with resting state networks might arise because lower motion periods could indicate periods of

low task involvement and consequently decreases in motion might indicate increases in resting state related activity. An alternative, and more likely, explanation is that these network regions are also prone to exhibit cardiorespiratory related correlations (Birn et al., 2006; Shmueli et al., 2007; van Buuren et al., 2009). Therefore, EEG as a very sensitive measure of voluntary and physiological motion could reveal similar correlations with the default mode network as cardiorespiratory measures. Together, our reported EEG-BOLD correlations seem to be more directly connected to motion and not to cortical activity connected to brain oscillatory responses. We hypothesize that when large movements are present, the correlations that we observe are primarily driven by voluntary movements (e.g. speech) causing MRI artifacts, such as spin history effects, as significant correlations are observed in wide-spread areas without convolution of the EEG/motion regressor with the HRF. However, when only small movements are present we suggest the primary driver of the correlations that we observe are physiological in origin, i.e. related to changes in respiration with task, since little correlation is observed without convolution with the HRF.

Motion in simultaneous EEG-fMRI recordings also impacts on the success of the gradient and BCG artifact correction, which is an additional undesirable impact of motion on data quality. Specifically, movement changes the shape and amplitude of the gradient and BCG artifacts in EEG because of the changed position of electrodes in the magnetic field. Consequently, artifact templates do not explain the individual artifact occurrences well, resulting in a less accurate correction. Increased residual BCG artifacts caused by motion can, at least in part, explain the prolonged increases in the theta frequency activity during high motion trials (Figure 4D), as the BCG artifact shows highest amplitudes in the theta frequency range (LeVan et al., 2013). The OBS method used in this study (Niazy et al., 2005) allows for temporal variations in BCG artifact by fitting an optimal basis set to the data, but still assumes spatial stationarity. Average artifact subtraction methods that are widely used are theoretically even less adapted to account for variability in artifacts. Considering motion in-scanner might therefore also be the key to improve gradient and BCG artifact correction.

The relationship between motion and EEG power might explain the lack of distinct correlation patterns found between specific frequency bands and BOLD responses (de Munck, Goncalves, Mammoliti, Heethaar, & Lopes da Silva, 2009; Lavallee, Herrmann, Weerda, & Huster, 2014; Mantini et al., 2007), the lack of correlation of oscillatory EEG power in task-active regions (Ritter, Moosmann, & Villringer, 2009; Scheeringa et al., 2009), and the high variability in correlation patterns across participants (de Munck et al., 2007; de Munck et al.,

2009; Goncalves et al., 2006; Laufs et al., 2006; Meyer, van Oort, & Barth, 2013). In particular, we suggest that EEG-fMRI studies investigating the relationship between oscillatory EEG power and BOLD responses in resting state are particularly susceptible to spurious correlations, since in resting state studies, continuous power time series are typically correlated with BOLD time series similar to the analysis presented here. In contrast, the common approach of including trial-based average power as a task-specific parametric modulator in the fMRI model (Debener et al., 2006; Hanslmayr et al., 2011; Scheeringa et al., 2009; Zumer et al., 2014) could reduce the impact of motion as long as motion is not task correlated. Therefore one important implication of our results is to avoid correlations of EEG power with fMRI data unless there is evidence that the EEG power measures are not related to movement.

However, correlating continuous EEG and fMRI measures is difficult to avoid when investigating ongoing effects, and can provide high power to detect effects of interest. An interesting solution to control for motion on EEG-fMRI data is to record motion co-registered to EEG recordings with a sufficiently high sampling rate. Recently, several motion-recording approaches have been proposed (Abbott et al., 2014; Chowdhury, Mullinger, Glover, & Bowtell, 2014; LeVan et al., 2013). Currently none of these methods are used in standard EEG-fMRI setups or are validated in measurements of oscillatory activity during cognitive tasks. Using such techniques will likely improve the validity of reported EEG-fMRI results. Post-processing methods already available may also be of some help in addressing this problem. One potentially powerful de-noising strategy is beamforming, as separating spatial sources of the EEG signal is an efficient artifact removal strategy (Brookes et al., 2009; Zumer et al., 2014). This approach has the advantage for motion correction by not assuming spatially stationary sources, unlike ICA approaches, but does not lend itself to analysis of all types of EEG data(Brookes et al., 2009).

An approach that has been used for EEG-fMRI analysis is to remove outliers from the EEG power time series (Sadaghiani et al., 2010; Scheeringa et al., 2009; Yuan, Zotev, Phillips, & Bodurka, 2013) from any regressors created. However, these studies set quite liberal thresholds for outlier removal of 4 or 5 standard deviations above the mean, which is not effective to prevent correlations with motion (Figure 2). Outliers can also be determined by applying a threshold to data on the basis of realignment parameters. For instance, one of the first EEG-fMRI studies correlating continuous alpha power with BOLD changes excluded all scans with motion exceeding a threshold of one standard deviation above the mean (Goldman et al., 2002). A similar approach of censoring motion scans has been demonstrated as a useful approach in resting state fMRI studies (Power et al., 2014) and event related fMRI designs (J. S. Siegel et al.,

2014). However, our results suggest this is not stringent enough when considering EEG-BOLD signal correlations when motion may be correlated with the task due to anything from voluntary movements to a change in breathing. Despite all potential clean up techniques the gold standard to validate EEG effects obtained in the scanner is still contrasting in-scanner EEG data with data recorded outside of scanner. This is especially important for the low frequency range up to 20 Hz, in which motion and other artifacts are most pronounced during simultaneous recordings (Masterton, Abbott, Fleming, & Jackson, 2007).

## CONCLUSION

Simultaneous EEG-fMRI undoubtedly is a highly useful research tool, which could provide important insights into countless research questions. However, poor data quality of simultaneously recorded EEG, especially due to motion induced artifact, is still a major limitation for simultaneous EEG-fMRI studies. Preventing motion and controlling results for motion is therefore an important step in acquiring valid results. Artifacts related to small head motion that would be negligible in each modality alone, cause spurious results that are difficult to separate from real neurophysiological effects. Tools to record motion in the scanner and artifact correction methods incorporating those measures might be the key to reliable EEG-fMRI correlations in future studies.

## ACKNOWLEDGMENTS

The research presented in this work was supported by a grant from the Deutsche Forschungsgemeinschaft (Project HA 5622/1-1) awarded to Simon Hanslmayr.

# STUDY 4: SPECTRAL FINGERPRINTS OF MEMORY ENCODING: MATERIAL SPECIFIC AND MATERIAL UNSPECIFIC SUBSEQUENT MEMORY EFFECTS

The formation of a memory relies on two processes: the processing of to-be-encoded material in the cortex and the binding of these representations to a memory trace in medial temporal lobes. Contrasting activity during encoding depending on subsequent memory (i.e. remembered vs. forgotten) consequently represents activity related to cortical information processing as well as activity related to medial temporal lobe binding mechanisms. To disentangle these effects, the present study contrasts oscillatory memory encoding effects during word and unfamiliar face encoding in MEG and iEEG recordings. Processing of words and faces is well known to elicit activity in dissociable areas: left lateralized fronto-temporo-parietal regions for semantic word processing and right ventral occipito-temporal areas for processing of distinct visual features of unfamiliar faces. Decreases in alpha/beta power were found to index processing of faces and words in the predicted word and faces areas. These alpha/beta decreases specifically tracked successful encoding of words, whereas successful encoding of faces was related to visual gamma increases. Material unspecific memory encoding effects were found in the theta frequency range: theta decreases pre- and poststimulus were related to successful encoding for words and faces. These results imply that indeed typically reported memory encoding effects present a mix of concurrent activity of neural networks with dissociable spectral fingerprints: successful encoding of visual features is reflected in local gamma power increases, whereas semantic processing is related to alpha/beta power decreases, material unspecific memory binding is reflected in theta decreases.

## INTRODUCTION

Despite the hypothesized important role of oscillatory activity in neural processing (Buzsaki & Draguhn, 2004) and specifically in memory encoding (Buzsaki & Moser, 2013; Fell & Axmacher, 2011; Hanslmayr & Staudigl, 2014; Watrous et al., 2015) only few studies so far have carried out experiments to disentangle the role of different frequency bands during memory formation. Studies investigating oscillatory memory encoding effects usually contrast activity during encoding depending on subsequent memory, commonly termed subsequent memory effects (SME, Paller and Wagner (2002)). Typically these memory encoding studies report decreases in low frequency power up to ~30 Hz and increases in high frequency power from ~40 Hz to 100 Hz to correlate with successful memory encoding (Burke et al., 2014; Burke et al., 2013; Greenberg et al., 2015; Guderian et al., 2009; Long et al., 2014; Osipova et al., 2006). An open question remains whether these decreases in low frequency power and increases in high frequency power are an unspecific general marker of neural activity (Burke et al., 2015; Miller et al., 2014; Voytek & Knight, 2015) or if specific frequency bands index activity in specific neural networks thereby serving as spectral fingerprints of specific cognitive processes in the service of memory encoding (M. Siegel et al., 2012; Watrous et al., 2015).

According to computational memory models, i.e. complimentary learning systems, a division of labour is proposed between the cortex and hippocampus (Mcclelland et al., 1995): the processing of the to-encoded-information, which is commonly considered to involve cortical activity and the binding of this distributed cortical representation to a complex spatio-temporal memory trace, which is typically linked to medial-temporal lobe activity, specifically the hippocampus (Eichenbaum, 2000; Nadel et al., 2000; Staresina & Davachi, 2009). Consequently, subsequent memory effects (SME) as a contrast between subsequently remembered and subsequently forgotten items reflect both processes: cortical processing of the stimulus material and stimulus independent medial temporal lobe activity. Medial temporal lobe connected memory binding processes have been extensively studied (Fell et al., 2001; Staresina & Davachi, 2009; Staudigl & Hanslmayr, 2013). Theta oscillations in the MTL are assumed to be crucially involved in memory binding mechanisms (Buzsaki & Moser, 2013; Lisman & Jensen, 2013). In contrast, alpha/beta and gamma power are commonly reported as a correlate of cortical information processing (Fries, 2009; Hanslmayr, Staudigl, et al., 2012; M. Siegel et al., 2012), however their role in memory encoding remains to be studied.

From fMRI studies it is well known that encoding of different materials leads to activity in dissociable cortical networks: for example encoding of verbalizable material in contrast non-

verbalizable material (e.g. faces) is related to increased BOLD activity in areas involved in semantic processes (Golby et al., 2001; Kelley et al., 1998; Kim, 2011). From previous cognitive studies it is known that encoding of words and unfamiliar faces is supported by different cognitive operations: extensive semantic processing enhances memory for words (Craik & Lockhart, 1972), whereas encoding of unfamiliar faces profits from distinct coding of visual features (Sporer, 1991; Winograd, 1981). Brain oscillatory activity related to distinct cortical information processing should therefore vary with the type of to be encoded material, whereas brain oscillatory activity related to MTL memory binding should not differ depending on material.

To investigate if memory related oscillatory activity in different frequency bands indeed reflects spectral fingerprints of differing neural networks, we measured oscillatory power during word and face encoding in MEG and in intracranial recordings (see Figure 1A). As alpha/beta decreases and gamma increases have been linked to cortical information processing (Fries, 2009; Hanslmayr, Staudigl, et al., 2012), we expected that SMEs in these frequency bands vary depending on the type of to-be-encoded material. Theta oscillatory activity during memory encoding is usually being linked to MTL processes (Buzsaki & Moser, 2013; Ekstrom & Watrous, 2014; Hanslmayr & Staudigl, 2014) and has been found in previous studies to not vary depending on the encoding task (Fellner et al., 2013; Fellner et al., submitted). Therefore theta SMEs should be related to material unspecific memory binding processes.

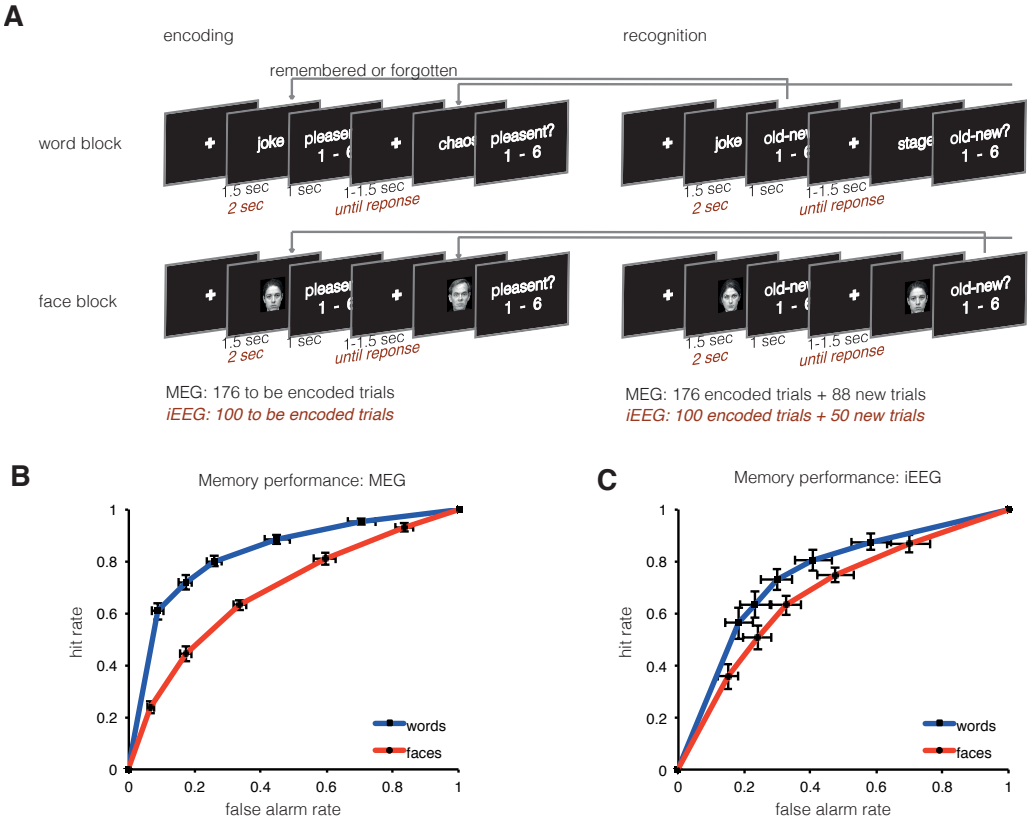


**Figure 1: paradigm and behavior**

(A) Paradigm. The experiment was split in two blocks: a word block and a face block. During each block participants were presented with to-be-encoded items, which they rated regarding pleasantness. Encoding was followed by a short distractor phase and the recognition phase. During recognition items presented previously were presented mixed with new items and participants had to rate on a 6-point confidence scale the items as old or new. The paradigm was slightly adapted for the iEEG patient sample, i.e. less items were presented, and each item was presented with a longer duration (B) & (C) Behavioral performance in the MEG dataset and iEEG dataset. ROC curves show memory performance for faces and words. On x axis percentage of a ratings to new items is plotted (i.e. false alarm rate), y- axis shows percentage of ratings for old/previously-encoded items (i.e. hit rate), error bars plot SEM. A left upward shift of the ROC indicates better recognition performance, i.e. more hits and less false alarms.

## METHODS AND MATERIAL

### *PARTICIPANTS*

Thirty-two volunteers participated in the MEG experiment, they were compensated either with course credit or 10 €/hour financial compensation. All of the participants gave written informed consent before the experiment, which was approved by the ethics committee of the University of Konstanz. Data from eleven participants had to be excluded because of low trial numbers in one of the conditions after excluding EEG artifacts and trials with early response button presses (>30 trials), one dataset had to be excluded because of a erroneous headshape, resulting in a sample of twenty subjects used in analysis. Participants in the remaining sample were aged between eighteen to thirty-three years (M=23.5), fourteen participants were female. All subjects spoke German as their native language, reported no history of neurologic or psychiatric disease, and had normal or corrected to normal vision. All participants gave their written informed consent, and the experimental protocol was approved by the local ethical review board.

Additional twenty-two patients with pharmaco-resistant epilepsy who had been implanted with intracranial electrodes for diagnostic purposes volunteered to participate in a matching memory encoding study. Data of seventeen patients was recorded at the University Hospital Erlangen, data of five patients was recorded in cooperation with University College London at the National Hospital for Neurology & Neurosurgery. Data of eight patients was excluded from reported analyses, due to either technical problems during recordings, insufficient memory performance or no electrodes in one of the regions of interest. In the remaining dataset of fourteen patients nine patients were native German speaker, four native English speaker, and one Slovenian. Word material and instructions were translated accordingly.

### *PARADIGM*

In the MEG sample every participant had to complete two task blocks: one block consisting of word encoding and recognition and another block consisting of encoding faces and face recognition. During encoding phase participants were presented with the 176 to-be-encoded items and were instructed to judge each item for pleasantness on a 1-6 scale. Participants were told that judging pleasantness facilitates later memory performance. Before the real encoding phase started participants had to complete a short practice phase (4 trials) resembling the encoding phase to familiarize them with the paradigm. Each encoding item (face or word) was presented for 1.5 sec followed by a 1sec response interval, between trials a fixation

cross was shown with a variable length (1-1.5sec), in total 176 items were presented. The encoding phase was followed by a distractor task in order to prevent working memory contributions to the memory test. The distractor task was a variation of the inattentional blindness task as used in (Hanslmayr, Backes, et al., 2013). During the recognition phase all 176 old items of the encoding phase were presented intermixed with 88 new items, not previously shown. Participants were instructed to give confidence ratings ranging from 1, very sure old, to 6, very sure new. In contrast to binary yes/no ratings, this graded confidence ratings provide a more fine grained scale of memory performance.

During both task blocks MEG was recorded, responses were given using two response boxes with 3 buttons placed on the right and left side of the body. Word material was drawn from the MRC Psycholinguistic Database (Coltheart, 2007), translated into German and separated in three lists of equal length matched for word length, frequency, concreteness and imageability and according to pleasantness ratings acquired in a pilot study. Faces were drawn from several face material databases. All face stimuli had an emotionally neutral expression and were presented in black and white on a black background. Face material was similarly divided in three sets matched for gender, approximate age, hair color and piloted pleasantness rating. Two subsets of material (faces, words) were used as to-be-encoded material and one subset was used as new material during recognition. Material was randomized for each participant, and counterbalanced across participants. Order of word and face block and response hand use was also counterbalanced across the sample.

The paradigm for intracranial implanted patients was slightly adapted to match the clinical setting and the cognitive abilities of the patients. To this end the paradigm was shortened to 100 items during each encoding block. During recognition these 100 old items were presented with 50 new items. The presentation was self paced, items were presented for 2 sec instead 1.5 in the MEG, and the response screen was shown until a response button was pressed. Due to the test setting in the hospital bed response hand use was not controlled, as flexible response hand use was not always possible.

### *ROC ANALYSIS*

An ROC approach was used to analyze recognition data. A recognition memory test can be conceptualized as a variation of a signal detection task, therefore ROC analysis can be used for in-depth analysis of the data. A single process unequal variance model was fitted to the data to obtain bias free measures of memory strength (Spitzer & Bauml, 2007; Wixted, 2007) and classify hits and misses relative to individually defined neutral response criterion for MEG/iEEG

analysis (for details of fitting procedures see (Fellner et al., 2013; Hanslmayr et al., 2009)). In short, this approach assumes that memory strength can be modeled by separate normal distributions for new and old items, i.e. each memory strength has a certain probability to be elicited by a new or old word. The distance d' of the mean of these distributions yields a bias free measure of memory strength. The model assumes that subjects respond with a certain confidence rating i, whenever their subjective memory strength exceeds a certain criterion ci. The crossover of the distributions of new and old items represents the point of the neutral response criterion because this point represents the memory strength that has an equal probability to be elicited by new and old items. An item that during recognition received confidence rating i was classified as a hit if the corresponding estimated criterion $c_i$ was higher than the individually estimated neutral criterion, otherwise the trial was classified as a miss. As demonstrated previously this procedure enhances signal to noise ratio by taking into account individual differences in the use of confidence ratings (Fellner et al., 2013).

### *MEG RECORDING AND PROCESSING*

MEG was recorded with a 148-channel whole-cortex magnetometer (MAGNES 2500 WH, 4D Neuroimaging, San Diego, USA) in a magnetically shielded room, while participants were in a supine position. Data were continuously recorded at a sampling rate of 678.17 Hz, and bandwidth of 0.1-200 Hz. The participants' nasion, left and right ear canal, and head shape were digitized prior to each session with a Polhemus 3Space Fasttrack.

All analyses were carried out running under MATLAB (The MathWorks, Natick, MA) using self written scripts and fieldtrip toolbox (www.ru.nl/fcdonders/fieldtrip, (Oostenveld et al., 2011)). Data of the encoding phases were epoched in trials -1.5 to 3 sec around each item onset during encoding. Data was visually inspected. Idiographic artifacts (channel jumps, muscle artifacts, noisy channels) were excluded from further analysis. Infomax independent component analysis was applied to correct for residual artifacts (e.g. eyeblinks, eye movements, heart beat related activity or tonic muscle activity). On average 105.8 word hit trials (SD=18.7, range: 75-129), 51.6 word miss trials (SD=18.4, range 31-88) and 85.8 face hit trials (SD=17.3, range: 39-111) and 71.8 faces miss trials (M=71.8, SD=18.0, range: 49-111) passed artifact correction and were used for further analysis.

Data was filtered to obtain lower frequency oscillatory power between 2 Hz and 30 Hz using wavelets with a 5 cycle length, resulting time-frequency data was smoothed with a Gaussian kernel (FWHM 200ms and 2 Hz) to control for inter-individual differences and to control for the time-frequency resolution trade-off across frequencies. To obtain higher

frequency oscillatory power in the gamma range (40-120 Hz) a multi-taper approach was used with a 300 ms window and a spectral smoothing of 10 Hz resulting in the use of 5 tapers. Resulting data was z-transformed to the respective mean and standard deviation across channels for every time-frequency bin separately for word and face trials. The data was therefore normalized across channels (not time) in order to maximize sensitivity towards topographical differences between conditions.

Source analysis was carried out using a linearly constrained minimal variance (LCMV) beamformer (Van Veen et al., 1997), calculating a spatial filter based on the whole length of all trials, with each trial bandpass filtered in the frequency range of interest. Individual structural MR images were aligned into the MEG sensor coordinates using NUT-MEG (Dalal et al., 2004). Individual single-shell headmodels (Nolte, 2003) were constructed using structural MRs of each participant. The brain was divided in 10 mm grid voxels and normalized to the MNI brain using a warping procedure. The source time-course for each grid point was calculated and subjected to a wavelet analysis. As the beamformer already acts as a spatial filter, data in the source domain was not z transformed across the across the spatial dimension as sensor level data, but across time dimension (i.e. to the mean/standard deviation for each grid voxel-frequency combination).

### *IEEG RECORDING AND PROCESSING*

Intracranial data was recorded from subdural grid, strip, and depth electrodes. Location of electrodes was determined using co-registered postoperative MRIs and postoperative CTs. Electrode locations were then transformed to MNI coordinate, anatomical labels were derived using the aal atlas (Automated Anatomical Labeling, Tzourio-Mazoyer et al. (2002)).

Data were continuously recorded at a sampling rate between 512 Hz and 4096 Hz. Data of the encoding phases were epoched in trials from -1.5 to 3 sec around each item onset during encoding and downsampled to a sampling rate of 512 Hz. Data was converted to a bipolar montage in order to obtain maximally focal spatial resolution, therefore each electrode was re-referenced to its neighboring electrode (for grid electrodes across the horizontal and vertical dimension). Coordinates of these bipolar "virtual" channels were calculated situated between the neighboring electrodes. Only bipolar contacts in one of the regions of interest defined by the MEG source analysis results was subjected to further analysis (Word areas: left IFG, left superior and middle temporal gyrus and left supramarginal gyrus; face area: occipital electrodes, and left inferior occipital gyrus, fusiform gyrus and inferior temporal gyrus). Data was carefully visually inspected, electrodes with epileptogenic activity was excluded form analysis. This resulted in a

dataset of 128 bipolar contacts. Data was filtered to obtain oscillatory power and smoothed using the same settings as MEG data. Data was z-transformed across the time dimension (i.e. to the mean/standard deviation for each electrode and frequency), similarly as in previous iEEG studies (e.g. Burke et al. (2013)).

### *STATISTICAL ANALYSIS*

Statistical analysis of MEG data was carried out using the fieldtrip cluster permutation approach (Maris & Oostenveld, 2007). To identify significant differences between conditions summed t-values of multi-dimensional clusters were contrasted in the data to a distribution of summed t-values obtained by randomizing conditions, which effectively controls for type-I errors due to multiple testing. For sensor analysis three dimensional clusters were built by identifying neighboring time-frequency-channel bins below a p-value of 0.01 and involving at least two neighboring channels. For source space analysis clusters were formed across space. To identify iEEG electrodes with significant differences between word and face processing clustering was performed across time-and frequency in each electrode separately.

Conjunction analysis was carried out following the analysis scheme describe by (Nichols, Brett, Andersson, Wager, & Poline, 2005). For this analysis the two task contrasts in questions were calculated (e.g. average power of the difference of faces-words and face-hit and face-miss). To test for the conjunction only the least favorable value (e.g. smallest absolute value) was kept for each grid point. To test the conjunction for significance, these values were tested against zero on the group level. This analysis tests the logical "*and*" of two effects, as this conjunction can only reach significance for grid voxels in which both contrast show concurrent decreases across subjects. Note also that according to (Nichols et al., 2005) this test is applicable for dependent contrasts.

# RESULTS

## BEHAVIORAL RESULTS

ROC curves depicting memory performance in both samples are shown in Figure 1B and 1C. Memory performance was higher for words (mean d'=1.99) than faces (mean d'=0.83, T(19)=7.836 p<.0001). This effect was highly significant and shows that words by providing the possibility of a pictorial as well as semantic coding are more efficiently encoded. In the iEEG sample there was also a tendency of a higher memory performance for words (mean d'=1.33) than faces (mean d'=0.85, T(13)=2.043 one-sided p=0.032). Note the higher variance in performance in the patient sample, which might explain the only one-sided significant difference in memory performance between words and faces in the patient sample.

## MEG RESULTS

### Material specific effects

As a first step we aimed to identify material dependent power effects in order to investigate which oscillations differentiate between the processing of different material (i.e. words vs faces). To this end low frequency power (2-30 Hz) was contrasted between words and face trials. A significant power decrease cluster for faces in contrast to words was found ranging from 0.3 -1.5 sec poststimulus in the alpha/beta frequency range (8-25 Hz) at posterior sensors ($p_{corr}$<0.05, Figure 2A). In the word condition stronger power decreases were evident in the beta frequency range (10-20 Hz) poststimulus (0.5-1.5 s) at left frontal sensors ($p_{corr}$<0.005, Figure 2B). This pattern of posterior alpha/beta power decreases for faces and left frontal decreases for words matches typical regions showing material dependent effects in fMRI (i.e. occipital cortex in pictorial processing and left frontal cortex in verbal processing, see Kim (2011).

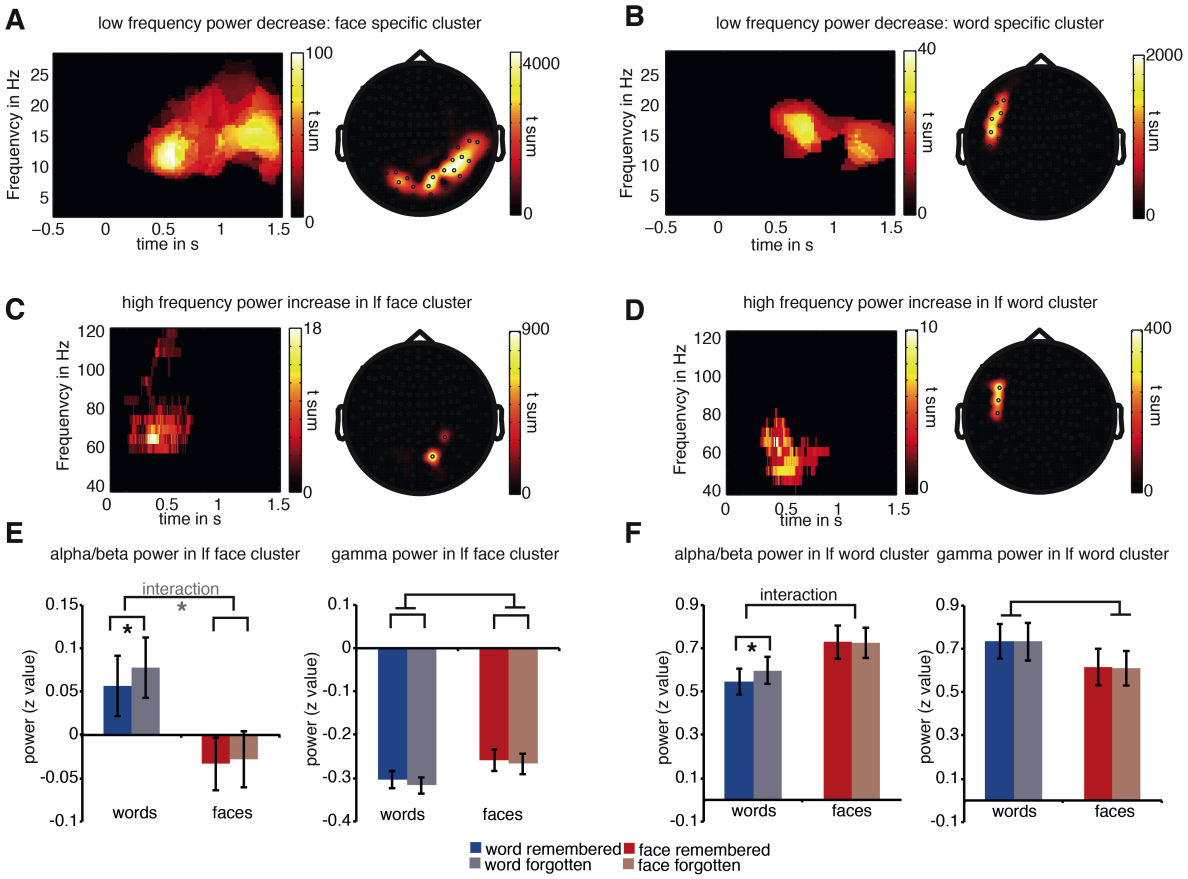


**Figure 2: Material specific decreases in alpha/beta power**

(A) Significant decreases in alpha/beta power (~10-20 Hz) for faces relative to words were found poststimulus at posterior sensor locations. (B) Significant decreases in alpha/beta power (~10-20 Hz) for words relative to faces were found poststimulus at left frontal sensor locations. Time frequency plots show the summed cluster t-values across channels of the significant cluster, topography plots show summed cluster t-values across cluster time-frequency bins. (C & D) A cluster permutation statistic restricted to channels exhibiting the alpha/beta decreases depicted in A and B revealed material specific increases in gamma concurrent to the decreases in alpha/beta power. (E) Average power was extracted from the alpha/beta (left) and gamma cluster (right) showing face specific effects shown in A & C. Alpha/beta and gamma power in the face cluster significantly differed between remembered and forgotten items. A significant trend was found for stronger memory effects for words than faces (F) Average power was also extracted for the word clusters shown in B & D. Significant memory effects were only evident for words in the alpha/beta cluster, no significant memory effect was evident for faces or in the gamma cluster. Stars denote significant post-hoc tests, non-significant trends are shown in grey.

Low frequency power decreases are often reported to co-occur with high frequency power increases. Therefore we tested for material dependent gamma power effects restricted to the time window and sensors, which exhibited low frequency decreases. Significant gamma power increases were found in the occipital face cluster ($p_{corr}<0.05$, 0.2-0.7 s, 60-80 Hz, Figure 2C) and in the left frontal word cluster ($p_{corr}<0.05$, 0.3-0.8 Hz, 40-80 Hz, Figure 2D). These gamma increases mirrored the effects in the alpha/beta but were spatially more focal.

To test if these material specific oscillatory signatures of pictorial and verbal material processing are predictive for later encoding, i.e. show subsequent memory effects (SME), average power for each cluster was extracted for remembered and forgotten items for faces and words and subjected to a 2x2 ANOVA (memory x material). Power in the low frequency face cluster (Figure 2A) showed a significant main effect of memory ($F(1,19)=10.488$, $p<0.01$); Successfully remembered items were related to decreases in alpha/beta similarly during word and face encoding (Figure 2E). In addition, a trend for an interaction was observed ($F(1,19)=3.172$, $p<0.1$), indicating that the SME for words in alpha/beta is marginally stronger compared to the SME for faces. Gamma power increases in the posterior face cluster (Figure 2C) exhibited a similar pattern of results. A significant main effect of memory was found ($F(1,19)=5.863$, $p<0.05$), with Gamma power increases indicating successful memory formation. However no significant interaction or trend for an interaction was evident. Increases in posterior gamma power therefore were similarly involved in successful encoding for word and face stimuli. A different pattern of results was obtained for alpha/beta power in the left frontal word cluster (Figure 2F), were no significant main effect for memory was found. However, the memory related power decreases differed between words and faces as indicated by a significant interaction ($F(1,19)=5.172$, $p<0.05$). Post-hoc tests revealed that a significant memory effect was only evident during word encoding ($T(19)=-3.059$, $p<0.01$), but not during face encoding ($T(19)=-0.853$). No significant memory effects were evident in the left frontal gamma cluster.

To investigate the sources of these effects the sensor data was projected into source space using an LCMV beamformer. Average alpha/beta power during word and face processing was contrasted averaged for the time frequency window in which sensor level effects were found (10-20 Hz, 500 to 1500 ms poststimulus, Figure 2A&B). Stronger alpha/beta power decreases for words were found in left frontal and temporal areas (cluster $p< 0.05$, blue areas in Figure 3A). Stronger power decreases for faces compared to words were evident in occipital areas and the right ventral occipito-temporal stream (cluster $p<0.001$, yellow areas in Figure 3A). The same analysis was carried out for the higher frequency ranges in the time frequency windows of

sensor level effects (40-80 Hz, 200-800 ms). This analysis revealed that word processing was related to stronger increases in gamma power in left temporal and temporo-parietal regions compared to face processing (cluster $p<0.1$, Figure 3B). Note, that this effect was only marginally significant on cluster level (i.e. the plot show uncorrected t-values for word related gamma increases) and was found in regions located posterior to the alpha/beta decrease for words (see Figure 3A). In contrast, face processing induced a stronger increase in occipital and parietal gamma power compared to word processing (cluster $p<0.001$, Figure 3B). Together these results fit with the sensor level data in suggesting that alpha/beta power decreases are mirrored by gamma power increases, especially in posterior regions. Specifically face related alpha/beta decreases seem to greatly overlap with face related gamma increases.

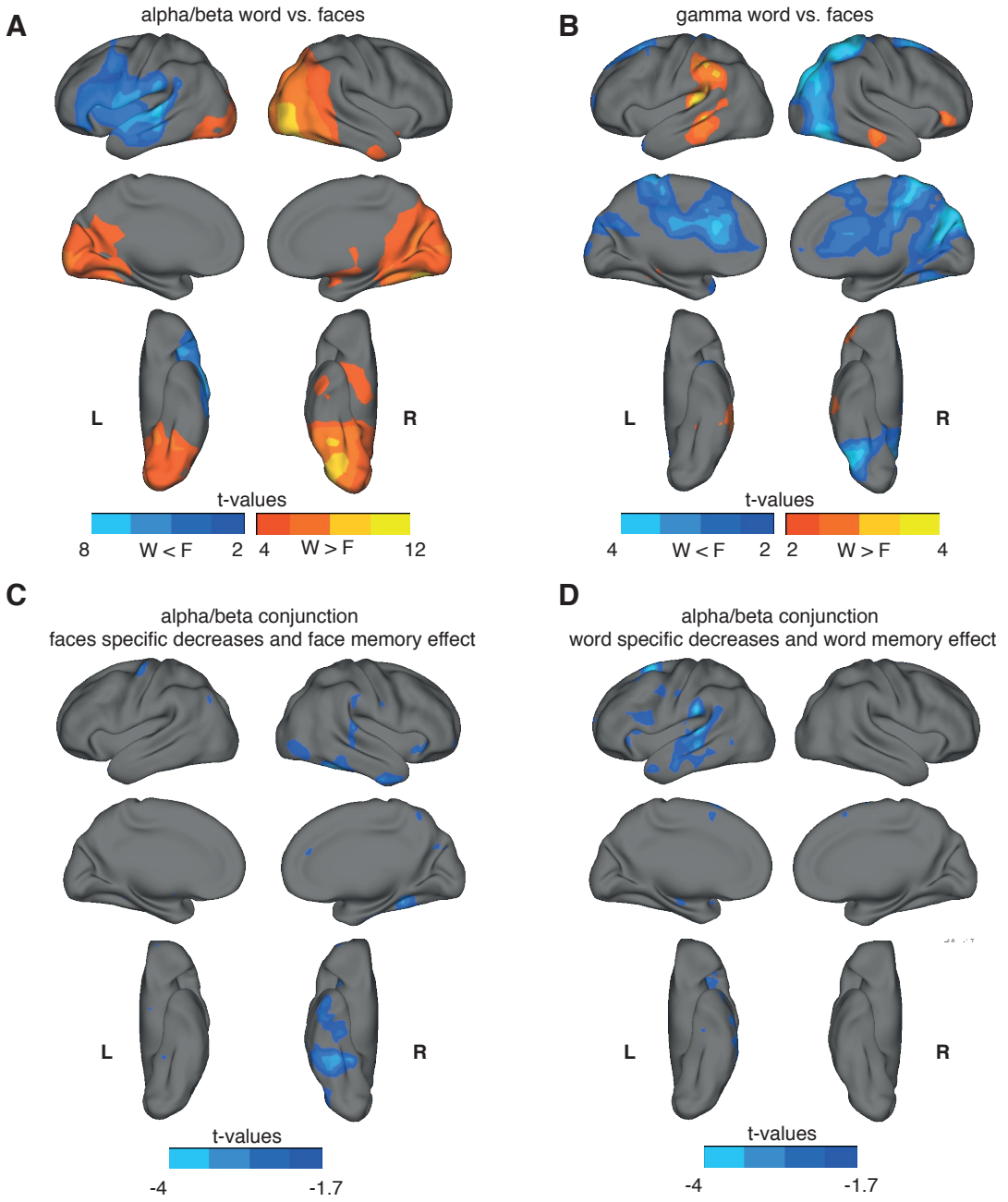


**Figure 3: Source of material specific alpha/beta decreases and gamma effects.**

The contrast words vs. faces is plotted on the source level in (A & B). Material specific alpha/beta power decreases are shown in (A), material specific increase in gamma power in (B) Analysis was carried out on the time-frequency window defined in the sensor level data, 10-20 Hz, 500-1500 ms for alpha/beta effects and 200 ms-800ms, 40-80 Hz. Stronger decreases in alpha/beta power for words is shown in blue, stronger decreases for faces in orange. Accordingly, stronger gamma power increases for words are plotted in orange, stronger increases for faces in blue. (B) shows the conjunction of face related alpha/beta decreases and face encoding effects (remembered vs. forgotten), in (C) the conjunction of word processing and word encoding effects (remembered vs. forgotten).

To investigate if regions exhibiting material specific alpha/beta decreases are also exhibiting material specific memory encoding effects we calculated the conjunction between face specific power decreases and face SME (face remembered vs. face forgotten) and word specific power decreases and word SME (word remembered vs. word forgotten). Such a conjunction analysis reveals areas that show similarly significant effects across two task contrasts. Therefore an area showing a significant conjunction is recruited by both tasks, i.e. word/face processing and memory. Concerning alpha/beta power decreases during face processing (relative to word processing) and face SME the conjunction analysis revealed power decreases in the right ventro-occipito-temporal stream (cluster $p<0.06$, 10-20 Hz, 500-1500ms). Concerning alpha/beta power decreases during word processing and word SMEs the conjunction analysis revealed areas in the left IFG and left temporal cortex (cluster $p<0.05$, 10-20 Hz, 500-1500ms).

These results show that alpha/beta power decreases strongly vary with the processed material and are evident in regions typically involved in processing faces or words respectively. Interestingly, gamma increases seem to co-occur with alpha/beta decreases. Alpha/beta decreases in frontal areas are specifically predictive for successful memory formation of word material, but not for memory formation of faces. Alpha/beta decreases also occur in conjunction with face alpha/beta SMEs in the visual ventral stream. However, also in posterior regions showing face specific effects, alpha/beta decreases seem to more strongly index memory formation for words. In contrast to posterior alpha/beta decreases, posterior gamma power increases are predicting successful memory formation for both types of material.

### *Material unspecific memory effects*

Additional to material specific effects in the alpha/beta range there are material unspecific effects. As theta oscillations are typically implicated in memory encoding, an additional cluster permutation statistic was carried out restricted to theta (2-7Hz) investigating SMEs irrespective of material (i.e. all remembered and all forgotten trials).

Two clusters of memory related decreases in theta power were found: one pre- to peristimulus cluster (3-7Hz, -0.5 to 0.3 s, Figure 3A, $p_{corr}<0.05$), and a second cluster in the poststimulus time window (2-6Hz, 0.5-1.5s, Figure 3B, $p_{corr}<0.05$), with both clusters showing a widespread topography. Theta power in these clusters did not vary with material (prestimulus cluster: $F(1,19)=0.051$; $p>0.82$; poststimulus cluster: $F(1,19)=0.016$; $p>0.9$). Source analysis revealed that these theta memory effects prestimulus (3-7 Hz, -500 to 300 ms) and poststimulus

(2-6 Hz, 800-1500 ms) are found in a distributed network including typical regions involved in memory encoding. Prestimulus theta power decreases related to memory encoding were found bilaterally in temporal, medial temporal, frontal and parietal regions (cluster $p<0.001$, Figure 4C). Post-stimulus theta power decreases during memory formation are evident in similar regions (cluster $p<0.001$, Figure 4D), additional to the prestimulus sources poststimulus theta decreases were also found in retrosplenial areas. Summed up, source localization revealed that memory related theta decrease are evident in a widespread cortical network including MTL and retrosplenial cortex, regions typically implicated in memory encoding.

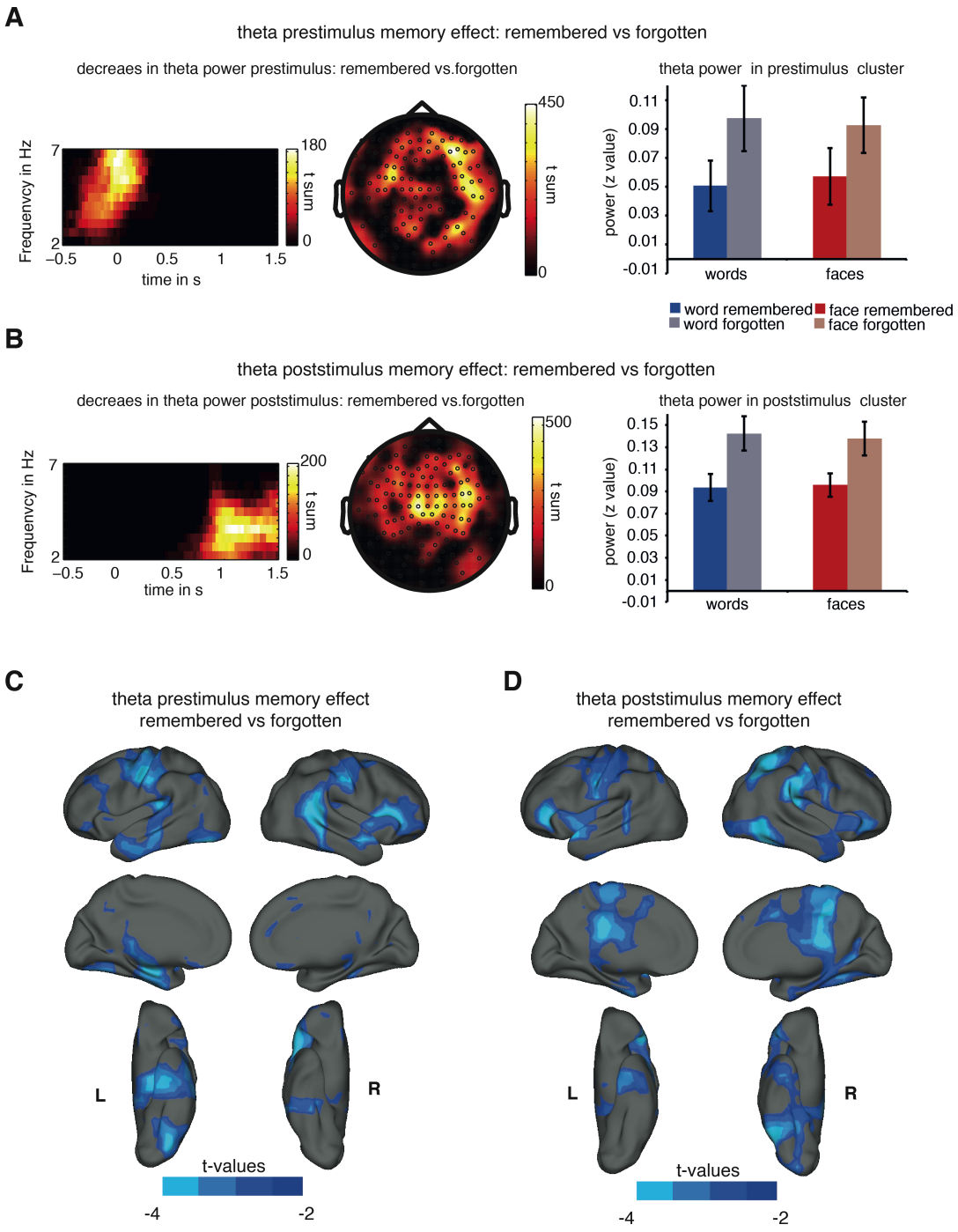


**Figure 4: Material unspecific memory effect in theta power**

A cluster permutation statistic restricted to the theta frequency band (2-7 Hz) revealed two significant clusters: A decrease in theta power prestimulus (~-500-300 ms, 3-7 Hz) (A) and poststimulus (~800-1500 ms, 2-6 Hz) (B) was stronger during successfully encoded items contrast to later forgotten items. (C) Average power in these clusters did not differ between material and memory encoding effect did not vary with to be encoded material. Time frequency plots show the summed cluster t-values across channels, topography plots show summed cluster t-values across cluster time-frequency bins. Source of the prestimulus memory encoding effect are shown in (C), sources of the poststimulus effects are shown in (D).

### *IEEG RESULTS*

Similarly as in the MEG analysis the first step of analysis in iEEG data was to define electrodes that exhibited differences in alpha/beta power between face and word processing. To this end we contrasted oscillatory activity for words and faces in each electrode, testing for a significant difference in the time-frequency window found in the MEG data (10-20 Hz, 500-1500 ms). Electrodes, which showed a significant cluster indicating a relative decrease during word than face processing where classified as "word electrodes" (Figure 5A in blue), electrodes showing significant cluster indicating a relative decrease for faces were labeled "face electrodes (Figure 5A in red). To test if these word and face electrodes were more prevalent in the respective word and face areas as identified by the previous MEG source analysis, numbers of "face" and "word electrodes" in face and word areas was counted (see Table 1, areas defined as in table legend). A $X^2$ contingency test revealed that indeed the distribution of word and face electrodes is dependent on the region ($X^2(2)=23.284$, $p<0.0001$).

**Table 1:** Number of significant electrodes showing a significant relative alpha/beta decrease for words or faces in words areas or face areas respectively.

| | Number of electrode showing significant effects | | |
|---|---|---|---|
| | decrease words | decrease faces | no effect |
| word areas | 21 | 7 | 45 |
| face areas | 9 | 26 | 20 |

Words areas: left IFG, left superior temporal, left temporal pole, left supramarginal gyrus; Face areas: occipital cortex, right fusiform gyrus, right inferior temporal gyrus)

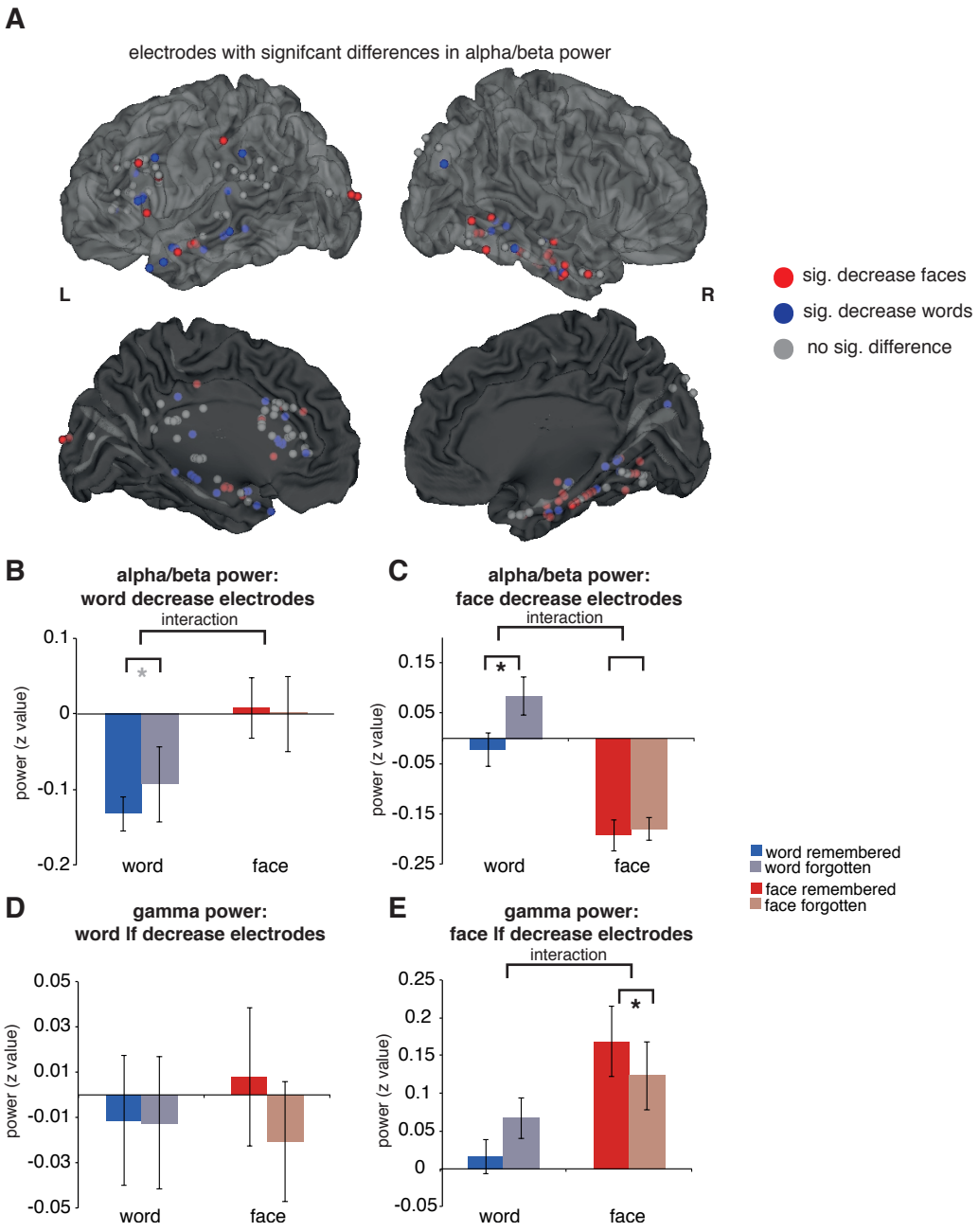


**Figure 5: Material specific encoding effects in iEEG data.** All electrodes included in the analysis are plotted in (A). Electrodes showing a significant difference in alpha/beta power (10-20 Hz) between word and face processing are highlighted in colors: red electrodes showed a higher decrease during face processing, blue electrodes during word processing. (B-E) Average alpha/beta power (10-20 Hz, 500-1500 ms) and gamma power (40-80 Hz, 200-800 ms) was calculated for each electrode showing face selective or word selective alpha/beta decreases. (B) Memory encoding effects at electrodes showing word related decreases did differ in alpha/beta power, but not in gamma power (D). Memory related decreases in alpha/beta power were also stronger at electrodes showing face selective effects (C), memory encoding related increases in gamma power however were stronger for face encoding at these electrodes. Stars indicate significant post-hoc tests, non-significant trend are highlighted in grey.

Keeping with the MEG analysis, further calculations were restricted to electrodes exhibiting word and face specific alpha/beta power decreases. Average alpha/beta and gamma power for these electrodes was calculated separately for hits and misses in each condition using the time frequency windows identified in MEG analysis (alpha/beta 10-20 Hz, 500-1500 ms, gamma: 40-80 Hz, 200-800ms) and subjected to a 2x2 ANOVA with factors memory and material.

In order to test if material specific alpha/beta decreases are accompanied by memory related alpha/beta decreases we contrasted alpha/beta decreases in word electrodes (Figure 5B). No significant main effect of memory was found ($F(1,29)=1.37$, $p>0.25$), but alpha/beta SMEs in these electrodes differed significantly between words and faces as indicated by a significant interaction ($F(1,29)=4.35$, $p<0.05$). Post hoc tests revealed a trend for a significant memory effect for words (one sided t-test: $t(29)=-1.926$, $p<0.05$), no significant memory effect was found for faces ($t(29)=0.56$). These results replicate the MEG results in showing material specific memory effects in electrodes showing word related alpha/beta power decreases during processing of verbal material.

To test for material specific effects in electrodes showing face related alpha/beta power decrease a similar 2-way ANOVA was carried out (Figure 5C). Again, a significant interaction was obtained ($F(1,32)=9.05$, $p<0.005$) but no significant main effect of memory ($F(1,32)=11.68$, $p<0.005$). Post-hoc tests revealed that the memory effect was only present for word encoding ($t(32)=-3.54$, $p<0.001$), but not for face encoding ($t(32)=-0.96$). These results suggest that even electrodes which show a face specific alpha/beta power decrease also show memory related power decreases for words, but not for faces, this tendency is also evident in MEG data, however only as non-significant trend (see Figure 2E).

Concerning power in the higher frequency ranges, increases in gamma power were found which mirrored the power decreases in alpha/beta, replicating the MEG findings. We also investigated whether the SME in gamma power varies with material, i.e. whether "face" and "word" electrodes show an interaction between Material and Memory. As above, face and word electrodes were defined according to whether they show material specific alpha/beta power decreases, regardless of later memory. For "word" electrodes, no significant interaction or main effects were obtained; Interaction: $F(1,29)=1.63$ $p<0.21$, Material effect: $F(1,29)=0.097$, $p<0.76$, Memory effect $F(1,29)=1.154$, $p<0.29$ (see Figure 5D). For "face" electrodes a significant Material by Memory interaction was obtained ($F(1,32)=5.89$, $p<0.05$), which was due to a positive SME in gamma power for faces (i.e. more power for later remembered compared to

later forgotten items; $t(32)=2.95$ $p<0.01$), compared to a tendency for a negative SME for words ($t(32)=-1.68$; $p<0.1$). These results are in accordance with the MEG results in showing that areas which are involved in face processing show concomitant alpha/beta decreases and gamma power increase. In contrast to MEG data the gamma power increases in intracranial recorded data are specifically related to encoding of non-verbal material (i.e. faces). This difference in results might be due to the higher spatial resolution of effects in iEEG.

## DISCUSSION

In this study we identified specific spectral fingerprints of dissociable cortical memory encoding networks. Encoding information into memory can be broken down to two processes: processing of the to be encoded material and binding of these representations to a unified memory trace (Mcclelland et al., 1995; Paller & Wagner, 2002). We hypothesized, that cortical information processing is reflected by alpha/beta power decreases and gamma power increases. As an index of cortical information processing power in these frequency bands should vary with to-be-encoded material. In contrast to alpha/beta and gamma oscillations, MTL theta oscillation are typically considered to be related to material independent memory binding processes. Indeed, memory encoding of verbalizable, familiar word material elicit stronger alpha/beta decreases in the well characterized, left lateralized semantic network (Pulvermuller, 2013), including left IFG, left superior and middle temporal gyrus and temporo-parietal areas. In contrast, successful encoding of non-verbalizable, unfamiliar, pictorial face items was related to alpha/beta power decreases and concurrent gamma power increases in cortical areas involved in visual processing in occipital cortex and along the right ventro-occipito-temporal stream, a cortical network typically involved in shape processing and faces in particular (Kanwisher & Yovel, 2006). Decreases in theta power were found during successful encoding for material types at widespread cortical areas resembling a potential MTL-cortical network. The findings provide evidence that commonly found memory encoding effects indeed index separable memory encoding networks: Whereas theta decreases are related to material independent memory binding processes, alpha/beta decreases index semantic information processing and gamma increases index processing of visual features.

Interestingly, alpha/beta decreases closely followed activations usually found in fMRI studies during word and face processing (e.g. (Guerin & Miller, 2009) suggesting alpha/beta decreases as a general correlate of cortical activity similar to the BOLD response (Scheeringa et al., 2011; Zumer et al., 2014). Processing words leads to alpha/beta decreases in the semantic network in contrast to processing faces. Processing faces lead to alpha/beta decreases in occipital and the ventro-occipito-temporal areas. A conjunction analysis of MEG data showed that memory related alpha/beta decreases and material related decreases are evident in regions typically reported during processing of the specific material: in left lateralized IFG, and temporal, and temporo-parietal regions for words and right ventro-occipito-temporal regions for faces. However, alpha/beta decreases were not equally involved in the encoding of words and faces. An interaction analysis of these decreases revealed that left frontal word related decreases exclusively index memory formation for words matching findings in fMRI studies (Kirchhoff et

al., 2000; Otten & Rugg, 2001b). More surprisingly stronger memory related alpha/beta decreases during word memory formation were also evident in posterior areas exhibiting stronger task related alpha/beta decreases for faces. These effects were replicated in the iEEG data: again alpha/beta decreases in word sensitive areas exclusively indicated successful encoding of word material and again also in face electrodes alpha/beta decrease related to memory encoding were stronger for words than faces. Combined the matching pattern in both experiments, in MEG and iEEG, demonstrate that alpha/beta decreases are generally more involved in the encoding of verbal material than unfamiliar pictorial stimuli like faces.

Alpha/beta decreases during memory formation seem to be specific spectral fingerprints of semantic processing. Previous studies have shown that decreases in alpha/beta power are specifically related to semantic encoding (Hanslmayr et al., 2014; Hanslmayr et al., 2009). Especially beta oscillations have been connected to language and semantic processes (Wang et al., 2012; Weiss & Mueller, 2012). On a more general level alpha activity has been hypothesized to reflect access to a semantic memory system (Klimesch, 2012) and alpha/beta decreases have been linked to cortical information processing in general (Hanslmayr, Staudigl, et al., 2012). Interestingly alpha/beta decreases here are not generally indexing successful memory encoding, as alpha/beta face SMEs are weaker or absent even in face processing areas. Following the notion that decreases in power might be related to increases in long range connectivity (Popov et al., 2013; Weisz et al., 2014), the stronger alpha/beta decreases during word encoding might mirror the larger cortical network involved in semantic memory formation in contrast to the encoding of visual features. Research inspired by the levels of processing framework of memory encoding (Craik & Lockhart, 1972) has shown that memory formation is strongly dependent on the way information is processed during encoding, with semantic processing being the most efficient encoding strategy for words. The reported stronger alpha/beta decreases during successful encoding of words might therefore be a oscillatory marker of the recruitment of semantic cortical networks.

Successful encoding of unfamiliar faces, material that is not strongly linked to prior knowledge and semantic associations, was not linked to decreases in alpha/beta power, but to increases in gamma power. In MEG, gamma increases in the posterior cluster showing face processing related alpha/beta decreases were found to index successful memory formation for both materials, faces and words. In iEEG data, gamma increases were exclusively found for electrodes showing face specific alpha/beta decreases. Gamma increases have been reported previously during memory encoding in visual cortex (Osipova et al., 2006) and in ventral

occipito-temporal regions (Burke et al., 2014; Burke et al., 2013). Co-occuring alpha/beta decreases and gamma increases in occipital cortex have also been reported during working memory maintenance of visual features (Jokisch & Jensen, 2007). Occipital gamma is hypothesized as correlate of visual feature binding (Fries, 2009) or more broadly as a general correlate of local cortical activity (Burke et al., 2015; Miller et al., 2014). As successful encoding of unfamiliar faces especially relies on the coding of distinct visual features (Sporer, 1991; Winograd, 1981), increases in gamma power, as observed in this study, likely index local visual pictorial encoding processes. The lack of alpha/beta memory encoding effects might be related to the lack of semantic processing employed to encode unfamiliar faces. For instance patients with semantic dementia are still able to recognize familiar faces even without being able to retrieve semantic knowledge about the familiar face (Simons, Graham, Galton, Patterson, & Hodges, 2001)

In contrast to the material specific memory encoding effects in alpha/beta and gamma power, theta power decreases were found during successful encoding unspecific for to-be-encoded material. Similarly as in previous studies, we found theta power decreases during successful encoding (Burke et al., 2013; Guderian et al., 2009; Long et al., 2014; Sederberg et al., 2007), which did not vary with the type of encoding processes employed (Fellner et al. submitted). Sources of these theta power decreases were found in a widespread cortical network including MTL, frontal lobe, temporal, and parietal areas matching memory encoding related theta decreases reported before (Burke et al., 2013; Greenberg et al., 2015). On a general level, theta activity has been related to MTL related memory binding processes (Hanslmayr & Staudigl, 2014; Nyhus & Curran, 2010). MTL neurons have been shown to code stimuli independent of stimulus modalities, i.e. respond similar to the picture of a person as to the written name (Quiroga et al., 2008; Quiroga et al., 2005). Widespread theta activity as shown in the presented study might provide these neurons with the input necessary for this stimulus type independent coding. The presented results yield further evidence in favor of the theta-MTL-memory binding hypothesis, as we demonstrate that theta oscillatory power independently of the to-be-encoded material indexes successful memory formation.

Notably, stimulus coding of words and faces is of course not exclusively differential. For example the processing of written words also involves processing of visual features in a word, also coded in the ventral occipito-temporal stream (McCandliss et al., 2003). Especially as the present study employed a recognition test, recognizing words could also be supported by successfully encoding visual features of a word. Previous research has shown that word form

and face selective areas in the ventral stream are highly overlapping (Matsuo et al., 2015). The reported iEEG electrodes in the ventral stream showing word selective activity therefore might not be false positives, but indeed reflect word selective processing that is beneficial for memory. Vice versa, unfamiliar faces can also carry a resemblance to a familiar person and therefore lead to activity in the semantic system. Consequently, other cortical areas than the ventral stream should also be involved in face processing. However, as previous behavioral research has shown, words should be especially well remembered if semantically processed (Craik & Lockhart, 1972), whereas faces are more likely to be later recognized if distinctive visual features are coded (Sporer, 1991; Winograd, 1981). Note, that the general pattern of results implicate that word encoding employs semantic and perceptual feature processing, face encoding more exclusively relies on only perceptual feature processing. This use of two different codes might explain the better memory performance for word material (see Figure 1 A &B), as the use of two code (semantic and visual) might support higher memory performance (Paivio, 1991).

On a more functional level, the presented results do not yet answer how low frequency power decreases and gamma power increases produce a later retrievable memory trace. Low frequency decreases might be a prerequisite for long range connectivity. On this note, semantic encoding, a cognitive operation involving widely separated cortical regions (Pulvermuller, 2013) and MTL memory binding operations should show stronger power decreases, which is in line with the reported alpha/beta and theta decreases. Decreases in low frequency power might be needed to form fine-grained cortical networks enabling semantic processing and memory binding. Therefor an open question that remains unanswered in the current analysis is whether the reported power decreases are related to increases in long range phase synchrony (see for example (Burke et al., 2013). Alternatively, low frequency power decreases might interact with local gamma increases and thereby provide a flexible code of distributed (semantic) features and more focal (pictorial) features (Donner & Siegel, 2011; Lisman & Jensen, 2013).

## CONCLUSIONS

The presented data provide evidence that commonly reported decreases in low frequency power and concurrent increases in high frequency power during memory encoding do not reflect a general marker of neural activity, but indeed reflect spectral fingerprints of dissociable memory encoding processes. Common theories assume that memory encoding relies on two subprocesses (Mcclelland et al., 1995; Tulving, 2002): cortical information processing and MTL based memory binding. The present results suggest whereas alpha/beta power decreases and gamma power increases index cortical information processing, theta decreases reflect memory binding processes.

# REFERENCES

Abbott, D. F., Masterton, R. A., Archer, J. S., Fleming, S. W., Warren, A. E., & Jackson, G. D. (2014). Constructing Carbon Fiber Motion-Detection Loops for Simultaneous EEG-fMRI. *Front Neurol, 5*, 260. doi:10.3389/fneur.2014.00260

Addis, D. R., Wong, A. T., & Schacter, D. L. (2007). Remembering the past and imagining the future: common and distinct neural substrates during event construction and elaboration. *Neuropsychologia, 45*(7), 1363-1377. doi:10.1016/j.neuropsychologia.2006.10.016

Allen, P. J., Polizzi, G., Krakow, K., Fish, D. R., & Lemieux, L. (1998). Identification of EEG events in the MR scanner: the problem of pulse artifact and a method for its subtraction. *Neuroimage, 8*(3), 229-239. doi:10.1006/nimg.1998.0361

Aslan, A., & Bauml, K. H. (2012). Adaptive memory: young children show enhanced retention of fitness-related information. *Cognition, 122*(1), 118-122. doi:10.1016/j.cognition.2011.10.001

Axmacher, N., Mormann, F., Fernandez, G., Elger, C. E., & Fell, J. (2006). Memory formation by neuronal synchronization. *Brain Res Rev, 52*(1), 170-182. doi:10.1016/j.brainresrev.2006.01.007

Baayen, R. H., Piepenbrock, R., & van H, R. (1993). The {CELEX} lexical data base on {CD-ROM}.

Bauml, K. H., Hanslmayr, S., Pastotter, B., & Klimesch, W. (2008). Oscillatory correlates of intentional updating in episodic memory. *Neuroimage, 41*(2), 596-604. doi:10.1016/j.neuroimage.2008.02.053

Binder, J. R., & Desai, R. H. (2011). The neurobiology of semantic memory. *Trends Cogn Sci, 15*(11), 527-536. doi:10.1016/j.tics.2011.10.001

Binder, J. R., Desai, R. H., Graves, W. W., & Conant, L. L. (2009). Where is the semantic system? A critical review and meta-analysis of 120 functional neuroimaging studies. *Cereb Cortex, 19*(12), 2767-2796. doi:10.1093/cercor/bhp055

Bird, C. M., & Burgess, N. (2008). The hippocampus and memory: insights from spatial processing. *Nat Rev Neurosci, 9*(3), 182-194. doi:10.1038/nrn2335

Birn, R. M., Bandettini, P. A., Cox, R. W., & Shaker, R. (1999). Event-related fMRI of tasks involving brief motion. *Hum Brain Mapp, 7*(2), 106-114. doi:10.1002/(sici)1097-0193(1999)7:2<106::aid-hbm4>3.0.co;2-o

Birn, R. M., Diamond, J. B., Smith, M. A., & Bandettini, P. A. (2006). Separating respiratory-variation-related fluctuations from neuronal-activity-related fluctuations in fMRI. *Neuroimage, 31*(4), 1536-1548. doi:10.1016/j.neuroimage.2006.02.048

Birn, R. M., Murphy, K., Handwerker, D. A., & Bandettini, P. A. (2009). fMRI in the presence of task-correlated breathing variations. *Neuroimage, 47*(3), 1092-1104. doi:10.1016/j.neuroimage.2009.05.030

Blair, R. C., & Karniski, W. (1993). An alternative method for significance testing of waveform difference potentials. *Psychophysiology, 30*(5), 518-524. doi:10.1111/j.1469-8986.1993.tb02075.x

Brewer, J. B., Zhao, Z., Desmond, J. E., Glover, G. H., & Gabrieli, J. D. E. (1998). Making memories: Brain activity that predicts how well visual experience will be remembered. *Science, 281*(5380), 1185-1187. doi:DOI 10.1126/science.281.5380.1185

Bright, M. G., Whittaker, J., Driver, I., & Murphy, K. (2015). Task-correlated physiology reveals vascular-neural networks. *Proc. Intl. Soc. Mag. Reson. Med., 23*. Retrieved from http://scholar.google.com/scholar?q=Task-correlated physiology reveals vascular-neural networks&btnG=&hl=en&num=20&as_sdt=0%2C22

Brookes, M. J., Vrba, J., Mullinger, K. J., Geirsdottir, G. B., Yan, W. X., Stevenson, C. M., . . . Morris, P. G. (2009). Source localisation in concurrent EEG/fMRI: applications at 7T. *Neuroimage, 45*(2), 440-452. doi:10.1016/j.neuroimage.2008.10.047

Brookes, M. J., Woolrich, M., Luckhoo, H., Price, D., Hale, J. R., Stephenson, M. C., . . . Morris, P. G. (2011). Investigating the electrophysiological basis of resting state networks using magnetoencephalography. *Proc Natl Acad Sci U S A, 108*(40), 16783-16788. doi:10.1073/pnas.1112685108

Buffalo, E. A. (2015). Bridging the gap between spatial and mnemonic views of the hippocampal formation. *Hippocampus, 25*(6), 713-718. doi:10.1002/hipo.22444

Buffalo, E. A., Fries, P., Landman, R., Buschman, T. J., & Desimone, R. (2011). Laminar differences in gamma and alpha coherence in the ventral stream. *Proc Natl Acad Sci U S A, 108*(27), 11262-11267. doi:10.1073/pnas.1011284108

Burgess, N. (2008). Spatial cognition and the brain. *Ann N Y Acad Sci, 1124*, 77-97. doi:10.1196/annals.1440.002

Burgess, N., Barry, C., & O'Keefe, J. (2007). An oscillatory interference model of grid cell firing. *Hippocampus, 17*(9), 801-812. doi:10.1002/hipo.20327

Burgess, N., Maguire, E. A., & O'Keefe, J. (2002). The human hippocampus and spatial and episodic memory. *Neuron, 35*(4), 625-641. doi:10.1016/s0896-6273(02)00830-9

Burke, J. F., Long, N. M., Zaghloul, K. A., Sharan, A. D., Sperling, M. R., & Kahana, M. J. (2014). Human intracranial high-frequency activity maps episodic memory formation in space and time. *Neuroimage, 85 Pt 2*, 834-843. doi:10.1016/j.neuroimage.2013.06.067

Burke, J. F., Ramayya, A. G., & Kahana, M. J. (2015). Human intracranial high-frequency activity during memory processing: neural oscillations or stochastic volatility? *Curr Opin Neurobiol, 31*, 104-110. doi:10.1016/j.conb.2014.09.003

Burke, J. F., Zaghloul, K. A., Jacobs, J., Williams, R. B., Sperling, M. R., Sharan, A. D., & Kahana, M. J. (2013). Synchronous and asynchronous theta and gamma activity during episodic memory formation. *J Neurosci, 33*(1), 292-304. doi:10.1523/JNEUROSCI.2057-12.2013

Burns, D. J., Burns, S. A., & Hwang, A. J. (2011). Adaptive memory: determining the proximate mechanisms responsible for the memorial advantages of survival processing. *J Exp Psychol Learn Mem Cogn, 37*(1), 206-218. doi:10.1037/a0021325

Butler, A. C., Kang, S. H., & Roediger, H. L., 3rd. (2009). Congruity effects between materials and processing tasks in the survival processing paradigm. *J Exp Psychol Learn Mem Cogn, 35*(6), 1477-1486. doi:10.1037/a0017024

Buzsaki, G. (1996). The hippocampo-neocortical dialogue. *Cereb Cortex, 6*(2), 81-92. Retrieved from http://www.ncbi.nlm.nih.gov/pubmed/8670641

Buzsaki, G. (2005). Theta rhythm of navigation: link between path integration and landmark navigation, episodic and semantic memory. *Hippocampus, 15*(7), 827-840. doi:10.1002/hipo.20113

Buzsaki, G. (2010). Neural syntax: cell assemblies, synapsembles, and readers. *Neuron, 68*(3), 362-385. doi:10.1016/j.neuron.2010.09.023

Buzsaki, G., Anastassiou, C. A., & Koch, C. (2012). The origin of extracellular fields and currents--EEG, ECoG, LFP and spikes. *Nat Rev Neurosci, 13*(6), 407-420. doi:10.1038/nrn3241

Buzsaki, G., & Draguhn, A. (2004). Neuronal oscillations in cortical networks. *Science, 304*(5679), 1926-1929. doi:10.1126/science.1099745

Buzsaki, G., & Moser, E. I. (2013). Memory, navigation and theta rhythm in the hippocampal-entorhinal system. *Nat Neurosci, 16*(2), 130-138. doi:10.1038/nn.3304

Canolty, R. T., Edwards, E., Dalal, S. S., Soltani, M., Nagarajan, S. S., Kirsch, H. E., . . . Knight, R. T. (2006). High gamma power is phase-locked to theta oscillations in human neocortex. *Science, 313*(5793), 1626-1628. doi:10.1126/science.1128115

Cashdollar, N., Malecki, U., Rugg-Gunn, F. J., Duncan, J. S., Lavie, N., & Duzel, E. (2009). Hippocampus-dependent and -independent theta-networks of active maintenance. *Proc Natl Acad Sci U S A, 106*(48), 20493-20498. doi:10.1073/pnas.0904823106

Chowdhury, M. E., Mullinger, K. J., Glover, P., & Bowtell, R. (2014). Reference layer artefact subtraction (RLAS): a novel method of minimizing EEG artefacts during simultaneous fMRI. *Neuroimage, 84*, 307-319. doi:10.1016/j.neuroimage.2013.08.039

Cohen, M. X. (2014). A neural microcircuit for cognitive conflict detection and signaling. *Trends Neurosci, 37*(9), 480-490. doi:10.1016/j.tins.2014.06.004

Coltheart, M. (2007). The MRC psycholinguistic database. *The Quarterly Journal of Experimental Psychology Section A, 33*(4), 497-505. doi:10.1080/14640748108400805

Conner, C. R., Ellmore, T. M., Pieters, T. A., DiSano, M. A., & Tandon, N. (2011). Variability of the relationship between electrophysiology and BOLD-fMRI across cortical regions in humans. *J Neurosci, 31*(36), 12855-12865. doi:10.1523/JNEUROSCI.1457-11.2011

Corkin, S. (2002). What's new with the amnesic patient H.M.? *Nat Rev Neurosci, 3*(2), 153-160. doi:10.1038/nrn726

Craik, F. I. M. (2002). Levels of processing: past, present. and future? *Memory, 10*(5-6), 305-318. doi:10.1080/09658210244000135

Craik, F. I. M., & Lockhart, R. S. (1972). Levels of processing: A framework for memory research. *Journal of Verbal Learning and Verbal Behavior, 11*(6), 671-684. doi:10.1016/s0022-5371(72)80001-x

Craik, F. I. M., & Tulving, E. (1975). Depth of processing and the retention of words in episodic memory. *Journal of Experimental Psychology: General, 104*(3), 268-294. doi:10.1037/0096-3445.104.3.268

Dalal, S. S., Sekihara, K., & Nagarajan, S. S. (2006). Modified beamformers for coherent source region suppression. *IEEE Trans Biomed Eng, 53*(7), 1357-1363. doi:10.1109/TBME.2006.873752

Dalal, S. S., Zumer, J. M., Agrawal, V., Hild, K. E., Sekihara, K., & Nagarajan, S. S. (2004). NUTMEG: a neuromagnetic source reconstruction toolbox. *Neurol Clin Neurophysiol, 2004*, 52. Retrieved from http://www.ncbi.nlm.nih.gov/pubmed/16012626

Davachi, L. (2006). Item, context and relational episodic encoding in humans. *Curr Opin Neurobiol, 16*(6), 693-700. doi:10.1016/j.conb.2006.10.012

Davachi, L., & DuBrow, S. (2015). How the hippocampus preserves order: the role of prediction and context. *Trends Cogn Sci, 19*(2), 92-99. doi:10.1016/j.tics.2014.12.004

de Munck, J. C., Goncalves, S. I., Faes, T. J., Kuijer, J. P., Pouwels, P. J., Heethaar, R. M., & Lopes da Silva, F. H. (2008). A study of the brain's resting state based on alpha band power, heart rate and fMRI. *Neuroimage, 42*(1), 112-121. doi:10.1016/j.neuroimage.2008.04.244

de Munck, J. C., Goncalves, S. I., Huijboom, L., Kuijer, J. P., Pouwels, P. J., Heethaar, R. M., & Lopes da Silva, F. H. (2007). The hemodynamic response of the alpha rhythm: an EEG/fMRI study. *Neuroimage, 35*(3), 1142-1151. doi:10.1016/j.neuroimage.2007.01.022

de Munck, J. C., Goncalves, S. I., Mammoliti, R., Heethaar, R. M., & Lopes da Silva, F. H. (2009). Interactions between different EEG frequency bands and their effect on alpha-fMRI correlations. *Neuroimage, 47*(1), 69-76. doi:10.1016/j.neuroimage.2009.04.029

Debener, S., Mullinger, K. J., Niazy, R. K., & Bowtell, R. W. (2008). Properties of the ballistocardiogram artefact as revealed by EEG recordings at 1.5, 3 and 7 T static magnetic field strength. *Int J Psychophysiol, 67*(3), 189-199. doi:10.1016/j.ijpsycho.2007.05.015

Debener, S., Ullsperger, M., Siegel, M., & Engel, A. K. (2006). Single-trial EEG-fMRI reveals the dynamics of cognitive function. *Trends Cogn Sci, 10*(12), 558-563. doi:10.1016/j.tics.2006.09.010

Debener, S., Ullsperger, M., Siegel, M., Fiehler, K., von Cramon, D. Y., & Engel, A. K. (2005). Trial-by-trial coupling of concurrent electroencephalogram and functional magnetic

resonance imaging identifies the dynamics of performance monitoring. *J Neurosci, 25*(50), 11730-11737. doi:10.1523/JNEUROSCI.3286-05.2005

Deco, G., Tononi, G., Boly, M., & Kringelbach, M. L. (2015). Rethinking segregation and integration: contributions of whole-brain modelling. *Nat Rev Neurosci, 16*(7), 430-439. doi:10.1038/nrn3963

Diana, R. A., Yonelinas, A. P., & Ranganath, C. (2007). Imaging recollection and familiarity in the medial temporal lobe: a three-component model. *Trends Cogn Sci, 11*(9), 379-386. doi:10.1016/j.tics.2007.08.001

Dickerson, B. C., Miller, S. L., Greve, D. N., Dale, A. M., Albert, M. S., Schacter, D. L., & Sperling, R. A. (2007). Prefrontal-hippocampal-fusiform activity during encoding predicts intraindividual differences in free recall ability: an event-related functional-anatomic MRI study. *Hippocampus, 17*(11), 1060-1070. doi:10.1002/hipo.20338

Donner, T. H., & Siegel, M. (2011). A framework for local cortical oscillation patterns. *Trends Cogn Sci, 15*(5), 191-199. doi:10.1016/j.tics.2011.03.007

Dunn, J. C. (2004). Remember-know: a matter of confidence. *Psychol Rev, 111*(2), 524-542. doi:10.1037/0033-295X.111.2.524

Duzel, E., Penny, W. D., & Burgess, N. (2010). Brain oscillations and memory. *Curr Opin Neurobiol, 20*(2), 143-149. doi:10.1016/j.conb.2010.01.004

Eichenbaum, H. (2000). A cortical-hippocampal system for declarative memory. *Nat Rev Neurosci, 1*(1), 41-50. doi:10.1038/35036213

Ekstrom, A. D. (2010). How and when the fMRI BOLD signal relates to underlying neural activity: the danger in dissociation. *Brain Res Rev, 62*(2), 233-244. doi:10.1016/j.brainresrev.2009.12.004

Ekstrom, A. D. (2014). Cognitive neuroscience: navigating human verbal memory. *Curr Biol, 24*(4), R167-168. doi:10.1016/j.cub.2013.12.043

Ekstrom, A. D., Caplan, J. B., Ho, E., Shattuck, K., Fried, I., & Kahana, M. J. (2005). Human hippocampal theta activity during virtual navigation. *Hippocampus, 15*(7), 881-889. doi:10.1002/hipo.20109

Ekstrom, A. D., Suthana, N., Millett, D., Fried, I., & Bookheimer, S. (2009). Correlation between BOLD fMRI and theta-band local field potentials in the human hippocampal area. *J Neurophysiol, 101*(5), 2668-2678. doi:10.1152/jn.91252.2008

Ekstrom, A. D., & Watrous, A. J. (2014). Multifaceted roles for low-frequency oscillations in bottom-up and top-down processing during navigation and memory. *Neuroimage, 85 Pt 2*, 667-677. doi:10.1016/j.neuroimage.2013.06.049

Ent, D. v. t., Braber, A. d., Rotgans, E., Geus, E. J. C. d., & Munck, J. C. d. (2014). The use of fMRI to detect neural responses to cognitive interference and planning: evidence for a contribution of task related changes in heart rate? *Journal of Neuroscience Methods, 229*, 97-107. Retrieved from http://www.ncbi.nlm.nih.gov/pubmed/24768574

Epstein, R. A. (2008). Parahippocampal and retrosplenial contributions to human spatial navigation. *Trends Cogn Sci, 12*(10), 388-396. doi:10.1016/j.tics.2008.07.004

Fell, J., & Axmacher, N. (2011). The role of phase synchronization in memory processes. *Nat Rev Neurosci, 12*(2), 105-118. doi:10.1038/nrn2979

Fell, J., Klaver, P., Lehnertz, K., Grunwald, T., Schaller, C., Elger, C. E., & Fernandez, G. (2001). Human memory formation is accompanied by rhinal-hippocampal coupling and decoupling. *Nat Neurosci, 4*(12), 1259-1264. doi:10.1038/nn759

Fell, J., Ludowig, E., Staresina, B. P., Wagner, T., Kranz, T., Elger, C. E., & Axmacher, N. (2011). Medial temporal theta/alpha power enhancement precedes successful memory encoding: evidence based on intracranial EEG. *J Neurosci, 31*(14), 5392-5397. doi:10.1523/JNEUROSCI.3668-10.2011

Fellner, M. C., Bauml, K. H., & Hanslmayr, S. (2013). Brain oscillatory subsequent memory effects differ in power and long-range synchronization between semantic and survival processing. *Neuroimage, 79*, 361-370. doi:10.1016/j.neuroimage.2013.04.121

Fellner, M. C., Volberg, G., Wimber, M., Goldhacker, M., Greenlee, M. W., & Hanslmayr, S. (submitted). Spatial mnemonic encoding is related to theta power decreases and medial temporal lobe BOLD increases.

Foster, B. L., & Parvizi, J. (2012). Resting oscillations and cross-frequency coupling in the human posteromedial cortex. *Neuroimage, 60*(1), 384-391. doi:10.1016/j.neuroimage.2011.12.019

Fox, M. D., & Raichle, M. E. (2007). Spontaneous fluctuations in brain activity observed with functional magnetic resonance imaging. *Nat Rev Neurosci, 8*(9), 700-711. doi:10.1038/nrn2201

Fries, P. (2005). A mechanism for cognitive dynamics: neuronal communication through neuronal coherence. *Trends Cogn Sci, 9*(10), 474-480. doi:10.1016/j.tics.2005.08.011

Fries, P. (2009). Neuronal gamma-band synchronization as a fundamental process in cortical computation. *Annu Rev Neurosci, 32*, 209-224. doi:10.1146/annurev.neuro.051508.135603

Fries, P., Nikolic, D., & Singer, W. (2007). The gamma cycle. *Trends Neurosci, 30*(7), 309-316. doi:10.1016/j.tins.2007.05.005

Friese, U., Koster, M., Hassler, U., Martens, U., Trujillo-Barreto, N., & Gruber, T. (2013). Successful memory encoding is associated with increased cross-frequency coupling between frontal theta and posterior gamma oscillations in human scalp-recorded EEG. *Neuroimage, 66*, 642-647. doi:10.1016/j.neuroimage.2012.11.002

Friston, K. J., Williams, S., Howard, R., Frackowiak, R. S., & Turner, R. (1996). Movement-related effects in fMRI time-series. *Magn Reson Med, 35*(3), 346-355. doi:10.1002/mrm.1910350312

Fuster, J. M. (1997). Network memory. *Trends Neurosci, 20*(10), 451-459. doi:10.1016/S0166-2236(97)01128-4

Gabrieli, J. D. E., Desmond, J. E., Demb, J. B., Wagner, A. D., Stone, M. V., Vaidya, C. J., & Glover, G. H. (1996). Functional magnetic resonance imaging of semantic memory processes in the frontal lobes. *Psychological Science, 7*(5), 278-283. doi:DOI 10.1111/j.1467-9280.1996.tb00374.x

Garoff, R. J., Slotnick, S. D., & Schacter, D. L. (2005). The neural origins of specific and general memory: the role of the fusiform cortex. *Neuropsychologia, 43*(6), 847-859. doi:10.1016/j.neuropsychologia.2004.09.014

Godden, D. R., & Baddeley, A. D. (1975). Context-Dependent Memory in Two Natural Environments: On Land and Underwater. *British Journal of psychology, 66*(3), 325-331. doi:10.1111/j.2044-8295.1975.tb01468.x

Golby, A. J., Poldrack, R. A., Brewer, J. B., Spencer, D., Desmond, J. E., Aron, A. P., & Gabrieli, J. D. (2001). Material-specific lateralization in the medial temporal lobe and prefrontal cortex during memory encoding. *Brain, 124*(Pt 9), 1841-1854. doi:10.1093/brain/124.9.1841

Goldman, R. I., Stern, J. M., Engel, J., Jr., & Cohen, M. S. (2002). Simultaneous EEG and fMRI of the alpha rhythm. *Neuroreport, 13*(18), 2487-2492. doi:10.1097/01.wnr.0000047685.08940.d0

Goncalves, S. I., de Munck, J. C., Pouwels, P. J., Schoonhoven, R., Kuijer, J. P., Maurits, N. M., . . . Lopes da Silva, F. H. (2006). Correlating the alpha rhythm to BOLD using simultaneous EEG/fMRI: inter-subject variability. *Neuroimage, 30*(1), 203-213. doi:10.1016/j.neuroimage.2005.09.062

Greenberg, J. A., Burke, J. F., Haque, R., Kahana, M. J., & Zaghloul, K. A. (2015). Decreases in theta and increases in high frequency activity underlie associative memory encoding. *Neuroimage, 114*, 257-263. doi:10.1016/j.neuroimage.2015.03.077

Gruber, M. J., & Otten, L. J. (2010). Voluntary control over prestimulus activity related to encoding. *J Neurosci, 30*(29), 9793-9800. doi:10.1523/JNEUROSCI.0915-10.2010

Gruber, M. J., Watrous, A. J., Ekstrom, A. D., Ranganath, C., & Otten, L. J. (2013). Expected reward modulates encoding-related theta activity before an event. *Neuroimage, 64*, 68-74. doi:10.1016/j.neuroimage.2012.07.064

Guderian, S., Schott, B. H., Richardson-Klavehn, A., & Duzel, E. (2009). Medial temporal theta state before an event predicts episodic encoding success in humans. *Proc Natl Acad Sci U S A, 106*(13), 5365-5370. doi:10.1073/pnas.0900289106

Guerin, S. A., & Miller, M. B. (2009). Lateralization of the parietal old/new effect: an event-related fMRI study comparing recognition memory for words and faces. *Neuroimage, 44*(1), 232-242. doi:10.1016/j.neuroimage.2008.08.035

Haegens, S., Nacher, V., Luna, R., Romo, R., & Jensen, O. (2011). alpha-Oscillations in the monkey sensorimotor network influence discrimination performance by rhythmical inhibition of neuronal spiking. *Proc Natl Acad Sci U S A, 108*(48), 19377-19382. doi:10.1073/pnas.1117190108

Halgren, E., Babb, T. L., & Crandall, P. H. (1978). Human hippocampal formation EEG desynchronizes during attentiveness and movement. *Electroencephalogr Clin Neurophysiol, 44*(6), 778-781. doi:10.1016/0013-4694(78)90212-2

Hämäläinen, M., Hari, R., Ilmoniemi, R. J., Knuutila, J., & Lounasmaa, O. V. (1993). Magnetoencephalography theory, instrumentation, and applications to noninvasive studies of the working human brain. *Reviews of modern Physics, 65*(2), 413. Retrieved from http://journals.aps.org/rmp/abstract/10.1103/RevModPhys.65.413

Hannula, D. E., & Ranganath, C. (2009). The eyes have it: hippocampal activity predicts expression of memory in eye movements. *Neuron, 63*(5), 592-599. doi:10.1016/j.neuron.2009.08.025

Hanslmayr, S., Aslan, A., Staudigl, T., Klimesch, W., Herrmann, C. S., & Bauml, K. H. (2007). Prestimulus oscillations predict visual perception performance between and within subjects. *Neuroimage, 37*(4), 1465-1473. doi:10.1016/j.neuroimage.2007.07.011

Hanslmayr, S., Backes, H., Straub, S., Popov, T., Langguth, B., Hajak, G., . . . Landgrebe, M. (2013). Enhanced resting-state oscillations in schizophrenia are associated with decreased synchronization during inattentional blindness. *Hum Brain Mapp, 34*(9), 2266-2275. doi:10.1002/hbm.22064

Hanslmayr, S., Matuschek, J., & Fellner, M. C. (2014). Entrainment of prefrontal beta oscillations induces an endogenous echo and impairs memory formation. *Curr Biol, 24*(8), 904-909. doi:10.1016/j.cub.2014.03.007

Hanslmayr, S., Spitzer, B., & Bauml, K. H. (2009). Brain oscillations dissociate between semantic and nonsemantic encoding of episodic memories. *Cereb Cortex, 19*(7), 1631-1640. doi:10.1093/cercor/bhn197

Hanslmayr, S., & Staudigl, T. (2014). How brain oscillations form memories--a processing based perspective on oscillatory subsequent memory effects. *Neuroimage, 85 Pt 2*(2), 648-655. doi:10.1016/j.neuroimage.2013.05.121

Hanslmayr, S., Staudigl, T., & Fellner, M. C. (2012). Oscillatory power decreases and long-term memory: the information via desynchronization hypothesis. *Front Hum Neurosci, 6*, 74. doi:10.3389/fnhum.2012.00074

Hanslmayr, S., Volberg, G., Wimber, M., Dalal, S. S., & Greenlee, M. W. (2013). Prestimulus oscillatory phase at 7 Hz gates cortical information flow and visual perception. *Curr Biol, 23*(22), 2273-2278. doi:10.1016/j.cub.2013.09.020

Hanslmayr, S., Volberg, G., Wimber, M., Oehler, N., Staudigl, T., Hartmann, T., . . . Bauml, K. H. (2012). Prefrontally driven downregulation of neural synchrony mediates goal-directed forgetting. *J Neurosci, 32*(42), 14742-14751. doi:10.1523/JNEUROSCI.1777-12.2012

Hanslmayr, S., Volberg, G., Wimber, M., Raabe, M., Greenlee, M. W., & Bauml, K. H. (2011). The relationship between brain oscillations and BOLD signal during memory formation: a combined EEG-fMRI study. *J Neurosci, 31*(44), 15674-15680. doi:10.1523/JNEUROSCI.3140-11.2011

Hassabis, D., & Maguire, E. A. (2007). Deconstructing episodic memory with construction. *Trends Cogn Sci, 11*(7), 299-306. doi:10.1016/j.tics.2007.05.001

Hasselmo, M. E., & Stern, C. E. (2006). Mechanisms underlying working memory for novel information. *Trends Cogn Sci, 10*(11), 487-493. doi:10.1016/j.tics.2006.09.005

Hasselmo, M. E., & Stern, C. E. (2014). Theta rhythm and the encoding and retrieval of space and time. *Neuroimage, 85 Pt 2*(2), 656-666. doi:10.1016/j.neuroimage.2013.06.022

Hebb, D. O. (1949). *The organization of behavior: a neuropsychological theory*: Wiley.

Hermes, D., Miller, K. J., Vansteensel, M. J., Edwards, E., Ferrier, C. H., Bleichner, M. G., . . . Ramsey, N. F. (2014). Cortical theta wanes for language. *Neuroimage, 85 Pt 2*(2), 738-748. doi:10.1016/j.neuroimage.2013.07.029

Hipp, J. F., & Siegel, M. (2015). BOLD fMRI Correlation Reflects Frequency-Specific Neuronal Correlation. *Curr Biol, 25*(10), 1368-1374. doi:10.1016/j.cub.2015.03.049

Howe, M. L., & Otgaar, H. (2013). Proximate Mechanisms and the Development of Adaptive Memory. *Current Directions in Psychological Science, 22*(1), 16-22. doi:10.1177/0963721412469397

Huijbers, W., Pennartz, C. M., Beldzik, E., Domagalik, A., Vinck, M., Hofman, W. F., . . . Daselaar, S. M. (2014). Respiration phase-locks to fast stimulus presentations: implications for the interpretation of posterior midline "deactivations". *Hum Brain Mapp, 35*(9), 4932-4943. doi:10.1002/hbm.22523

Hunt, R. R., & Einstein, G. O. (1981). Relational and item-specific information in memory. *Journal of Verbal Learning and Verbal Behavior*. Retrieved from http://www.sciencedirect.com/science/article/pii/S0022537181901389

Huster, R. J., Debener, S., Eichele, T., & Herrmann, C. S. (2012). Methods for simultaneous EEG-fMRI: an introductory review. *J Neurosci, 32*(18), 6053-6060. doi:10.1523/JNEUROSCI.0447-12.2012

Jacobs, J., Kahana, M. J., Ekstrom, A. D., & Fried, I. (2007). Brain oscillations control timing of single-neuron activity in humans. *J Neurosci, 27*(14), 3839-3844. doi:10.1523/JNEUROSCI.4636-06.2007

Jafarpour, A., Fuentemilla, L., Horner, A. J., Penny, W., & Duzel, E. (2014). Replay of very early encoding representations during recollection. *J Neurosci, 34*(1), 242-248. doi:10.1523/JNEUROSCI.1865-13.2014

Jafarpour, A., Horner, A. J., Fuentemilla, L., Penny, W. D., & Duzel, E. (2013). Decoding oscillatory representations and mechanisms in memory. *Neuropsychologia, 51*(4), 772-780. doi:10.1016/j.neuropsychologia.2012.04.002

Jansen, M., White, T. P., Mullinger, K. J., Liddle, E. B., Gowland, P. A., Francis, S. T., . . . Liddle, P. F. (2012). Motion-related artefacts in EEG predict neuronally plausible patterns of activation in fMRI data. *Neuroimage, 59*(1), 261-270. doi:10.1016/j.neuroimage.2011.06.094

Jensen, O., Bonnefond, M., Marshall, T. R., & Tiesinga, P. (2015). Oscillatory mechanisms of feedforward and feedback visual processing. *Trends Neurosci, 38*(4), 192-194. doi:10.1016/j.tins.2015.02.006

Jensen, O., Gelfand, J., Kounios, J., & Lisman, J. E. (2002). Oscillations in the alpha band (9-12 Hz) increase with memory load during retention in a short-term memory task. *Cerebral Cortex, 12*(8), 877-882. doi:DOI 10.1093/cercor/12.8.877

Jensen, O., Gips, B., Bergmann, T. O., & Bonnefond, M. (2014). Temporal coding organized by coupled alpha and gamma oscillations prioritize visual processing. *Trends Neurosci, 37*(7), 357-369. doi:10.1016/j.tins.2014.04.001

Jensen, O., Kaiser, J., & Lachaux, J. P. (2007). Human gamma-frequency oscillations associated with attention and memory. *Trends Neurosci, 30*(7), 317-324. doi:10.1016/j.tins.2007.05.001

Jensen, O., & Mazaheri, A. (2010). Shaping functional architecture by oscillatory alpha activity: gating by inhibition. *Front Hum Neurosci, 4*, 186. doi:10.3389/fnhum.2010.00186

Jokisch, D., & Jensen, O. (2007). Modulation of gamma and alpha activity during a working memory task engaging the dorsal or ventral stream. *J Neurosci, 27*(12), 3244-3251. doi:10.1523/JNEUROSCI.5399-06.2007

Kahana, M. J. (2006). The cognitive correlates of human brain oscillations. *J Neurosci, 26*(6), 1669-1672. doi:10.1523/JNEUROSCI.3737-05c.2006

Kanwisher, N., & Yovel, G. (2006). The fusiform face area: a cortical region specialized for the perception of faces. *Philos Trans R Soc Lond B Biol Sci, 361*(1476), 2109-2128. doi:10.1098/rstb.2006.1934

Kaplan, R., Doeller, C. F., Barnes, G. R., Litvak, V., Duzel, E., Bandettini, P. A., & Burgess, N. (2012). Movement-related theta rhythm in humans: coordinating self-directed hippocampal learning. *PLoS Biol, 10*(2), e1001267. doi:10.1371/journal.pbio.1001267

Kapur, S., Craik, F. I., Tulving, E., Wilson, A. A., Houle, S., & Brown, G. M. (1994). Neuroanatomical correlates of encoding in episodic memory: levels of processing effect. *Proc Natl Acad Sci U S A, 91*(6), 2008-2011. doi:10.1073/pnas.91.6.2008

Kelley, W. M., Miezin, F. M., McDermott, K. B., Buckner, R. L., Raichle, M. E., Cohen, N. J., . . . Petersen, S. E. (1998). Hemispheric specialization in human dorsal frontal cortex and medial temporal lobe for verbal and nonverbal memory encoding. *Neuron, 20*(5), 927-936. Retrieved from http://www.ncbi.nlm.nih.gov/pubmed/9620697

Khader, P. H., Heil, M., & Rosler, F. (2005). Material-specific long-term memory representations of faces and spatial positions: evidence from slow event-related brain potentials. *Neuropsychologia, 43*(14), 2109-2124. doi:10.1016/j.neuropsychologia.2005.03.012

Khader, P. H., Jost, K., Ranganath, C., & Rosler, F. (2010). Theta and alpha oscillations during working-memory maintenance predict successful long-term memory encoding. *Neurosci Lett, 468*(3), 339-343. doi:10.1016/j.neulet.2009.11.028

Khader, P. H., & Rosler, F. (2011). EEG power changes reflect distinct mechanisms during long-term memory retrieval. *Psychophysiology, 48*(3), 362-369. doi:10.1111/j.1469-8986.2010.01063.x

Khursheed, F., Tandon, N., Tertel, K., Pieters, T. A., Disano, M. A., & Ellmore, T. M. (2011). Frequency-specific electrocorticographic correlates of working memory delay period fMRI activity. *Neuroimage, 56*(3), 1773-1782. doi:10.1016/j.neuroimage.2011.02.062

Kim, H. (2011). Neural activity that predicts subsequent memory and forgetting: a meta-analysis of 74 fMRI studies. *Neuroimage, 54*(3), 2446-2461. doi:10.1016/j.neuroimage.2010.09.045

Kirchhoff, B. A., Wagner, A. D., Maril, A., & Stern, C. E. (2000). Prefrontal-temporal circuitry for episodic encoding and subsequent memory. *J Neurosci, 20*(16), 6173-6180. Retrieved from http://www.ncbi.nlm.nih.gov/pubmed/10934267

Klein, K., & Saltz, E. (1976). Specifying the mechanisms in a levels-of-processing approach to memory. *Journal of Experimental Psychology: Human Learning & Memory, 2*(6), 671-679. doi:10.1037/0278-7393.2.6.671

Klimesch, W. (1996). Memory processes, brain oscillations and EEG synchronization. *Int J Psychophysiol, 24*(1-2), 61-100. Retrieved from http://www.ncbi.nlm.nih.gov/pubmed/8978436

Klimesch, W. (2012). alpha-band oscillations, attention, and controlled access to stored information. *Trends Cogn Sci, 16*(12), 606-617. doi:10.1016/j.tics.2012.10.007

Klimesch, W. (2013). An algorithm for the EEG frequency architecture of consciousness and brain body coupling. *Front Hum Neurosci, 7*, 766. doi:10.3389/fnhum.2013.00766

Klimesch, W., Doppelmayr, M., Russegger, H., & Pachinger, T. (1996). Theta band power in the human scalp EEG and the encoding of new information. *Neuroreport, 7*(7), 1235-1240. Retrieved from http://www.ncbi.nlm.nih.gov/pubmed/8817539

Klimesch, W., Doppelmayr, M., Schimke, H., & Ripper, B. (1997). Theta synchronization and alpha desynchronization in a memory task. *Psychophysiology, 34*(2), 169-176. doi:10.1111/j.1469-8986.1997.tb02128.x

Klimesch, W., Freunberger, R., & Sauseng, P. (2010). Oscillatory mechanisms of process binding in memory. *Neurosci Biobehav Rev, 34*(7), 1002-1014. doi:10.1016/j.neubiorev.2009.10.004

Klimesch, W., Freunberger, R., Sauseng, P., & Gruber, W. (2008). A short review of slow phase synchronization and memory: evidence for control processes in different memory systems? *Brain Res, 1235*, 31-44. doi:10.1016/j.brainres.2008.06.049

Klimesch, W., Sauseng, P., & Hanslmayr, S. (2007). EEG alpha oscillations: the inhibition-timing hypothesis. *Brain Res Rev, 53*(1), 63-88. doi:10.1016/j.brainresrev.2006.06.003

Klimesch, W., Schimke, H., Doppelmayr, M., Ripper, B., Schwaiger, J., & Pfurtscheller, G. (1996). Event-related desynchronization (ERD) and the Dm effect: does alpha desynchronization during encoding predict later recall performance? *International*

*journal of psychophysiology : official journal of the International Organization of Psychophysiology, 24*(1-2), 47-60. Retrieved from http://www.ncbi.nlm.nih.gov/pubmed/8978435

Kroneisen, M., & Erdfelder, E. (2011). On the plasticity of the survival processing effect. *J Exp Psychol Learn Mem Cogn, 37*(6), 1553-1562. doi:10.1037/a0024493

Kroneisen, M., Erdfelder, E., & Buchner, A. (2013). The proximate memory mechanism underlying the survival-processing effect: richness of encoding or interactive imagery? *Memory, 21*(4), 494-502. doi:10.1080/09658211.2012.741603

Lachaux, J. P., Rodriguez, E., Martinerie, J., & Varela, F. J. (1999). Measuring phase synchrony in brain signals. *Hum Brain Mapp, 8*(4), 194-208. doi:10.1002/(sici)1097-0193(1999)8:4<194::aid-hbm4>3.0.co;2-c

Lakatos, P., Shah, A. S., Knuth, K. H., Ulbert, I., Karmos, G., & Schroeder, C. E. (2005). An oscillatory hierarchy controlling neuronal excitability and stimulus processing in the auditory cortex. *J Neurophysiol, 94*(3), 1904-1911. doi:10.1152/jn.00263.2005

Laufs, H., Holt, J. L., Elfont, R., Krams, M., Paul, J. S., Krakow, K., & Kleinschmidt, A. (2006). Where the BOLD signal goes when alpha EEG leaves. *Neuroimage, 31*(4), 1408-1418. doi:10.1016/j.neuroimage.2006.02.002

Lavallee, C. F., Herrmann, C. S., Weerda, R., & Huster, R. J. (2014). Stimulus-response mappings shape inhibition processes: a combined EEG-fMRI study of contextual stopping. *PLoS One, 9*(4), e96159. doi:10.1371/journal.pone.0096159

Lemieux, L., Salek-Haddadi, A., Lund, T. E., Laufs, H., & Carmichael, D. (2007). Modelling large motion events in fMRI studies of patients with epilepsy. *Magn Reson Imaging, 25*(6), 894-901. doi:10.1016/j.mri.2007.03.009

LeVan, P., Maclaren, J., Herbst, M., Sostheim, R., Zaitsev, M., & Hennig, J. (2013). Ballistocardiographic artifact removal from simultaneous EEG-fMRI using an optical motion-tracking system. *Neuroimage, 75*, 1-11. doi:10.1016/j.neuroimage.2013.02.039

Lisman, J. E., & Idiart, M. A. P. (1995). Storage of 7+/-2 Short-Term Memories in Oscillatory Subcycles. *Science, 267*(5203), 1512-1515. doi:DOI 10.1126/science.7878473

Lisman, J. E., & Jensen, O. (2013). The theta-gamma neural code. *Neuron, 77*(6), 1002-1016. doi:10.1016/j.neuron.2013.03.007

Liu, Z., de Zwart, J. A., van Gelderen, P., Kuo, L. W., & Duyn, J. H. (2012). Statistical feature extraction for artifact removal from concurrent fMRI-EEG recordings. *Neuroimage, 59*(3), 2073-2087. doi:10.1016/j.neuroimage.2011.10.042

Logothetis, N. K., Pauls, J., Augath, M., Trinath, T., & Oeltermann, A. (2001). Neurophysiological investigation of the basis of the fMRI signal. *Nature, 412*(6843), 150-157. doi:10.1038/35084005

Logothetis, N. K., Pauls, J., & Poggio, T. (1995). Shape representation in the inferior temporal cortex of monkeys. *Curr Biol, 5*(5), 552-563. doi:10.1016/S0960-9822(95)00108-4

Long, N. M., Burke, J. F., & Kahana, M. J. (2014). Subsequent memory effect in intracranial and scalp EEG. *Neuroimage, 84*, 488-494. doi:10.1016/j.neuroimage.2013.08.052

Macey, P. M., Macey, K. E., Kumar, R., & Harper, R. M. (2004). A method for removal of global effects from fMRI time series. *Neuroimage, 22*(1), 360-366. doi:10.1016/j.neuroimage.2003.12.042

Macmillan, N. A., & Creelman, C. D. (1991). *Detection Theory: A User's Guide*: Cambridge University Press.

Magri, C., Schridde, U., Murayama, Y., Panzeri, S., & Logothetis, N. K. (2012). The amplitude and timing of the BOLD signal reflects the relationship between local field potential power at different frequencies. *J Neurosci, 32*(4), 1395-1407. doi:10.1523/JNEUROSCI.3985-11.2012

Maguire, E. A., Valentine, E. R., Wilding, J. M., & Kapur, N. (2003). Routes to remembering: the brains behind superior memory. *Nat Neurosci, 6*(1), 90-95. doi:10.1038/nn988

Mantini, D., Perrucci, M. G., Del Gratta, C., Romani, G. L., & Corbetta, M. (2007). Electrophysiological signatures of resting state networks in the human brain. *Proc Natl Acad Sci U S A, 104*(32), 13170-13175. doi:10.1073/pnas.0700668104

Maris, E., & Oostenveld, R. (2007). Nonparametric statistical testing of EEG- and MEG-data. *J Neurosci Methods, 164*(1), 177-190. doi:10.1016/j.jneumeth.2007.03.024

Masterton, R. A., Abbott, D. F., Fleming, S. W., & Jackson, G. D. (2007). Measurement and reduction of motion and ballistocardiogram artefacts from simultaneous EEG and fMRI recordings. *Neuroimage, 37*(1), 202-211. doi:10.1016/j.neuroimage.2007.02.060

Matsuo, T., Kawasaki, K., Kawai, K., Majima, K., Masuda, H., Murakami, H., . . . Hasegawa, I. (2015). Alternating zones selective to faces and written words in the human ventral occipitotemporal cortex. *Cereb Cortex, 25*(5), 1265-1277. doi:10.1093/cercor/bht319

McCandliss, B. D., Cohen, L., & Dehaene, S. (2003). The visual word form area: expertise for reading in the fusiform gyrus. *Trends Cogn Sci, 7*(7), 293-299. Retrieved from http://www.ncbi.nlm.nih.gov/pubmed/12860187

Mcclelland, J. L., Mcnaughton, B. L., & Oreilly, R. C. (1995). Why There Are Complementary Learning-Systems in the Hippocampus and Neocortex - Insights from the Successes and Failures of Connectionist Models of Learning and Memory. *Psychological review, 102*(3), 419-457. doi:Doi 10.1037/0033-295x.102.3.419

Meeuwissen, E. B., Takashima, A., Fernandez, G., & Jensen, O. (2011). Increase in posterior alpha activity during rehearsal predicts successful long-term memory formation of word sequences. *Hum Brain Mapp, 32*(12), 2045-2053. doi:10.1002/hbm.21167

Merkow, M. B., Burke, J. F., Stein, J. M., & Kahana, M. J. (2014). Prestimulus theta in the human hippocampus predicts subsequent recognition but not recall. *Hippocampus, 24*(12), 1562-1569. doi:10.1002/hipo.22335

Meyer, M. C., van Oort, E. S., & Barth, M. (2013). Electrophysiological correlation patterns of resting state networks in single subjects: a combined EEG-fMRI study. *Brain Topogr, 26*(1), 98-109. doi:10.1007/s10548-012-0235-0

Miller, K. J., Honey, C. J., Hermes, D., Rao, R. P., denNijs, M., & Ojemann, J. G. (2014). Broadband changes in the cortical surface potential track activation of functionally diverse neuronal populations. *Neuroimage, 85 Pt 2*, 711-720. doi:10.1016/j.neuroimage.2013.08.070

Mitchell, J. F., Sundberg, K. A., & Reynolds, J. H. (2009). Spatial attention decorrelates intrinsic activity fluctuations in macaque area V4. *Neuron, 63*(6), 879-888. doi:10.1016/j.neuron.2009.09.013

Morris, C. D., Bransford, J. D., & Franks, J. J. (1977). Levels of Processing Versus Transfer Appropriate Processing. *Journal of Verbal Learning and Verbal Behavior, 16*(5), 519-533. doi:Doi 10.1016/S0022-5371(77)80016-9

Moser, E. I., & Moser, M. B. (2013). Grid cells and neural coding in high-end cortices. *Neuron, 80*(3), 765-774. doi:10.1016/j.neuron.2013.09.043

Mukamel, R., Gelbard, H., Arieli, A., Hasson, U., Fried, I., & Malach, R. (2005). Coupling between neuronal firing, field potentials, and FMRI in human auditory cortex. *Science, 309*(5736), 951-954. doi:10.1126/science.1110913

Mullinger, K. J., Havenhand, J., & Bowtell, R. (2013). Identifying the sources of the pulse artefact in EEG recordings made inside an MR scanner. *Neuroimage, 71*, 75-83. doi:10.1016/j.neuroimage.2012.12.070

Murphy, K., Birn, R. M., & Bandettini, P. A. (2013). Resting-state fMRI confounds and cleanup. *Neuroimage, 80*, 349-359. doi:10.1016/j.neuroimage.2013.04.001

Nadel, L., & Moscovitch, M. (1997). Memory consolidation, retrograde amnesia and the hippocampal complex. *Curr Opin Neurobiol, 7*(2), 217-227. doi:10.1016/S0959-4388(97)80010-4

Nadel, L., Samsonovich, A., Ryan, L., & Moscovitch, M. (2000). Multiple trace theory of human memory: computational, neuroimaging, and neuropsychological results. *Hippocampus, 10*(4), 352-368. doi:10.1002/1098-1063(2000)10:4<352::AID-HIPO2>3.0.CO;2-D

Nairne, J. S., & Pandeirada, J. N. S. (2008). Adaptive memory - Remembering with a stone-age brain. *Current Directions in Psychological Science, 17*(4), 239-243. doi:DOI 10.1111/j.1467-8721.2008.00582.x

Nairne, J. S., Thompson, S. R., & Pandeirada, J. N. (2007). Adaptive memory: survival processing enhances retention. *J Exp Psychol Learn Mem Cogn, 33*(2), 263-273. doi:10.1037/0278-7393.33.2.263

Niazy, R. K., Beckmann, C. F., Iannetti, G. D., Brady, J. M., & Smith, S. M. (2005). Removal of FMRI environment artifacts from EEG data using optimal basis sets. *Neuroimage, 28*(3), 720-737. doi:10.1016/j.neuroimage.2005.06.067

Nichols, T., Brett, M., Andersson, J., Wager, T., & Poline, J. B. (2005). Valid conjunction inference with the minimum statistic. *Neuroimage, 25*(3), 653-660. doi:10.1016/j.neuroimage.2004.12.005

Niessing, J., Ebisch, B., Schmidt, K. E., Niessing, M., Singer, W., & Galuske, R. A. (2005). Hemodynamic signals correlate tightly with synchronized gamma oscillations. *Science, 309*(5736), 948-951. doi:10.1126/science.1110948

Nolte, G. (2003). The magnetic lead field theorem in the quasi-static approximation and its use for magnetoencephalography forward calculation in realistic volume conductors. *Physics in medicine and biology, 48*(22), 3637-3652. doi:Doi 10.1088/0031-9155/48/22/002

Noppeney, U., Phillips, J., & Price, C. (2004). The neural areas that control the retrieval and selection of semantics. *Neuropsychologia, 42*(9), 1269-1280. doi:10.1016/j.neuropsychologia.2003.12.014

Nunez, P. L., Srinivasan, R., Westdorp, A. F., Wijesinghe, R. S., Tucker, D. M., Silberstein, R. B., & Cadusch, P. J. (1997). EEG coherency. I: Statistics, reference electrode, volume conduction, Laplacians, cortical imaging, and interpretation at multiple scales. *Electroencephalogr Clin Neurophysiol, 103*(5), 499-515. doi:10.1016/s0013-4694(97)00066-7

Nyhus, E., & Curran, T. (2010). Functional role of gamma and theta oscillations in episodic memory. *Neurosci Biobehav Rev, 34*(7), 1023-1035. doi:10.1016/j.neubiorev.2009.12.014

Oostenveld, R., Fries, P., Maris, E., & Schoffelen, J. M. (2011). FieldTrip: Open source software for advanced analysis of MEG, EEG, and invasive electrophysiological data. *Comput Intell Neurosci, 2011*, 156869. doi:10.1155/2011/156869

Osipova, D., Takashima, A., Oostenveld, R., Fernandez, G., Maris, E., & Jensen, O. (2006). Theta and gamma oscillations predict encoding and retrieval of declarative memory. *J Neurosci, 26*(28), 7523-7531. doi:10.1523/JNEUROSCI.1948-06.2006

Otten, L. J., Quayle, A. H., Akram, S., Ditewig, T. A., & Rugg, M. D. (2006). Brain activity before an event predicts later recollection. *Nat Neurosci, 9*(4), 489-491. doi:10.1038/nn1663

Otten, L. J., & Rugg, M. D. (2001a). Electrophysiological correlates of memory encoding are task-dependent. *Brain Res Cogn Brain Res, 12*(1), 11-18. doi:10.1016/s0926-6410(01)00015-5

Otten, L. J., & Rugg, M. D. (2001b). Task-dependency of the neural correlates of episodic encoding as measured by fMRI. *Cerebral Cortex, 11*(12), 1150-1160. doi:DOI 10.1093/cercor/11.12.1150

Paivio, A. (1991). Dual Coding Theory - Retrospect and Current Status. *Canadian Journal of Psychology-Revue Canadienne De Psychologie, 45*(3), 255-287. doi:DOI 10.1037/h0084295

Paller, K. A., McCarthy, G., & Wood, C. C. (1988). ERPs predictive of subsequent recall and recognition performance. *Biol Psychol, 26*(1-3), 269-276. Retrieved from http://www.ncbi.nlm.nih.gov/pubmed/3207786

Paller, K. A., & Wagner, A. D. (2002). Observing the transformation of experience into memory. *Trends in Cognitive Sciences, 6*(2), 93-102. doi:Doi 10.1016/S1364-6613(00)01845-3

Park, H. D., Correia, S., Ducorps, A., & Tallon-Baudry, C. (2014). Spontaneous fluctuations in neural responses to heartbeats predict visual detection. *Nat Neurosci, 17*(4), 612-618. doi:10.1038/nn.3671

Park, H. D., & Tallon-Baudry, C. (2014). The neural subjective frame: from bodily signals to perceptual consciousness. *Philos Trans R Soc Lond B Biol Sci, 369*(1641), 20130208. doi:10.1098/rstb.2013.0208

Patterson, K., Nestor, P. J., & Rogers, T. T. (2007). Where do you know what you know? The representation of semantic knowledge in the human brain. *Nat Rev Neurosci, 8*(12), 976-987. doi:10.1038/nrn2277

Pfurtscheller, G., & Aranibar, A. (1977). Event-related cortical desynchronization detected by power measurements of scalp EEG. *Electroencephalogr Clin Neurophysiol, 42*(6), 817-826. doi:10.1016/0013-4694(77)90235-8

Popov, T., Miller, G. A., Rockstroh, B., & Weisz, N. (2013). Modulation of alpha power and functional connectivity during facial affect recognition. *J Neurosci, 33*(14), 6018-6026. doi:10.1523/JNEUROSCI.2763-12.2013

Power, J. D., Mitra, A., Laumann, T. O., Snyder, A. Z., Schlaggar, B. L., & Petersen, S. E. (2014). Methods to detect, characterize, and remove motion artifact in resting state fMRI. *Neuroimage, 84*, 320-341. doi:10.1016/j.neuroimage.2013.08.048

Pulvermuller, F. (2013). How neurons make meaning: brain mechanisms for embodied and abstract-symbolic semantics. *Trends Cogn Sci, 17*(9), 458-470. doi:10.1016/j.tics.2013.06.004

Quiroga, R. Q., Kreiman, G., Koch, C., & Fried, I. (2008). Sparse but not 'grandmother-cell' coding in the medial temporal lobe. *Trends Cogn Sci, 12*(3), 87-91. doi:10.1016/j.tics.2007.12.003

Quiroga, R. Q., Reddy, L., Kreiman, G., Koch, C., & Fried, I. (2005). Invariant visual representation by single neurons in the human brain. *Nature, 435*(7045), 1102-1107. doi:10.1038/nature03687

Ranganath, C. (2010). A unified framework for the functional organization of the medial temporal lobes and the phenomenology of episodic memory. *Hippocampus, 20*(11), 1263-1290. doi:10.1002/hipo.20852

Rice, J. K., Rorden, C., Little, J. S., & Parra, L. C. (2013). Subject position affects EEG magnitudes. *Neuroimage, 64*, 476-484. doi:10.1016/j.neuroimage.2012.09.041

Ritter, P., Moosmann, M., & Villringer, A. (2009). Rolandic alpha and beta EEG rhythms' strengths are inversely related to fMRI-BOLD signal in primary somatosensory and motor cortex. *Hum Brain Mapp, 30*(4), 1168-1187. doi:10.1002/hbm.20585

Roediger, H. L. (1980). The effectiveness of four mnemonics in ordering recall. *Journal of Experimental Psychology: Human Learning and Memory, 6*(5). Retrieved from psycnet.apa.org

Roux, F., & Uhlhaas, P. J. (2014). Working memory and neural oscillations: alpha-gamma versus theta-gamma codes for distinct WM information? *Trends Cogn Sci, 18*(1), 16-25. doi:10.1016/j.tics.2013.10.010

Rutishauser, U., Ross, I. B., Mamelak, A. N., & Schuman, E. M. (2010). Human memory strength is predicted by theta-frequency phase-locking of single neurons. *Nature, 464*(7290), 903-907. doi:10.1038/nature08860

Sadaghiani, S., Scheeringa, R., Lehongre, K., Morillon, B., Giraud, A. L., & Kleinschmidt, A. (2010). Intrinsic connectivity networks, alpha oscillations, and tonic alertness: a simultaneous electroencephalography/functional magnetic resonance imaging study. *J Neurosci, 30*(30), 10243-10250. doi:10.1523/JNEUROSCI.1004-10.2010

Salinas, E., & Sejnowski, T. J. (2001). Correlated neuronal activity and the flow of neural information. *Nat Rev Neurosci, 2*(8), 539-550. doi:10.1038/35086012

Sammer, G., Blecker, C., Gebhardt, H., Bischoff, M., Stark, R., Morgen, K., & Vaitl, D. (2007). Relationship between regional hemodynamic activity and simultaneously recorded EEG-theta associated with mental arithmetic-induced workload. *Hum Brain Mapp, 28*(8), 793-803. doi:10.1002/hbm.20309

Sanquist, T. F., Rohrbaugh, J. W., Syndulko, K., & Lindsley, D. B. (1980). Electrocortical signs of levels of processing: perceptual analysis and recognition memory. *Psychophysiology, 17*(6), 568-576. doi:10.1111/j.1469-8986.1980.tb02299.x

Satterthwaite, T. D., Wolf, D. H., Ruparel, K., Erus, G., Elliott, M. A., Eickhoff, S. B., . . . Gur, R. C. (2013). Heterogeneous impact of motion on fundamental patterns of developmental changes in functional connectivity during youth. *Neuroimage, 83*, 45-57. doi:10.1016/j.neuroimage.2013.06.045

Sauseng, P., Klimesch, W., Doppelmayr, M., Pecherstorfer, T., Freunberger, R., & Hanslmayr, S. (2005). EEG alpha synchronization and functional coupling during top-down processing in a working memory task. *Hum Brain Mapp, 26*(2), 148-155. doi:10.1002/hbm.20150

Scheeringa, R., Fries, P., Petersson, K. M., Oostenveld, R., Grothe, I., Norris, D. G., . . . Bastiaansen, M. C. (2011). Neuronal dynamics underlying high- and low-frequency EEG oscillations contribute independently to the human BOLD signal. *Neuron, 69*(3), 572-583. doi:10.1016/j.neuron.2010.11.044

Scheeringa, R., Petersson, K. M., Oostenveld, R., Norris, D. G., Hagoort, P., & Bastiaansen, M. C. (2009). Trial-by-trial coupling between EEG and BOLD identifies networks related to

alpha and theta EEG power increases during working memory maintenance. *Neuroimage, 44*(3), 1224-1238. doi:10.1016/j.neuroimage.2008.08.041

Schneidman, E., Puchalla, J. L., Segev, R., Harris, R. A., Bialek, W., & Berry, M. J., 2nd. (2011). Synergy from silence in a combinatorial neural code. *J Neurosci, 31*(44), 15732-15741. doi:10.1523/JNEUROSCI.0301-09.2011

Schott, B. H., Henson, R. N., Richardson-Klavehn, A., Becker, C., Thoma, V., Heinze, H. J., & Duzel, E. (2005). Redefining implicit and explicit memory: the functional neuroanatomy of priming, remembering, and control of retrieval. *Proc Natl Acad Sci U S A, 102*(4), 1257-1262. doi:10.1073/pnas.0409070102

Schott, B. H., Wustenberg, T., Wimber, M., Fenker, D. B., Zierhut, K. C., Seidenbecher, C. I., . . . Richardson-Klavehn, A. (2013). The relationship between level of processing and hippocampal-cortical functional connectivity during episodic memory formation in humans. *Hum Brain Mapp, 34*(2), 407-424. doi:10.1002/hbm.21435

Scoville, W. B., & Milner, B. (1957). Loss of recent memory after bilateral hippocampal lesions. *J Neurol Neurosurg Psychiatry, 20*(1), 11-21. doi:10.1136/jnnp.20.1.11

Sederberg, P. B., Kahana, M. J., Howard, M. W., Donner, E. J., & Madsen, J. R. (2003). Theta and gamma oscillations during encoding predict subsequent recall. *J Neurosci, 23*(34), 10809-10814. Retrieved from http://www.ncbi.nlm.nih.gov/pubmed/14645473

Sederberg, P. B., Schulze-Bonhage, A., Madsen, J. R., Bromfield, E. B., McCarthy, D. C., Brandt, A., . . . Kahana, M. J. (2007). Hippocampal and neocortical gamma oscillations predict memory formation in humans. *Cereb Cortex, 17*(5), 1190-1196. doi:10.1093/cercor/bhl030

Shadlen, M. N., & Movshon, J. A. (1999). Synchrony unbound: a critical evaluation of the temporal binding hypothesis. *Neuron, 24*(1), 67-77, 111-125. doi:10.1016/S0896-6273(00)80822-3

Sharon, L. T.-S. (2003). Neuroimaging studies of semantic memory: inferring "how" from "where". *Neuropsychologia, 41*(3), 280-292. Retrieved from http://www.sciencedirect.com/science/article/pii/S0028393202001616

Shmueli, K., van Gelderen, P., de Zwart, J. A., Horovitz, S. G., Fukunaga, M., Jansma, J. M., & Duyn, J. H. (2007). Low-frequency fluctuations in the cardiac rate as a source of variance in the resting-state fMRI BOLD signal. *Neuroimage, 38*(2), 306-320. doi:10.1016/j.neuroimage.2007.07.037

Siegel, J. S., Power, J. D., Dubis, J. W., Vogel, A. C., Church, J. A., Schlaggar, B. L., & Petersen, S. E. (2014). Statistical improvements in functional magnetic resonance imaging analyses produced by censoring high-motion data points. *Hum Brain Mapp, 35*(5), 1981-1996. doi:10.1002/hbm.22307

Siegel, M., Donner, T. H., & Engel, A. K. (2012). Spectral fingerprints of large-scale neuronal interactions. *Nat Rev Neurosci, 13*(2), 121-134. doi:10.1038/nrn3137

Simons, J. S., Graham, K. S., Galton, C. J., Patterson, K., & Hodges, J. R. (2001). Semantic knowledge and episodic memory for faces in semantic dementia. *Neuropsychology, 15*(1), 101-114. Retrieved from http://www.ncbi.nlm.nih.gov/pubmed/11216881

Singer, W., & Gray, C. M. (1995). Visual feature integration and the temporal correlation hypothesis. *Annu Rev Neurosci, 18*, 555-586. doi:10.1146/annurev.ne.18.030195.003011

Singh, K. D. (2012). Which "neural activity" do you mean? fMRI, MEG, oscillations and neurotransmitters. *Neuroimage, 62*(2), 1121-1130. doi:10.1016/j.neuroimage.2012.01.028

Soderstrom, N. C., & McCabe, D. P. (2011). Are survival processing memory advantages based on ancestral priorities? *Psychon Bull Rev, 18*(3), 564-569. doi:10.3758/s13423-011-0060-6

Spitzer, B., & Bauml, K. H. (2007). Retrieval-induced forgetting in item recognition: evidence for a reduction in general memory strength. *J Exp Psychol Learn Mem Cogn, 33*(5), 863-875. doi:10.1037/0278-7393.33.5.863

Sporer, S. L. (1991). Deep deeper deepest? Encoding strategies and the recognition of human faces. *Journal of Experimental Psychology: Learning, Memory, and Cognition, 17*(2), 323-333. doi:10.1037/0278-7393.17.2.323

Squire, L. R. (2004). Memory systems of the brain: a brief history and current perspective. *Neurobiol Learn Mem, 82*(3), 171-177. doi:10.1016/j.nlm.2004.06.005

Staresina, B. P., & Davachi, L. (2009). Mind the gap: binding experiences across space and time in the human hippocampus. *Neuron, 63*(2), 267-276. doi:10.1016/j.neuron.2009.06.024

Staudigl, T., & Hanslmayr, S. (2013). Theta oscillations at encoding mediate the context-dependent nature of human episodic memory. *Curr Biol, 23*(12), 1101-1106. doi:10.1016/j.cub.2013.04.074

Staudigl, T., Vollmar, C., Noachtar, S., & Hanslmayr, S. (2015). Temporal-pattern similarity analysis reveals the beneficial and detrimental effects of context reinstatement on human memory. *J Neurosci, 35*(13), 5373-5384. doi:10.1523/JNEUROSCI.4198-14.2015

Stern, C. E., Corkin, S., Gonzalez, R. G., Guimaraes, A. R., Baker, J. R., Jennings, P. J., . . . Rosen, B. R. (1996). The hippocampal formation participates in novel picture encoding: evidence from functional magnetic resonance imaging. *Proc Natl Acad Sci U S A, 93*(16), 8660-8665. Retrieved from http://www.ncbi.nlm.nih.gov/pubmed/8710927

Summerfield, C., & Mangels, J. A. (2005). Coherent theta-band EEG activity predicts item-context binding during encoding. *Neuroimage, 24*(3), 692-703. doi:10.1016/j.neuroimage.2004.09.012

Terrazas, A., Krause, M., Lipa, P., Gothard, K. M., Barnes, C. A., & McNaughton, B. L. (2005). Self-motion and the hippocampal spatial metric. *J Neurosci, 25*(35), 8085-8096. doi:10.1523/JNEUROSCI.0693-05.2005

Thibault, R. T., Lifshitz, M., Jones, J. M., & Raz, A. (2014). Posture alters human resting-state. *Cortex, 58*, 199-205. doi:10.1016/j.cortex.2014.06.014

Thut, G., & Miniussi, C. (2009). New insights into rhythmic brain activity from TMS-EEG studies. *Trends Cogn Sci, 13*(4), 182-189. doi:10.1016/j.tics.2009.01.004

Tort, A. B., Komorowski, R. W., Manns, J. R., Kopell, N. J., & Eichenbaum, H. (2009). Theta-gamma coupling increases during the learning of item-context associations. *Proc Natl Acad Sci U S A, 106*(49), 20942-20947. doi:10.1073/pnas.0911331106

Tulving, E. (1984). Precis of Tulving Elements of Episodic Memory (Oxford-University-Press, 1983). *Behavioral and Brain Sciences, 7*(2), 223-238. Retrieved from <Go to ISI>://WOS:A1984SX97600028

Tulving, E. (1993). What is episodic memory? *Current Directions in Psychological Science*. Retrieved from http://www.jstor.org/stable/20182204

Tulving, E. (2001). Episodic memory and common sense: how far apart? *Philos Trans R Soc Lond B Biol Sci, 356*(1413), 1505-1515. doi:10.1098/rstb.2001.0937

Tulving, E. (2002). Episodic memory: from mind to brain. *Annu Rev Psychol, 53*, 1-25. doi:10.1146/annurev.psych.53.100901.135114

Tulving, E., & Thomson, D. M. (1973). Encoding Specificity and Retrieval Processes in Episodic Memory. *Psychological review, 80*(5), 352-373. doi:DOI 10.1037/h0020071

Tzourio-Mazoyer, N., Landeau, B., Papathanassiou, D., Crivello, F., Etard, O., Delcroix, N., . . . Joliot, M. (2002). Automated anatomical labeling of activations in SPM using a macroscopic anatomical parcellation of the MNI MRI single-subject brain. *Neuroimage, 15*(1), 273-289. doi:10.1006/nimg.2001.0978

Uncapher, M. R., Otten, L. J., & Rugg, M. D. (2006). Episodic encoding is more than the sum of its parts: an fMRI investigation of multifeatural contextual encoding. *Neuron, 52*(3), 547-556. doi:10.1016/j.neuron.2006.08.011

van Buuren, M., Gladwin, T. E., Zandbelt, B. B., van den Heuvel, M., Ramsey, N. F., Kahn, R. S., & Vink, M. (2009). Cardiorespiratory effects on default-mode network activity as measured with fMRI. *Hum Brain Mapp, 30*(9), 3031-3042. doi:10.1002/hbm.20729

van Kesteren, M. T., Ruiter, D. J., Fernandez, G., & Henson, R. N. (2012). How schema and novelty augment memory formation. *Trends Neurosci, 35*(4), 211-219. doi:10.1016/j.tins.2012.02.001

Van Veen, B. D., van Drongelen, W., Yuchtman, M., & Suzuki, A. (1997). Localization of brain electrical activity via linearly constrained minimum variance spatial filtering. *IEEE Trans Biomed Eng, 44*(9), 867-880. doi:10.1109/10.623056

Vanderwolf, C. H. (1969). Hippocampal electrical activity and voluntary movement in the rat. *Electroencephalogr Clin Neurophysiol, 26*(4), 407-418. doi:10.1016/0013-4694(69)90092-3

Vann, S. D., Aggleton, J. P., & Maguire, E. A. (2009). What does the retrosplenial cortex do? *Nat Rev Neurosci, 10*(11), 792-802. doi:10.1038/nrn2733

Varela, F., Lachaux, J. P., Rodriguez, E., & Martinerie, J. (2001). The brainweb: phase synchronization and large-scale integration. *Nat Rev Neurosci, 2*(4), 229-239. doi:10.1038/35067550

Vargha-Khadem, F., Gadian, D. G., Watkins, K. E., Connelly, A., Van Paesschen, W., & Mishkin, M. (1997). Differential effects of early hippocampal pathology on episodic and semantic memory. *Science, 277*(5324), 376-380. doi:10.1126/science.277.5324.376

Vlemincx, E., Taelman, J., De Peuter, S., Van Diest, I., & Van den Bergh, O. (2011). Sigh rate and respiratory variability during mental load and sustained attention. *Psychophysiology, 48*(1), 117-120. doi:10.1111/j.1469-8986.2010.01043.x

von Stein, A., Chiang, C., & Konig, P. (2000). Top-down processing mediated by interareal synchronization. *Proc Natl Acad Sci U S A, 97*(26), 14748-14753. doi:10.1073/pnas.97.26.14748

Voytek, B., & Knight, R. T. (2015). Dynamic network communication as a unifying neural basis for cognition, development, aging, and disease. *Biol Psychiatry, 77*(12), 1089-1097. doi:10.1016/j.biopsych.2015.04.016

Wagner, A. D., Schacter, D. L., Rotte, M., Koutstaal, W., Maril, A., Dale, A. M., . . . Buckner, R. L. (1998). Building memories: Remembering and forgetting of verbal experiences as predicted by brain activity. *Science, 281*(5380), 1188-1191. doi:DOI 10.1126/science.281.5380.1188

Waldhauser, G. T., Johansson, M., & Hanslmayr, S. (2012). alpha/beta oscillations indicate inhibition of interfering visual memories. *J Neurosci, 32*(6), 1953-1961. doi:10.1523/JNEUROSCI.4201-11.2012

Wang, L., Jensen, O., van den Brink, D., Weder, N., Schoffelen, J. M., Magyari, L., . . . Bastiaansen, M. (2012). Beta oscillations relate to the N400m during language comprehension. *Hum Brain Mapp, 33*(12), 2898-2912. doi:10.1002/hbm.21410

Watrous, A. J., & Ekstrom, A. D. (2014). The spectro-contextual encoding and retrieval theory of episodic memory. *Front Hum Neurosci, 8*, 75. doi:10.3389/fnhum.2014.00075

Watrous, A. J., Fell, J., Ekstrom, A. D., & Axmacher, N. (2015). More than spikes: common oscillatory mechanisms for content specific neural representations during perception and memory. *Curr Opin Neurobiol, 31*, 33-39. doi:10.1016/j.conb.2014.07.024

Watrous, A. J., Fried, I., & Ekstrom, A. D. (2011). Behavioral correlates of human hippocampal delta and theta oscillations during navigation. *J Neurophysiol, 105*(4), 1747-1755. doi:10.1152/jn.00921.2010

Watrous, A. J., Lee, D. J., Izadi, A., Gurkoff, G. G., Shahlaie, K., & Ekstrom, A. D. (2013). A comparative study of human and rat hippocampal low-frequency oscillations during spatial navigation. *Hippocampus, 23*(8), 656-661. doi:10.1002/hipo.22124

Watrous, A. J., Tandon, N., Conner, C. R., Pieters, T., & Ekstrom, A. D. (2013). Frequency-specific network connectivity increases underlie accurate spatiotemporal memory retrieval. *Nat Neurosci, 16*(3), 349-356. doi:10.1038/nn.3315

Weiss, S., & Mueller, H. M. (2012). "Too Many betas do not Spoil the Broth": The Role of Beta Brain Oscillations in Language Processing. *Front Psychol, 3*, 201. doi:10.3389/fpsyg.2012.00201

Weiss, S., & Rappelsberger, P. (2000). Long-range EEG synchronization during word encoding correlates with successful memory performance. *Brain Res Cogn Brain Res, 9*(3), 299-312. Retrieved from http://www.ncbi.nlm.nih.gov/pubmed/10808141

Weisz, N., Wuhle, A., Monittola, G., Demarchi, G., Frey, J., Popov, T., & Braun, C. (2014). Prestimulus oscillatory power and connectivity patterns predispose conscious somatosensory perception. *Proc Natl Acad Sci U S A, 111*(4), E417-425. doi:10.1073/pnas.1317267111

White, T. P., Jansen, M., Doege, K., Mullinger, K. J., Park, S. B., Liddle, E. B., . . . Liddle, P. F. (2013). Theta power during encoding predicts subsequent-memory performance and default mode network deactivation. *Hum Brain Mapp, 34*(11), 2929-2943. doi:10.1002/hbm.22114

Wimber, M., Maass, A., Staudigl, T., Richardson-Klavehn, A., & Hanslmayr, S. (2012). Rapid memory reactivation revealed by oscillatory entrainment. *Curr Biol, 22*(16), 1482-1486. doi:10.1016/j.cub.2012.05.054

Winograd, E. (1981). Elaboration and distinctiveness in memory for faces. *J Exp Psychol Hum Learn, 7*(3), 181-190. doi:10.1037/0278-7393.7.3.181

Wixted, J. T. (2007). Dual-process theory and signal-detection theory of recognition memory. *Psychol Rev, 114*(1), 152-176. doi:10.1037/0033-295X.114.1.152

Worthen, J. B., & Hunt, R. R. (2008). Mnemonics: Underlying Processes and Practical Applications. In J. H. Byrne (Ed.), *Learning and Memory: A Comprehensive Reference* (pp. 145-156). Oxford: Academic Press.

Yan, C. G., Cheung, B., Kelly, C., Colcombe, S., Craddock, R. C., Di Martino, A., . . . Milham, M. P. (2013). A comprehensive assessment of regional variation in the impact of head micromovements on functional connectomics. *Neuroimage, 76*, 183-201. doi:10.1016/j.neuroimage.2013.03.004

Yonelinas, A. P. (2001). Consciousness, control, and confidence: the 3 Cs of recognition memory. *J Exp Psychol Gen, 130*(3), 361-379. Retrieved from http://www.ncbi.nlm.nih.gov/pubmed/11561915

Yuan, H., Zotev, V., Phillips, R., & Bodurka, J. (2013). Correlated slow fluctuations in respiration, EEG, and BOLD fMRI. *Neuroimage, 79*, 81-93. doi:10.1016/j.neuroimage.2013.04.068

Zotev, V., Yuan, H., Phillips, R., & Bodurka, J. (2012). EEG-assisted retrospective motion correction for fMRI: E-REMCOR. *Neuroimage, 63*(2), 698-712. doi:10.1016/j.neuroimage.2012.07.031

Zucker, H. R., & Ranganath, C. (2015). Navigating the human hippocampus without a GPS. *Hippocampus, 25*(6), 697-703. doi:10.1002/hipo.22447

Zumer, J. M., Scheeringa, R., Schoffelen, J. M., Norris, D. G., & Jensen, O. (2014). Occipital alpha activity during stimulus processing gates the information flow to object-selective cortex. *PLoS Biol, 12*(10), e1001965. doi:10.1371/journal.pbio.1001965

# SUPPLEMENTAL MATERIAL

## SUPPLEMENTAL MATERIAL TO STUDY 1

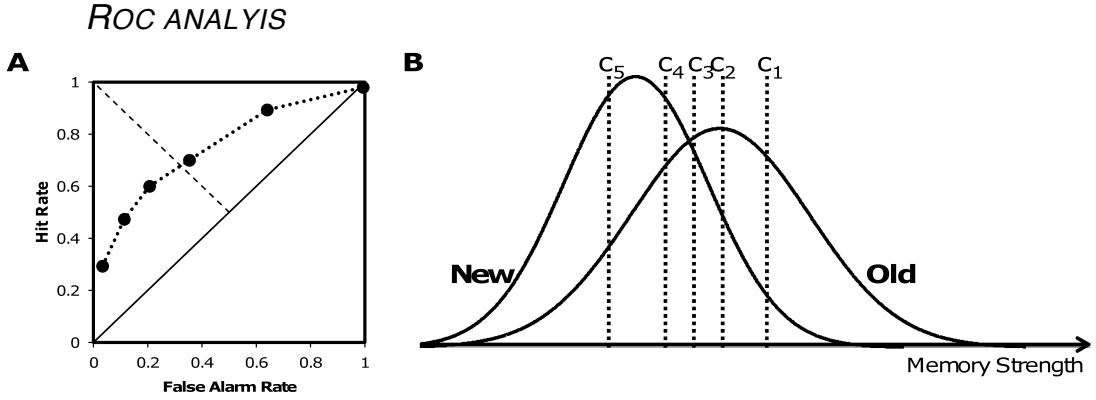


**Supplementary Figure 1:** A Example of an individual ROC. The cumulated hit rate is plotted on the y-axis, and the cumulated false alarm rate is plotted on the x-axis. These 10 data points (hit rate and false alarm rate for 5 criteria each) are used to estimate the model parameter. Each point on the ROC represents the false alarm and hit rate for a rating i.e. criterion with varying bias. B Assumed Model. The unequal variance signal detection model assumes that memory strength for new and old items can be modelled with normal distributions. The criterion values $c_i$ represent cutoff values. If an item elicits a certain memory strength higher than a criterion $c_i$ the item is rating with confidence rating i. The neutral response criterion is at the crossover of the distributions representing the criterion of no bias. Old items receiving a confidence rating with a criterion lower than the neutral criterion were classified as misses.

## *RESULTS USING A FIXED CRITERION FOR MISS CLASSIFICATION*

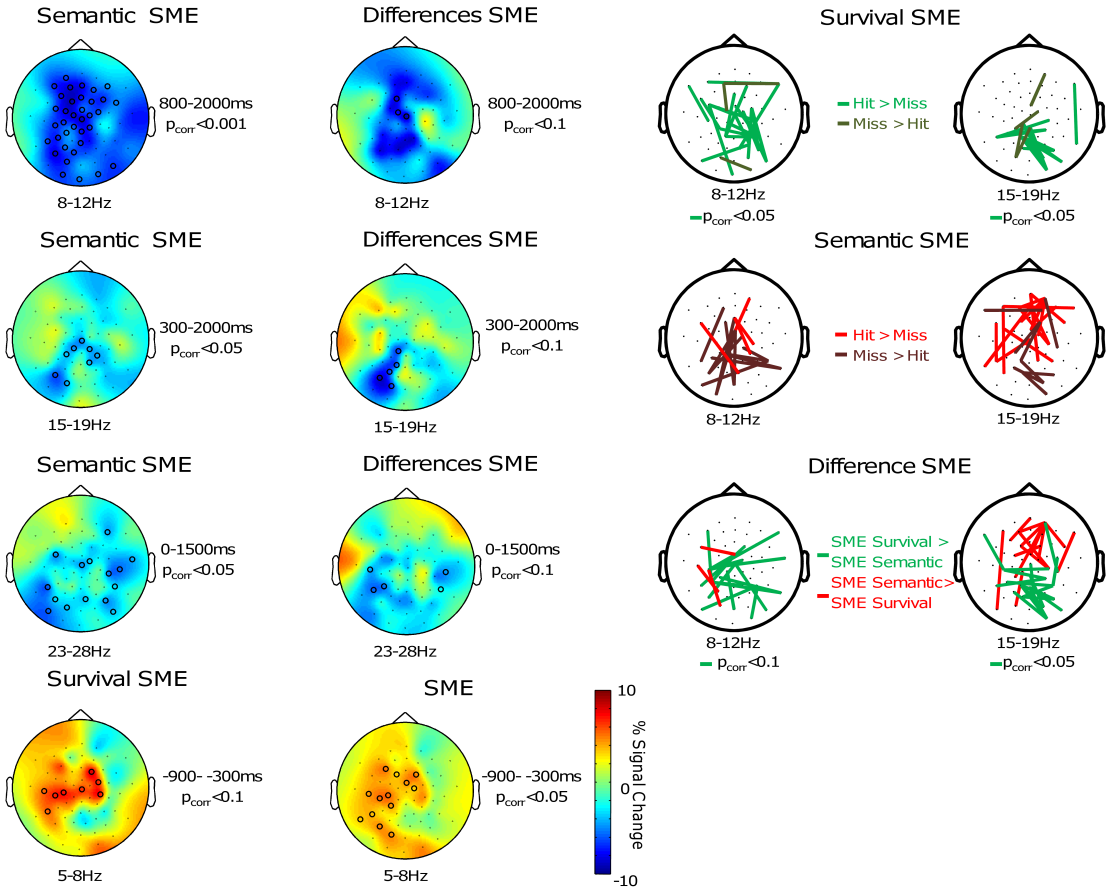


**Supplementary Figure 2:** Power and phase locking results using a fixed criterion for misses. All effects were calculated in the same time frequency bins as the effects employing individually defined criterion for classification of misses. Note the qualitatively very similar results. Although in line with the underlying theory, signal to noise ratio using a fixed criterion is decreased, resulting in some effects following short of significance.

# SUPPLEMENTAL MATERIAL TO STUDY 3

## *SUPPLEMENTAL FIGURES*

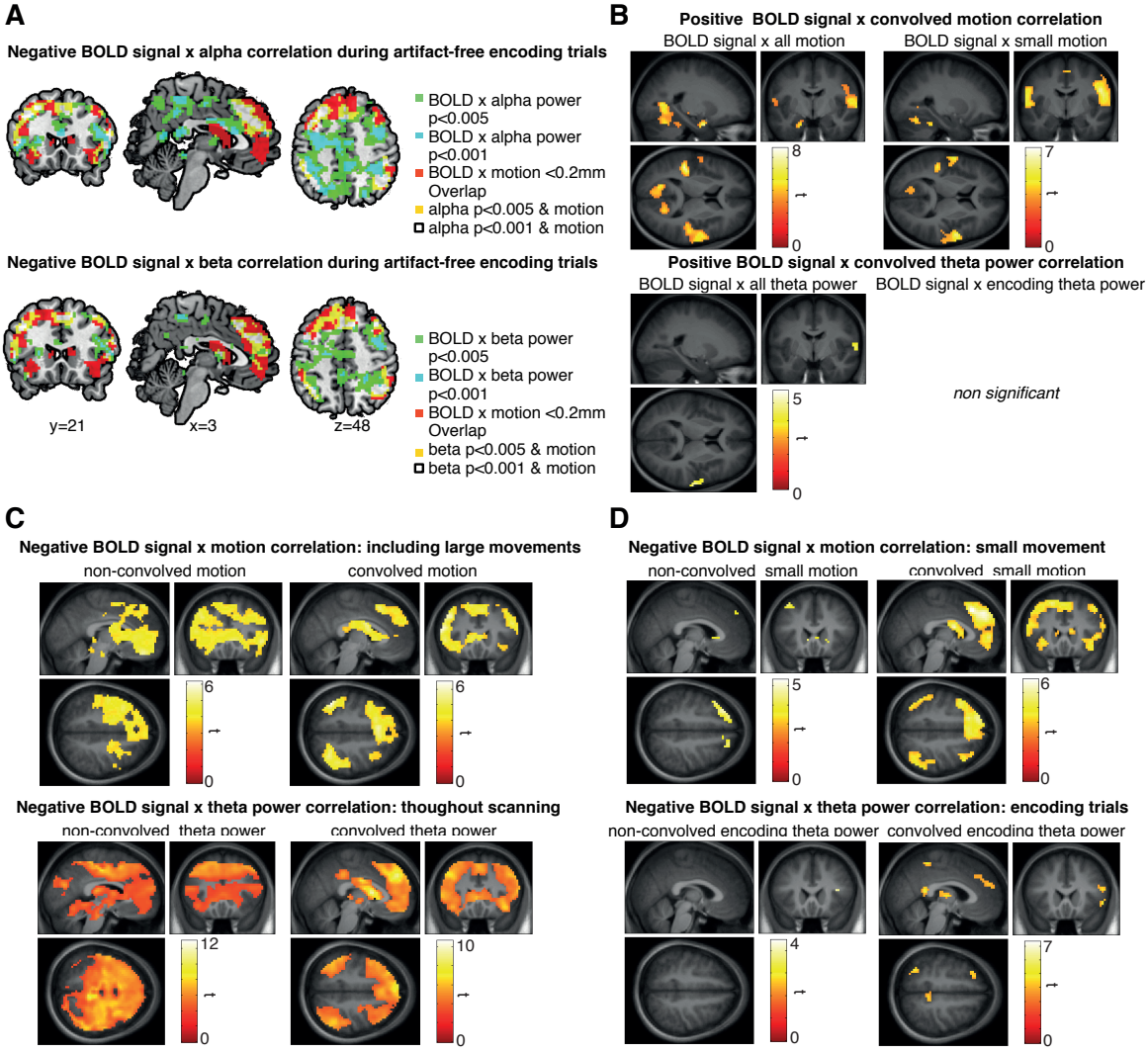


**Figure S1: Alpha/beta band EEG-BOLD correlations, positive EEG/motion BOLD correlations, and unconvolved EEG-BOLD correlations.**

(A) Negative alpha/beta power-BOLD signal correlations. Upper plots show continuous alpha power (8-12 Hz) of the low motion encoding trials convolved with the canonical HRF. Lower plots show the matching correlations for the beta frequency ranges (13-20 Hz). Clusters show correlations of convolved alpha or beta power during encoding and BOLD according to a statistical threshold of either p<0.001 (≥10 voxel, cyan) and p<0.005 (≥10 voxel, green). Areas in yellow/white show an overlap of motion correlation and the more liberally/conservatively thresholded power correlations, respectively. Note the similar pattern of alpha/beta power-BOLD correlations with theta power correlations in Figure 6B.

(B) Positive EEG-BOLD signal and positive motion-BOLD signal correlations are shown. Positive correlations between convolved continuous motion throughout the scanning session

and during small motion trials showed significant activity in areas typically involved in motion generation and execution (i.e. motor cortex, cerebellum). Correlating convolved continuous theta power during the scanning session yielded weaker effects in fewer motion related areas, correlating theta power during the low motion, artifact-free encoding trials showed no significant positive correlations. All plots show uncorrected effects with $p<0.001$ and clustersize≥10 voxel. Slice coordinates are x=-21, y=-7, z=10.

(C) Negative motion-BOLD and theta power-BOLD signal correlations before and after convolving motion or EEG power timecourse with the HRF. BOLD signal correlations with theta-power and motion throughout the scanning session (C) and during clean encoding trials and during small motion (D) are shown. Throughout the scanning session similar correlation pattern before and after convolution are evident, magnitude of t-values is reduced after convolution. (C). This pattern is different for small motion shown in (D): Correlations during small movements are more pronounced after convolution, suggesting that correlations during small motion are related to neural activity or physiological vascular responses driving the measured motion. Note, however the similarity in areas exhibiting effects to the areas showing GLM-allmotion correlations. All plots show uncorrected effects with $p<0.001$, clustersize≥10 voxel. Slice coordinates are x=3, y=-21, z=48. Convolved motion/power correlations are identical to the ones presented in Figure 6.

## RESULT TABLES

**Table S1**: Peak locations of significant convolved all theta power x BOLD correlations and convolved all motion x BOLD correlations (negative correlations shown in Figure 6, positive correlations in Figure S1)

| | | | | MNI coordinates | | | |
|---|---|---|---|---|---|---|---|
| Anatomical label | HS | BA | Size | x | y | z | Z |
| convolved all theta power x BOLD correlation | | | | | | | |
| negative correlations | | | | | | | |
| Caudate | R/L | | 10763 | -3 | 5 | 13 | 5.9 |
| Medial Frontal Gyrus | | 2 | | -3 | 44 | 34 | 5.67 |
| Cingulate Gyrus | | 23 | | 0 | -10 | 28 | 5.4 |
| Inferior Parietal Lobe | R/L | 40 | 651 | 45 | -49 | 52 | 4.58 |
| | | 40 | | 54 | -52 | 43 | 4.41 |
| | | 40 | | 48 | -37 | 46 | 4.04 |
| positive correlations | | | | | | | |
| Superior Temporal Gyrus | R | 22 | 71 | 63 | 2 | 1 | 4.27 |
| Transverse Temporal Gyrus | | 42 | | 66 | -16 | 10 | 3.87 |
| convolved all motion x BOLD correlation | | | | | | | |
| negative correlations | | | | | | | |
| Inferior Parietal Lobule | L | 40 | 452 | -39 | -52 | 52 | 4.59 |
| | | 40 | | -45 | -52 | 46 | 4.54 |
| Middle Temporal Gyrus | | 39 | | -42 | -64 | 37 | 4.25 |
| Inferior Parietal Lobule | R | 7 | 391 | 39 | -55 | 52 | 4.1 |
| Precuneus | | 7 | | 27 | -52 | 49 | 4.04 |
| Inferior Parietal Lobule | | 40 | | 45 | -43 | 49 | 3.96 |
| Inferior Frontal Gyrus | L | 44 | 4282 | -54 | 20 | 16 | 4.59 |
| Superior Frontal Gyrus | | 6 | | -6 | 17 | 52 | 4.57 |
| Caudate | | | | -18 | -31 | 25 | 4.49 |
| Middle Frontal Gyrus | R | 9 | 325 | 51 | 23 | 25 | 3.97 |
| | | 6 | | 36 | 5 | 40 | 3.46 |
| | | 9 | | 39 | 38 | 28 | 3.46 |
| Medial Frontal Gyrus | | 10 | 12 | 18 | 50 | -5 | 3.33 |
| Claustrum | R | | 21 | 33 | 23 | -8 | 3.36 |
| positive correlations | | | | | | | |
| Lingual Gyrus | R/L | 19 | 874 | -15 | -67 | 4 | 5.42 |
| Declive | | | | 27 | -61 | -20 | 5.01 |
| Posterior Cingulate | | 30 | | 0 | -70 | 16 | 4.39 |
| Precentral Gyrus | R | 6 | 552 | 63 | 2 | 4 | 5.24 |
| Superior Temporal Gyrus | | 22 | | 66 | -13 | 4 | 4.7 |
| Postcentral Gyrus | | 43 | | 63 | -10 | 13 | 4.53 |
| Superior Temporal Gyrus | L | 41 | 130 | -45 | -31 | 10 | 5.16 |
| Precentral Gyrus | L | 6 | 33 | -54 | -4 | 7 | 3.57 |
| Parahippocampal Gyrus | R | | 64 | -24 | -1 | -26 | 5.02 |
| Superior Temporal Gyrus | | 38 | | -33 | 5 | -23 | 4.82 |
| Parahippocampal Gyrus | L | | 12 | 24 | -1 | -23 | 3.85 |
| Cerebellum | | | 16 | -24 | -40 | -26 | 3.84 |

**Table S2:** Peak locations of convolved clean encoding theta power x BOLD and convolved small motion x BOLD correlations (negative correlations in Figure 6, positive correlations in Figure S1B)

| | | | | MNI coordinates | | | |
|---|---|---|---|---|---|---|---|
| Anatomical label | HS | BA | Size | x | y | z | Z |
| convolved clean encoding theta power x BOLD correlation | | | | | | | |
| negative correlations | | | | | | | |
| Medial Frontal Gyrus | R/L | 9 | 80 | -3 | 50 | 25 | 3.74 |
| Cingulate Gyrus | | 32 | | 3 | 32 | 34 | 3.22 |
| Paracentral Lobule | R/L | 31 | 15 | -3 | -16 | 46 | 4.19 |
| Lentiform Nucleus | L | | 50 | -21 | 2 | -14 | 4.93 |
| | | | | -12 | 8 | -2 | 3.82 |
| | | | | -18 | -1 | -2 | 3.4 |
| Claustrum | R | | 78 | 39 | -16 | -5 | 4.67 |
| Inferior Frontal Gyrus | R | 44 | 80 | 57 | 14 | 16 | 4.45 |
| Insula | | 13 | | 51 | 5 | 10 | 3.53 |
| Inferior Frontal Gyrus | | 9 | | 42 | 14 | 25 | 3.24 |
| Inferior Frontal Gyrus | R | | 22 | 54 | 20 | -5 | 4.04 |
| Culmen | L | | 27 | -36 | -58 | -20 | 4.33 |
| Fusiform Gyrus | | 37 | | -42 | -52 | -17 | 3.74 |
| Middle Temporal Gyrus | L | 37 | 101 | -45 | -64 | 7 | 4.24 |
| | | 22 | | -57 | -43 | 4 | 3.89 |
| Superior Temporal Gyrus | | 13 | | -45 | -49 | 19 | 3.39 |
| Precuneus | | 7 | 37 | 12 | -37 | 55 | 4.14 |
| Superior Temporal Gyrus | L | 22 | 19 | -57 | -7 | -14 | 4.05 |
| Middle Temporal Gyrus | | 21 | | -51 | -4 | -23 | 3.6 |
| Superior Temporal Gyrus | R | 13 | 279 | 51 | -49 | 19 | 3.98 |
| | | 22 | | 54 | -37 | 7 | 3.9 |
| | | 41 | | 54 | -25 | 7 | 3.84 |
| Thalamus | R/L | | 165 | 6 | -13 | 7 | 3.97 |
| | | | | -18 | -19 | 10 | 3.79 |
| | | | | -6 | -13 | 7 | 3.79 |
| Posterior Cingulate | | 29 | 97 | 0 | -46 | 13 | 3.92 |
| | | 29 | | 9 | -46 | 7 | 3.47 |
| Thalamus | | | | 12 | -34 | 4 | 3.41 |
| Insula | L | 13 | 22 | -60 | -31 | 19 | 3.83 |
| Superior Parietal Lobule | L | 7 | 28 | -33 | -61 | 52 | 3.81 |
| Sub-Gyral | R | 13 | 17 | 48 | 2 | -20 | 3.76 |
| | | 21 | | 42 | -4 | -20 | 3.41 |
| convolved small motion x BOLD correlation | | | | | | | |
| negative correlations | | | | | | | |
| Medial Frontal Gyrus | R/L | 8 | 3600 | 6 | 29 | 43 | 4.77 |
| Middle Frontal Gyrus | | 10 | | -36 | 50 | 13 | 4.69 |
| Anterior Cingulate | | 32 | | 0 | 47 | 13 | 4.67 |
| Thalamus | R/L | | 604 | 0 | -1 | 16 | 4.62 |
| Caudate | | | | -15 | -34 | 25 | 4.58 |
| Cingulate Gyrus | | 23 | | -3 | -7 | 22 | 4.46 |
| Inferior Parietal Lobule | R | 40 | 222 | 51 | -58 | 43 | 4.21 |
| | | 40 | | 57 | -43 | 49 | 3.86 |
| | | 40 | | 48 | -34 | 46 | 3.64 |
| Inferior Parietal Lobule | L | 40 | 249 | -45 | -52 | 46 | 4.08 |
| Middle Temporal Gyrus | | 39 | | -45 | -58 | 31 | 3.85 |
| Precuneus | | 39 | | -39 | -64 | 40 | 3.8 |
| Superior Temporal Gyrus | L | 22 | 24 | -51 | -22 | -8 | 3.61 |
| Middle Temporal Gyrus | | | | -54 | -34 | -2 | 3.35 |
| positive correlations | | | | | | | |
| Precentral Gyrus | R | 4 | 548 | 42 | -13 | 37 | 5.02 |
| | | 4 | | 66 | -1 | 22 | 4.99 |
| | | 6 | | 54 | -7 | 25 | 4.62 |
| Precentral Gyrus | L | 43 | 202 | -60 | -7 | 10 | 4.23 |
| Postcentral Gyrus | | 43 | | -60 | -4 | 22 | 4.17 |
| Precentral Gyrus | | 4 | | -54 | -10 | 28 | 4.05 |
| Transverse Temporal Gyrus | L | 41 | 79 | -42 | -34 | 13 | 4.25 |
| Superior Temporal Gyrus | | 42 | | -60 | -28 | 16 | 3.56 |
| Declive | R | | 74 | 27 | -64 | -17 | 4.04 |
| Fastigium | | | | 12 | -58 | -23 | 4.04 |

| | | | | | | | |
|---|---|---|---|---|---|---|---|
| | L | | 152 | -12 | -61 | -23 | 3.93 |
| Declive | | | | -24 | -64 | -20 | 3.78 |
| Culmen | | | | -33 | -55 | -23 | 3.24 |
| Cuneus | R | 18 | 125 | 6 | -76 | 25 | 3.71 |
| | | 18 | | 0 | -85 | 31 | 3.6 |
| Lingual Gyrus | | 18 | | -15 | -70 | 7 | 3.52 |
| Medial Frontal Gyrus | R | 6 | 10 | 3 | -7 | 55 | 3.66 |
| Parahippocampal Gyrus | R | 19 | 26 | 24 | -58 | 1 | 3.53 |

**Table S3:** Peak locations of significant convolved clean encoding alpha power x BOLD correlations and convolved clean encoding beta power x BOLD correlations (correlations shown in Figure S1A)

| | | | | MNI coordinates | | | |
|---|---|---|---|---|---|---|---|
| Anatomical label | HS | BA | Size | x | y | z | Z |
| convolved encoding clean alpha power x BOLD correlation | | | | | | | |
| negative correlations | | | | | | | |
| Paracentral Lobule | R/L | 5 | 541 | 9 | -37 | 55 | 4.82 |
| Superior Temporal Gyrus | | 41 | | 51 | -37 | 10 | 4.06 |
| Precuneus | | 31 | | 21 | -46 | 40 | 4.04 |
| Middle Frontal Gyrus | R | 6 | 61 | 39 | 2 | 49 | 4.76 |
| Caudate | R | | 684 | 27 | -4 | 28 | 4.47 |
| | | | | 21 | -4 | 22 | 4.44 |
| Precentral Gyrus | | 6 | | 42 | -1 | 25 | 4.34 |
| | L | 6 | 857 | -30 | -4 | 52 | 4.44 |
| Superior Parietal Lobule | | 7 | | -33 | -58 | 49 | 4.42 |
| Middle Frontal Gyrus | | 6 | | -18 | -13 | 52 | 4.17 |
| Anterior Cingulate | R/L | 32 | 364 | -6 | 35 | 19 | 4.25 |
| Medial Frontal Gyrus | | 8 | | 0 | 35 | 40 | 4.10 |
| | | 9 | | 0 | 38 | 28 | 4.01 |
| Lentiform Nucleus | L | | 410 | -21 | -7 | 7 | 4.10 |
| Thalamus | | | | -18 | -28 | 1 | 4.09 |
| | | | | -24 | -16 | 16 | 3.96 |
| Middle Frontal Gyrus | L | 10 | 58 | -33 | 44 | 13 | 4.05 |
| | | 10 | | -33 | 38 | 7 | 3.43 |
| Cingulate Gyrus | R/L | 31 | 23 | 0 | -43 | 40 | 4.05 |
| Lentiform Nucleus | L | | 27 | -27 | 2 | -14 | 3.88 |
| Extra-Nuclear | | 13 | | -36 | 11 | -14 | 3.34 |
| Posterior Cingulate | L | 23 | 17 | -9 | -31 | 31 | 3.87 |
| Claustrum | L | | 17 | -27 | 20 | 10 | 3.86 |
| no gray matter | R | | 89 | 45 | -70 | 25 | 3.81 |
| Precuneus | | 31 | | 36 | -73 | 31 | 3.56 |
| | | 31 | | 27 | -73 | 22 | 3.38 |
| Posterior Cingulate | R/L | 29 | 43 | 0 | -43 | 16 | 3.76 |
| | | 23 | | 3 | -34 | 19 | 3.42 |
| Culmen | | | 19 | 6 | -34 | -8 | 3.71 |
| Posterior Cingulate | R/L | 29 | 16 | 3 | -58 | 13 | 3.68 |
| Middle Frontal Gyrus | R | 8 | 23 | 33 | 35 | 46 | 3.67 |
| | | 6 | | 36 | 23 | 46 | 3.17 |
| Cingulate Gyrus | R/L | 24 | 28 | 3 | 5 | 28 | 3.66 |
| | | 23 | | -9 | -10 | 31 | 3.31 |
| Superior Frontal Gyrus | L | 9 | 16 | -24 | 44 | 25 | 3.59 |
| Insula | L | 13 | 17 | -30 | -40 | 25 | 3.54 |
| Precuneus | R | 7 | 24 | 21 | -70 | 52 | 3.52 |
| Culmen | R | | 12 | 18 | -46 | -26 | 3.49 |
| | | | | 21 | -34 | -23 | 3.30 |
| Paracentral Lobule | R | 31 | 14 | 6 | -13 | 49 | 3.47 |
| Cingulate Gyrus | L | 24 | 10 | -15 | 8 | 34 | 3.43 |
| Caudate | | | | -12 | 5 | 25 | 3.26 |
| Precuneus | L | 31 | 12 | -15 | -58 | 28 | 3.40 |
| | | | | MNI coordinates | | | |
| Anatomical label | HS | | Size | x | y | z | Z |
| convolved encoding clean beta power x BOLD correlation | | | | | | | |

| negative correlations | | | | | | | |
|---|---|---|---|---|---|---|---|
| Caudate | L | | 183 | -12 | 5 | 10 | 4.38 |
| Thalamus | | | | -21 | -10 | 10 | 3.72 |
| | | | | -15 | -16 | 16 | 3.67 |
| Inferior Frontal Gyrus | R | 45 | 123 | 54 | 26 | 7 | 4.34 |
| Middle Frontal Gyrus | | 9 | | 54 | 26 | 25 | 3.90 |
| | | 46 | | 48 | 20 | 16 | 3.50 |
| Caudate | R | | 301 | 18 | -13 | 22 | 4.17 |
| Thalamus | | | | 6 | 2 | 13 | 3.97 |
| | | | | 12 | -16 | 13 | 3.96 |
| Middle Frontal Gyrus | R | 6 | 64 | 39 | 2 | 49 | 4.16 |
| Precuneus | R | 7 | 42 | 9 | -40 | 55 | 4.09 |
| Middle Frontal Gyrus | L | 10 | 51 | -36 | 50 | 16 | 4.02 |
| Medial Frontal Gyrus | | 9 | | -24 | 41 | 13 | 3.65 |
| Middle Frontal Gyrus | | 10 | | -39 | 47 | 7 | 3.60 |
| Medial Frontal Gyrus | R/L | 8 | 314 | 0 | 29 | 43 | 4.01 |
| | | 6 | | 0 | 41 | 31 | 3.83 |
| | | 10 | | -6 | 53 | 7 | 3.63 |
| Middle Temporal Gyrus | L | 19 | 142 | -48 | -61 | 22 | 3.97 |
| Middle Occipital Gyrus | | 37 | | -42 | -67 | 1 | 3.77 |
| Inferior Parietal Lobule | | 7 | | -33 | -55 | 49 | 3.74 |
| Precentral Gyrus | L | 6 | 37 | -45 | 5 | 46 | 3.86 |
| Precuneus | R | 7 | 189 | 24 | -52 | 43 | 3.81 |
| Inferior Parietal Lobule | | 40 | | 45 | -55 | 49 | 3.67 |
| Cingulate Gyrus | | 31 | | 27 | -37 | 43 | 3.56 |
| Middle Temporal Gyrus | L | 22 | 65 | -54 | -37 | 10 | 3.76 |
| Cingulate Gyrus | L | 24 | 46 | -9 | -16 | 46 | 3.72 |
| Precentral Gyrus | | 6 | | -30 | -4 | 55 | 3.51 |
| Medial Frontal Gyrus | | 6 | | -12 | 2 | 55 | 3.29 |
| | R | 9 | 46 | 24 | 38 | 28 | 3.72 |
| | | 9 | | 27 | 47 | 19 | 3.58 |
| Middle Frontal Gyrus | R | 10 | 22 | 33 | 44 | 7 | 3.61 |
| Extra-Nuclear | L | 13 | 22 | -39 | 14 | -17 | 3.60 |
| Claustrum | | | | -33 | 8 | -14 | 3.56 |
| Lentiform Nucleus | | | | -27 | 2 | -14 | 3.19 |
| Precentral Gyrus | L | 44 | 36 | -51 | 14 | 1 | 3.59 |
| Inferior Frontal Gyrus | | 46 | | -51 | 32 | 7 | 3.53 |
| | | 44 | | -51 | 11 | 19 | 3.18 |
| Thalamus | R | | 15 | 24 | -19 | -2 | 3.54 |
| Cingulate Gyrus | L | 31 | 11 | -12 | -37 | 28 | 3.49 |
| Precentral Gyrus | L | 6 | 20 | -42 | -4 | 28 | 3.44 |
| Middle Frontal Gyrus | R | 6 | 13 | 36 | 23 | 46 | 3.43 |
| Precentral Gyrus | L | 9 | 16 | -45 | 23 | 34 | 3.41 |
| | L | 9 | | -39 | 20 | 40 | 3.41 |
| Superior Temporal Gyrus | R | 41 | 12 | 51 | -31 | 7 | 3.33 |
| | | 41 | | 54 | -40 | 10 | 3.32 |
| Claustrum | L | | 15 | -24 | 20 | 10 | 3.32 |
| | | | | -30 | 8 | 13 | 3.30 |

**Table S4:** Peak locations of significant non-convolved all theta power x BOLD correlations and non-convolved all motion x BOLD correlations (correlations shown in Figure S1C)

| | | | | MNI coordinates | | | |
|---|---|---|---|---|---|---|---|
| Anatomical label | HS | BA | Size | x | y | z | Z |
| non-convolved all motion x BOLD correlation | | | | | | | |
| negative correlations | | | | | | | |
| Precentral Gyrus | R/L | 9 | 13847 | -36 | 11 | 34 | 4.46 |
| Postcentral Gyrus | | 43 | | -60 | -16 | 16 | 4.36 |
| Anterior Cingulate | | 32 | | -18 | 47 | -14 | 4.16 |
| Superior Temporal Gyrus | R | 42 | 59 | 60 | -28 | 13 | 3.54 |
| Cerebellum | | | 88 | 3 | -37 | -14 | 3.40 |
| Midbrain | | | | 9 | -28 | -11 | 3.18 |
| Cerebellum | | | | 18 | -31 | -11 | 3.16 |
| Thalamus | | | 11 | -3 | -34 | 1 | 3.29 |
| Midbrain | | | 23 | -3 | -19 | -20 | 3.24 |
| | | | | -12 | -19 | -17 | 3.22 |
| Middle Temporal Gyrus | L | 37 | 12 | -39 | -61 | 10 | 3.19 |
| non-convolved all theta power x BOLD correlation | | | | | | | |
| negative correlations | | | | | | | |
| Paracentral Lobule | R/L | 5 | 20999 | -6 | -31 | 55 | 6.42 |
| Paracentral Lobule | | 5 | | 9 | -37 | 55 | 6.18 |
| Cingulate Gyrus | | 31 | | 6 | -28 | 46 | 5.81 |

**Table S5:** Peak locations of significant non-convolved clean encoding theta power x BOLD correlations and non-convolved small motion x BOLD correlations (correlations shown in Figure S1D)

| | | | | MNI coordinates | | | |
|---|---|---|---|---|---|---|---|
| Anatomical label | HS | BA | Size | x | y | z | Z |
| non-convolved clean encoding theta power x BOLD correlation | | | | | | | |
| negative correlations | | | | | | | |
| Claustrum | R | | 17 | 27 | 29 | -8 | 4.29 |
| no gray matter defined | R | | 14 | 36 | -46 | 28 | 3.86 |
| Insula | R | 13 | 17 | 36 | 26 | 10 | 3.74 |
| non-convolved small motion x BOLD correlation | | | | | | | |
| negative correlations | | | | | | | |
| Caudate | R | | 137 | 21 | 26 | -5 | 4.08 |
| Anterior Cingulate | | 32 | | 15 | 47 | -11 | 3.97 |
| no gray matter defined | | | | 33 | 44 | -5 | 3.69 |
| Superior Frontal Gyrus | L | 8 | 202 | -15 | 41 | 43 | 3.84 |
| | | 8 | | -27 | 32 | 49 | 3.79 |
| Middle Frontal Gyrus | | 8 | | -21 | 44 | 37 | 3.68 |
| Medial Frontal Gyrus | R | 9 | 43 | 18 | 50 | 16 | 3.77 |
| Caudate | L | | 29 | -21 | 26 | -5 | 3.76 |
| | | | | -9 | 23 | -2 | 3.53 |
| Middle Frontal Gyrus | L | 10 | 32 | -36 | 44 | 7 | 3.75 |
| Medial Frontal Gyrus | L | 10 | 41 | -15 | 56 | 10 | 3.62 |
| Superior Frontal Gyrus | R | 6 | 41 | 21 | 35 | 49 | 3.5 |
| Medial Frontal Gyrus | | 8 | | 12 | 26 | 46 | 3.34 |
| Anterior Cingulate | L | 32 | 16 | -9 | 47 | -11 | 3.33 |
| Caudate | R | | 10 | 6 | 14 | 1 | 3.33 |
| | | | | 6 | 26 | 1 | 3.2 |